



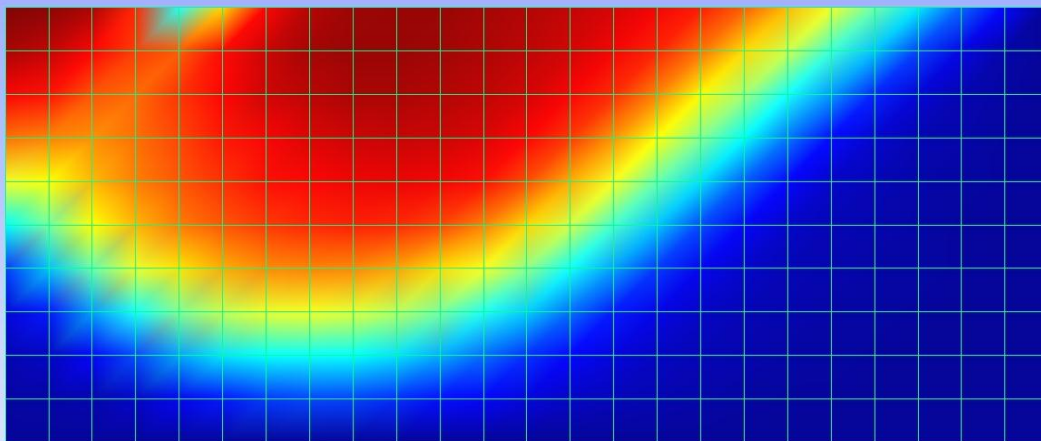
NATIONAL  
TECHNICAL  
UNIVERSITY  
ATHENS

School of Civil Engineering

**Institute of Structural Analysis & Seismic Research**

# Elastoplastic Constitutive Models in Finite Element Analysis

Manitaras Theofilos-Ioannis



Supervisor: Professor Manolis Papadrakakis

July 2012

NATIONAL TECHNICAL UNIVERSITY ATHENS

SCHOOL OF CIVIL ENGINEERING

Institute of Structural Analysis & Seismic Research

ELASTOPLASTIC CONSTITUTIVE MODELS  
IN FINITE ELEMENT ANALYSIS

Manitaras Theofilos-Ioannis

Supervisor: Professor Manolis Papadrakakis

July 2012

Athens



## Εισαγωγή

Η εκπόνηση της παρούσας μεταπτυχιακής εργασίας εντάσσεται στα πλαίσια του διεπιστημονικού-διατηρηματικού προγράμματος μεταπτυχιακών σπουδών “Δομοστατικός Σχεδιασμός και Ανάλυση Κατασκευών” της Σχολής Πολιτικών Μηχανικών του Εθνικού Μετσόβιου Πολυτεχνείου.

Κύριο αντικείμενο της εργασίας είναι η μελέτη, αλλά και εφαρμογή των αριθμητικών μεθόδων, οι οποίες χρησιμοποιούνται για τη μη γραμμική ανάλυση ελαστοπλαστικών στερεών με πεπερασμένα στοιχεία στα πλαίσια των μικρών παραμορφώσεων.

Αρχικά παρουσιάζεται μία σύντομη ανασκόπηση της θεωρίας των διανυσμάτων και τανυστών που χρησιμοποιούνται στη Μηχανική του Συνεχούς Μέσου και υιοθετούνται για την εκπόνηση της παρούσας εργασίας. Ακολουθεί περιγραφή και ανάλυση της θεωρίας της πλαστικότητας, η οποία είναι ανεξάρτητη από το ρυθμό επιβολής του φορτίου. Στη συνέχεια μελετάται ο τρόπος με τον οποίο εκτελείται η μη γραμμική ανάλυση με πεπερασμένα στοιχεία εξαιτίας της μη γραμμικότητας του υλικού. Παράλληλα, αναλύονται τα διάφορα βήματα που είναι απαραίτητα για την επιτυχή εκτέλεση της ανάλυσης που προαναφέρθηκε, αλλά και τα απαιτούμενα στοιχεία για την ενσωμάτωση ενός ελαστοπλαστικού καταστατικού νόμου υλικού σε έναν κώδικα πεπερασμένων στοιχείων. Επίσης, περιγράφονται τα καταστατικά μοντέλα υλικού von Mises και Drucker-Prager, ενώ ιδιαίτερη έμφαση δίδεται στον τρόπο με τον οποίο εκτελείται η ολοκλήρωση των τάσεων και η παραγωγή των εφαπτομενικών καταστατικών μητρώων. Τέλος, πραγματοποιούνται αναλύσεις με τη χρήση πεπερασμένων στοιχείων, όπου εφαρμόζονται όσα αναφέρθηκαν παραπάνω, αλλά ακολουθεί και σύγκριση με αναλυτικές λύσεις και με δημοσιευμένα αποτελέσματα, τα οποία επικυρώσουν την αποτελεσματικότητα των αριθμητικών μεθόδων που χρησιμοποιήθηκαν.

Ο προγραμματισμός των αριθμητικών τεχνικών που αποτελούν το κεντρικό θέμα της εργασίας πραγματοποιήθηκε στη γλώσσα προγραμματισμού Java. Για την επίτευξη της εφαρμογής των μεθόδων που περιγράφονται στη συνέχεια προηγήθηκε η ενσωμάτωση των μη γραμμικών ελαστοπλαστικών μοντέλων υλικού στον κώδικα πεπερασμένων στοιχείων *Solverize*. Ο κώδικας αυτός προέκυψε από την επέκταση και τον εμπλουτισμό του προγράμματος *AnalyzerSharp*, το οποίο αναπτύχθηκε από τον υποψήφιο διδάκτορα κ. Γεώργιο Σταυρουλάκη στα πλαίσια της διδακτορικής του διατριβής.

Στο σημείο αυτό οφείλω να ευχαριστήσω τον καθηγητή μου κ. Μανόλη Παπαδρακάκη, επιβλέποντα της παρούσας μεταπτυχιακής εργασίας, η καθοδήγηση του οποίου καθ' όλη τη διάρκεια εκπόνησής της υπήρξε πραγματικά πολύτιμη.

Επιπλέον, θεωρώ καθήκον μου να ευχαριστήσω και τον κ. Αλέξανδρο Καραταράκη, επίσης υποψήφιο διδάκτορα της Σχολής Πολιτικών Μηχανικών, η συνεργασία με τον οποίο έπαιξε καταλυτικό ρόλο στην επιτυχή περάτωση της παρούσας εργασίας. Η αξιόλογη εμπειρία του στον προγραμματισμό βοήθησε σημαντικά στην κατανόηση και υιοθέτηση των βέλτιστων προγραμματιστικών τεχνικών για την οριστική ενσωμάτωση των απαιτούμενων στοιχείων στον κώδικα *Solverize*.

## *Introduction*

The elaboration of the following master thesis was conducted on the basis of the master program “Analysis and Design of Earthquake Resistant Structures” organized by the School of Civil Engineering of the National Technical University of Athens.

The main subject of the current thesis focuses on the study and application of the numerical procedures used in nonlinear analysis of elastoplastic solids subjected to small strains and simulated with the finite element method.

Initially, a brief review introduces the reader to the theory of vectors and tensors mainly used in Continuum Mechanics, which are adopted throughout the thesis. Secondly, the theory of rate-independent plasticity is extensively described and analyzed, while studying the nonlinear analysis with finite elements due to material non-linearity. All the required steps for carrying out the aforementioned analysis successfully are furtherly examined, along with the essential components for incorporating an elastoplastic constitutive model into a finite element code. In addition, the constitutive models of von Mises and Drucker-Prager are described, emphasizing on the integration of stresses and the construction of the consistent tangent moduli. Finally, nonlinear finite element analyses taking into account the elastoplastic material response are executed followed by comparisons to analytical solutions and results available in international bibliography which validate the effectiveness and accuracy of the methods used.

The Java programming language has been chosen for the programming of the numerical procedures constituting the main subject of the current thesis. Application of the nonlinear procedures required the incorporation of the elastoplastic constitutive models mentioned above into the finite element code *Solverize*. This particular code has been the fruit of previous research as well as the extension of the *AnalyzerSharp* program, developed by George Stavroulakis for solving finite element problems during his PhD research.

At this point I would like to thank my professor Mr. Manolis Papadrakakis, supervisor of the current thesis, whose guidance and support has been indeed valuable throughout the whole study.

Additionally, it's my duty to thank Mr. Alexander Karatarakis, who is also a PhD candidate at the School of Civil Engineering of NTUA, the collaboration with whom has played a crucial role to the successful completion of the thesis. His programming experience was of utter importance during the programming procedure and especially the incorporation of the required elements into the *Solverize* code.

## *Contents*

Εισαγωγή.....	3
Introduction .....	4
Chapter 1: Review of Vectors and Tensors .....	9
1.1. Vectors and Scalars .....	9
1.1.1. Inner Product, Norm and Orthogonality.....	9
1.1.2. Orthonormal Bases and Cartesian Components.....	10
1.2. Second-order Tensors .....	11
1.2.1. Tensor Product.....	11
1.2.2. The Transpose, Symmetric and Skew Tensors.....	12
1.2.3. Trace, Contraction, Inner Product and Euclidean Norm.....	13
1.2.4. Inverse of a Tensor, Tensor Determinant and Positive Definiteness.....	14
1.2.5. Orthogonal Tensors and Changes of Basis.....	15
1.2.6. Spectral Decomposition – Principal Invariants .....	16
1.3. Higher-Order Tensors .....	17
1.3.1. Fourth-Order Tensors and Symmetry .....	17
1.3.2. Change of Basis for Fourth-Order Tensors.....	18
1.4. Isotropic Tensors.....	18
Chapter 2: Theory of Rate-Independent Plasticity – Classical Yield Criteria .....	21
The Mathematical Theory of Plasticity .....	21
2.1. Phenomenological Aspects .....	21
2.2. One-dimensional Constitutive Model.....	23
2.2.1. Elastoplastic Decomposition of the Axial Strain .....	24
2.2.2. The Elastic Uniaxial Constitutive Law.....	25
2.2.3. The Yield Function and the Yield Criterion .....	25
2.2.4. The Plastic Flow Rule. Loading/Unloading Conditions.....	26
2.2.5. The Hardening Law .....	27
2.2.6. Determination of the Plastic Multiplier .....	28
2.2.7. The Elastoplastic Tangent Modulus .....	29
2.3. General Elastoplastic Constitutive Model.....	30
2.3.1. Additive Decomposition of the Strain Tensor.....	30
2.3.2. The Free Energy Potential and the Elastic Law .....	30
2.3.3. Yield Criterion and Yield Surface.....	32
2.3.4. Plastic Flow Rule and Hardening Law .....	32

2.3.5. Flow Rules Defined from a Flow Potential.....	33
2.3.6. The Plastic Multiplier .....	33
2.3.7. Rate Form and the Elastoplastic Tangent Operator .....	34
2.4. Classical Yield Criteria .....	35
2.4.1. Von Mises Yield-Criterion .....	35
2.4.2. Drucker-Prager Yield-Criterion.....	37
Chapter 3: Numerical Solution of the Elastoplastic Constitutive Initial Value Problem with the Finite Element Method .....	41
3.1. The Incremental Finite Element Solution for Path-Dependent Materials.....	41
3.1.1. The Incremental Constitutive Function .....	41
3.1.2. The Incremental Boundary Value Problem.....	42
3.1.3. The Nonlinear Incremental Finite Element Equation .....	42
3.1.4. Nonlinear Solution. The Newton-Raphson Scheme.....	43
3.1.5. The Consistent Tangent Modulus .....	44
3.2. Preliminary Implementation Aspects for the Elastoplastic Constitutive Initial Value Problem .....	45
3.2.1 The Elastoplastic Constitutive Initial Value Problem .....	46
3.2.2. Euler Discretization: The Incremental Constitutive Problem.....	46
3.2.3. Solution of the incremental problem.....	47
3.2.4. The Elastic Predictor/Plastic Corrector Algorithm .....	48
Chapter 4:Numerical Implementation of Classical Elastoplastic Models .....	51
4.1. The von Mises Plasticity Model .....	51
4.1.1 The Implicit Elastic Predictor/Return Mapping Scheme .....	52
4.1.2. Single-equation return-mapping.....	53
4.1.3. Linear Isotropic Hardening and Perfect Plasticity: The Closed-Form Return Mapping .....	55
4.1.4. The Elastoplastic Consistent Tangent for the Von Mises Model with Isotropic Hardening.....	56
4.2. The Drucker-Prager Model.....	58
4.2.1. The Drucker-Prager constitutive equations .....	58
4.2.2. Integration Algorithm for the Drucker-Prager model.....	59
4.2.3. Return to the smooth portion of the cone .....	59
4.2.4. Return to the apex .....	60
4.2.5. Selection of the appropriate return-mapping .....	62
4.2.6. Consistent Tangent Operator for the Drucker-Prager Model.....	63
4.3. The Plane Stress-Projected von Mises Model.....	66

4.3.1 The plane stress-projected equations .....	67
4.3.2. Matrix Notation.....	68
4.3.3. The Plane Stress-Projected Integration Algorithm .....	69
4.3.4. The plane stress-projected return mapping .....	70
4.3.5. Newton-Raphson return-mapping solution.....	71
4.3.6. The Elastoplastic Consistent Tangent Operator.....	73
Chapter 5: Applications.....	77
5.1. Internally pressurized thick-walled cylinder .....	77
5.2. Collapse of an End-Loaded Cantilever .....	80
5.3. Strip-Footing Collapse .....	83
5.3.1. Results for the von Mises material model .....	85
5.3.2. Results for the Drucker-Prager material model.....	87
References .....	89





# Chapter 1: Review of Vectors and Tensors

## 1.1. Vectors and Scalars

A physical quantity that can be completely described by a single real number is called a *scalar*. It is designated by  $\alpha, \beta, \gamma \dots$ . Quantities such as temperature, density, mass, work are scalars. Comparison between scalar quantities is possible only if they have the same physical dimensions.

However there are cases when someone must deal with quantities, called vectors whose specification requires a direction as well as a numerical value. Displacement, velocity, acceleration, force, moment are typical quantities that can be adequately described by using vectors. Vectors are designated by  $\mathbf{u}, \mathbf{v}, \mathbf{w}, \dots$

The notion of a vector can be generalized for n-dimensions for an Euclidean space  $\mathcal{E}$ . Then by letting  $\mathcal{U}$  be the space of n-dimensional vectors associated to  $\mathcal{E}$ , points of  $\mathcal{E}$  and vectors  $\mathcal{U}$  must satisfy the basic rules of vector algebra.

### 1.1.1. Inner Product, Norm and Orthogonality

The expression:

$$\mathbf{u} \cdot \mathbf{v}$$

denotes the *inner product* or *scalar product* between two arbitrary vectors of space  $\mathcal{U}$ .

The vector  $\mathbf{u}$  is said to be *orthogonal* or *perpendicular* to another vector  $\mathbf{v}$  if their inner product is zero:

$$\mathbf{u} \cdot \mathbf{v} = 0$$

The *Euclidean norm* or simply *norm* of a vector  $\mathbf{u}$  is defined as:

$$\|\mathbf{u}\| = \sqrt{\mathbf{u} \cdot \mathbf{u}}$$

and  $\mathbf{u}$  is said to be a *unit vector* if its norm is equal to unity:

$$\|\mathbf{u}\| = 1$$

The *zero vector*  $\mathbf{o}$  is a vector that has zero norm:

$$\|\mathbf{o}\| = 0$$

### 1.1.2. Orthonormal Bases and Cartesian Components

An *orthonormal basis* for  $\mathcal{U}$  is defined as a set  $\{\mathbf{e}_i\} = \{\mathbf{e}_1, \mathbf{e}_2, \dots, \mathbf{e}_n\}$  of mutually orthogonal unit vectors. They satisfy the following:

$$\mathbf{e}_i \cdot \mathbf{e}_j = \delta_{ij}$$

Where  $\delta_{ij}$  is the Krönecker delta:

$$\delta_{ij} = \begin{cases} 1 & \text{if } i = j \\ 0 & \text{if } i \neq j \end{cases}$$

Then any vector  $\mathbf{u} \in \mathcal{U}$  can be represented as:

$$\mathbf{u} = u_1 \mathbf{e}_1 + u_2 \mathbf{e}_2 + \dots + u_n \mathbf{e}_n = \sum_{i=1}^n u_i \mathbf{e}_i$$

where:

$$u_i = \mathbf{u} \cdot \mathbf{e}_i$$

are the Cartesian components of  $\mathbf{u}$  relative to the basis  $\{\mathbf{e}_i\}$ . Any vector  $\mathbf{u} \in \mathcal{U}$  can be uniquely defined by its Cartesian components relative to a given basis. This allows us to represent any vector  $\mathbf{u}$  as a single column matrix denoted by  $[\mathbf{u}]$ :

$$[\mathbf{u}] = \begin{bmatrix} u_1 \\ u_2 \\ \vdots \\ u_n \end{bmatrix}$$

At this point, it is essential to introduce the *summation convention* (Einstein convention) which is going to be used throughout the text. According to the summation convention, when an index appears twice in the same product, summation over the repeated index is applied unless otherwise stated. The summation convention allows us to express relations including vectors and tensors in a more compact and efficient way. The following example will make things clearer so that the use and application of the summation convention is completely understood:

$$u_i \mathbf{e}_i = \sum_{i=1}^3 u_i \mathbf{e}_i = u_1 \mathbf{e}_1 + u_2 \mathbf{e}_2 + u_3 \mathbf{e}_3$$

By making use of the summation convention, it is easy to express the inner product of two vectors  $\mathbf{u}, \mathbf{v}$  in terms of their vector components relative to a Cartesian basis:

$$\mathbf{u} \cdot \mathbf{v} = u_i v_i$$

Note that in the above expression, the value of the inner product does not depend on the particular letter chosen for an index of summation. For this reason, indices of summation are often called “dummy” indices.

## 1.2. Second-order Tensors

Second-order tensors (or simply tensors) denoted by bold capital italic letters are linear transformations (mappings) which transform any vector into another vector. We can write this by using mathematical symbols for a second order tensor  $\mathbf{T}$  and the vector space  $\mathcal{U}$ :

$$\mathbf{T}: \mathcal{U} \rightarrow \mathcal{U}$$

Let  $\mathbf{T}$ ,  $\mathbf{S}$  be second order tensors and  $\mathbf{a}$ ,  $\mathbf{b}$  two vectors. Then due to the fact that  $\mathbf{T}$  is a linear transformation:

$$\mathbf{c} = \mathbf{T}\mathbf{a},$$

$$\mathbf{T}(\mathbf{a} + \mathbf{b}) = \mathbf{T}\mathbf{a} + \mathbf{T}\mathbf{b},$$

$$(\mathbf{S} + \mathbf{T})\mathbf{a} = \mathbf{S}\mathbf{a} + \mathbf{T}\mathbf{a},$$

$$\mathbf{T}(\alpha\mathbf{a}) = \alpha\mathbf{T}\mathbf{a}$$

where  $\alpha$  and is a scalar and  $\mathbf{c}$  is another vector.

The product of two tensors  $\mathbf{S}$  and  $\mathbf{T}$  is the tensor  $\mathbf{ST}$  defined by:

$$\mathbf{ST}\mathbf{u} = \mathbf{S}(\mathbf{T}\mathbf{u})$$

In general:

$$\mathbf{ST} \neq \mathbf{TS}$$

### 1.2.1. Tensor Product

The *tensor product* or the *dyad* or *dyadic product* of two vectors  $\mathbf{u}$ ,  $\mathbf{v}$  is denoted by:

$$\mathbf{u} \otimes \mathbf{v}$$

and is a second order tensor which transforms a vector  $\mathbf{w}$  to another vector with the direction of vector  $\mathbf{u}$  according to the following relation:

$$(\mathbf{u} \otimes \mathbf{v})\mathbf{w} = \mathbf{u}(\mathbf{v} \cdot \mathbf{w}) = (\mathbf{v} \cdot \mathbf{w})\mathbf{u}$$

The dyadic product, is very important to second-order tensors in general, because any second-order tensor can be expressed as a linear combination of dyads formed by the Cartesian basis  $\{\mathbf{e}_i\}$ :

$$\mathbf{T} = T_{ij} \mathbf{e}_i \otimes \mathbf{e}_j$$

where:

$$T_{ij} = \mathbf{e}_i \cdot \mathbf{T} \mathbf{e}_j$$

A tensor resolved along basis vectors that are orthonormal is called a Cartesian tensor of order two. The components of this Cartesian tensor with respect to the n-dimensional basis  $\{\mathbf{e}_i\}$ , are represented as above by  $T_{ij}$  and form the entries of a matrix:

$$\begin{bmatrix} T_{11} & T_{12} & \cdots & T_{1n} \\ T_{21} & T_{22} & \cdots & T_{2n} \\ \vdots & \vdots & \ddots & \vdots \\ T_{n1} & T_{n2} & \cdots & T_{nn} \end{bmatrix}$$

The above relation is known as the *matrix notation* of tensor  $\mathbf{T}$ . The Cartesian components of the identity tensor  $\mathbf{I}$  which reads:

$$I_{ij} = \delta_{ij}$$

are written in matrix form:

$$[\mathbf{I}] = \begin{bmatrix} 1 & 0 & \cdots & 0 \\ 0 & 1 & \cdots & 0 \\ \vdots & \vdots & \ddots & \vdots \\ 0 & 0 & \cdots & 1 \end{bmatrix}$$

It is also very useful to show the relation which provides the Cartesian components of a vector  $\mathbf{v}$  which is the result of the transformation of another vector  $\mathbf{u}$  via the second order tensor  $\mathbf{T}$ :

$$\mathbf{v} = \mathbf{T} \mathbf{u}$$

$$\begin{aligned} v_i &= [T_{jk} (\mathbf{e}_j \otimes \mathbf{e}_k) u_l \mathbf{e}_l] \cdot \mathbf{e}_i = T_{jk} u_l (\mathbf{e}_j \cdot \mathbf{e}_i) (\mathbf{e}_k \cdot \mathbf{e}_l) = \\ &= T_{jk} u_l \delta_{ji} \delta_{kl} = T_{ik} u_k \end{aligned}$$

Thus is clear that column vector of Cartesian components of  $\mathbf{v}$  is obtained from the matrix-vector multiplication:

$$\begin{bmatrix} v_1 \\ v_2 \\ \vdots \\ v_n \end{bmatrix} = \begin{bmatrix} T_{11} & T_{12} & \cdots & T_{1n} \\ T_{21} & T_{22} & \cdots & T_{2n} \\ \vdots & \vdots & \ddots & \vdots \\ T_{n1} & T_{n2} & \cdots & T_{nn} \end{bmatrix} \begin{bmatrix} u_1 \\ u_2 \\ \vdots \\ u_n \end{bmatrix}$$

### 1.2.2. The Transpose, Symmetric and Skew Tensors

The *transpose*  $\mathbf{T}^T$  of a second-order tensor  $\mathbf{T}$ , is the unique tensor governed by the following identity:

$$\mathbf{v} \cdot \mathbf{T}^T \mathbf{u} = \mathbf{u} \cdot \mathbf{T} \mathbf{v} = \mathbf{T} \mathbf{v} \cdot \mathbf{u}, \quad \forall \mathbf{u}, \mathbf{v} \in \mathcal{U}$$

The second order tensor is said to be *symmetric* if the following relation holds:

$$\mathbf{T} = \mathbf{T}^T$$

and *skew symmetric* if:

$$\mathbf{T} = -\mathbf{T}^T$$

Any tensor  $\mathbf{T}$  can be decomposed as the sum of a symmetric tensor here denoted by  $\mathbf{S}$  and a skew symmetric (antisymmetric) tensor here denoted by  $\mathbf{W}$ . Hence:

$$\mathbf{T} = \text{sym}(\mathbf{T}) + \text{skew}(\mathbf{T}) = \mathbf{S} + \mathbf{W}$$

$$\text{sym}(\mathbf{T}) = \mathbf{S} = \frac{1}{2}(\mathbf{T} + \mathbf{T}^T),$$

$$\text{skew}(\mathbf{T}) = \mathbf{W} = \frac{1}{2}(\mathbf{T} - \mathbf{T}^T)$$

There are many useful properties involving the transpose of a tensor, symmetric and skew symmetric tensors. The most important are the following:

- a)  $(\alpha \mathbf{A} + \beta \mathbf{B})^T = \alpha \mathbf{A}^T + \beta \mathbf{B}^T$
- b)  $(\mathbf{A}\mathbf{B})^T = \mathbf{B}^T \mathbf{A}^T$
- c)  $(\mathbf{u} \otimes \mathbf{v})^T = (\mathbf{v} \otimes \mathbf{u})^T$
- d)  $(\mathbf{A}^T)_{ij} = \mathbf{A}_{ji}$

where  $\mathbf{A}, \mathbf{B}$  are second-order tensors,  $\mathbf{u}, \mathbf{v}$  are vectors and  $\alpha, \beta$  are scalars.

### 1.2.3. Trace, Contraction, Inner Product and Euclidean Norm

The trace of a tensor  $\mathbf{A}$  is a scalar denoted as  $\text{tr}\mathbf{A}$ . For a second order tensor, the trace is calculated by summing up the diagonal terms of its matrix representation relative to a Cartesian basis. The trace of the dyadic product between two vectors  $\mathbf{u}$  and  $\mathbf{v}$  gives their inner product:

$$\text{tr}(\mathbf{u} \otimes \mathbf{v}) = \mathbf{u} \cdot \mathbf{v} = u_i v_i$$

For a generic second order tensor  $\mathbf{T}$  which can be expressed as a linear combination of dyads formed by the Cartesian basis  $\{\mathbf{e}_i\}$

$$\mathbf{T} = T_{ij} \mathbf{e}_i \otimes \mathbf{e}_j$$

$$\rightarrow \text{tr}\mathbf{T} = T_{ij} \text{tr}(\mathbf{e}_i \otimes \mathbf{e}_j) = T_{ij} \delta_{ij} = T_{ii}$$

In index notation, *contraction* means to identify two indices and to apply summation over them by using them as dummy indices. Between two second-order tensors  $\mathbf{S}$  and  $\mathbf{T}$  a *double contraction* is denoted as:

$$\mathbf{S}:\mathbf{T}$$

and yields a scalar. It is also known as *inner product* between  $\mathbf{S}$  and  $\mathbf{T}$  and in Cartesian component form, it defined as:

$$\mathbf{S}:\mathbf{T} = \text{tr}(\mathbf{S}^T\mathbf{T}) = S_{ij}T_{ij}$$

The Euclidean norm of a second-order tensor  $\mathbf{T}$  is defined easily by using the double contraction:

$$\|\mathbf{T}\| = \sqrt{\mathbf{T}:\mathbf{T}} = \sqrt{T_{11}^2 + T_{12}^2 + \dots + T_{nn}^2}$$

#### 1.2.4. Inverse of a Tensor, Tensor Determinant and Positive Definiteness

A tensor  $\mathbf{T}$  is said to be *invertible* if there exists a tensor which is denoted  $\mathbf{T}^{-1}$  which satisfies:

$$\mathbf{T}\mathbf{T}^{-1} = \mathbf{T}^{-1}\mathbf{T} = \mathbf{I}$$

This tensor  $\mathbf{T}^{-1}$  is the *inverse* of tensor  $\mathbf{T}$  and if it exists it is unique.

Let  $[\mathbf{T}]$  be the matrix representation of the Cartesian components of tensor  $\mathbf{T}$  relative to a basis  $\{\mathbf{e}_i\}$ . Then the determinant of the matrix  $[\mathbf{T}]$  is called the *determinant* of tensor  $\mathbf{T}$ . A tensor  $\mathbf{T}$  is invertible if and only if its determinant is non-zero:

$$\det\mathbf{T} \neq 0$$

A tensor  $\mathbf{T}$  is said to be *positive definite* if:

$$\mathbf{T}\mathbf{u} \cdot \mathbf{u} > 0 \quad \forall \mathbf{u} \neq \mathbf{o}$$

Any positive definite tensor is also invertible.

The basic relations that hold for matrix determinants and inverse matrices are also valid for tensors. Let  $\mathbf{T}$  and  $\mathbf{S}$  be tensors:

- a)  $\det(\mathbf{ST}) = \det(\mathbf{S}) \det(\mathbf{T})$
- b)  $\det(\mathbf{T}^{-1}) = (\det\mathbf{T})^{-1}$
- c)  $(\mathbf{ST})^{-1} = \mathbf{T}^{-1}\mathbf{S}^{-1}$
- d)  $(\mathbf{T}^{-1})^T = (\mathbf{T}^T)^{-1}$

### 1.2.5. Orthogonal Tensors and Changes of Basis

Generally, the inner product between two vectors  $\mathbf{u}, \mathbf{v}$  is not preserved under a transformation by a tensor. A tensor  $\mathbf{Q}$  which preserves the inner product of two vectors under the transformation:

$$\mathbf{Q}\mathbf{u} \cdot \mathbf{Q}\mathbf{v} = \mathbf{u} \cdot \mathbf{v}$$

is called an *orthogonal tensor*. A tensor  $\mathbf{Q}$  is orthogonal if and only if:

$$\mathbf{Q}^T = \mathbf{Q}^{-1}$$

The determinant of an orthogonal tensor has a value of either +1 or -1. An orthogonal tensor is called *proper orthogonal* if the value of its determinant is equal to 1. A *proper orthogonal* tensor is also called a *rotation*.

Now that we have defined proper orthogonal tensors (or rotations), we can introduce the key property of tensors, which is the *transformation law* of its components, i.e., the way its components in one coordinate system are related to its components in another coordinate system.

Let  $\{\mathbf{e}_i\}$  and  $\{\mathbf{e}'_i\}$  be two orthonormal bases of  $\mathcal{U}$ . These two bases are related via a proper orthogonal tensor  $\mathbf{R}$  (a rotation) by the following relation:

$$\mathbf{e}'_i = \mathbf{R}\mathbf{e}_i, \quad \text{for } i = 1, 2, \dots, n$$

Let  $\mathbf{T}$  and  $\mathbf{u}$  be respectively a tensor and a vector. The matrix representations of their components relative to basis  $\{\mathbf{e}_1\}$  are  $[\mathbf{T}]$  and  $[\mathbf{u}]$ . The transformation law, states that the matrix representation of tensor  $\mathbf{T}$  and  $\mathbf{u}$  relative to the second basis  $\{\mathbf{e}'_1\}$  can be calculated via the following relations:

$$[\mathbf{T}'] = [\mathbf{R}]^T [\mathbf{T}] [\mathbf{R}],$$

$$[\mathbf{u}'] = [\mathbf{R}]^T [\mathbf{u}]$$

The above relations can be equivalently written in component form:

$$T'_{ij} = R_{ki} T_{kl} R_{lj},$$

$$u'_i = R_{ji} u_j$$

Finally, the matrix representation of the rotation tensor  $\mathbf{R}$  can be calculated by:

$$[\mathbf{R}] = \begin{bmatrix} \mathbf{e}_1 \cdot \mathbf{e}'_1 & \mathbf{e}_1 \cdot \mathbf{e}'_2 & \cdots & \mathbf{e}_1 \cdot \mathbf{e}'_n \\ \mathbf{e}_2 \cdot \mathbf{e}'_1 & \mathbf{e}_2 \cdot \mathbf{e}'_2 & \cdots & \mathbf{e}_2 \cdot \mathbf{e}'_n \\ \vdots & \vdots & \ddots & \vdots \\ \mathbf{e}_n \cdot \mathbf{e}'_1 & \mathbf{e}_n \cdot \mathbf{e}'_2 & \cdots & \mathbf{e}_n \cdot \mathbf{e}'_n \end{bmatrix}$$

or, in component form:



$$R_{ij} = \mathbf{e}_i \cdot \mathbf{e}_j$$

### 1.2.6. Spectral Decomposition – Principal Invariants

Let  $\mathbf{T}$  be a second-order tensor. A non-zero vector  $\mathbf{v}$ , is called an eigenvector of  $\mathbf{T}$  if there is a scalar say  $\lambda$  such that the following relation holds:

$$\mathbf{T}\mathbf{v} = \lambda\mathbf{v}$$

Then  $\lambda$  is called the *eigenvalue* of  $\mathbf{T}$  corresponding to the *eigenvector*  $\mathbf{v}$ . The previous relation defines a set of  $n$  homogeneous equations which has non-trivial solutions for  $\mathbf{v}$  if and only if:

$$\det(\mathbf{T} - \lambda\mathbf{I}) = 0.$$

This is called the characteristic equation for  $\mathbf{T}$  and can be also written in terms of Cartesian components as:

$$\det(T_{ij} - \lambda\delta_{ij}) = 0.$$

Let  $\mathbf{T}$  be a symmetric second-order tensor. Then  $\mathbf{T}$  can be represented as:

$$\mathbf{T} = \sum_{i=1}^n \lambda_i \mathbf{e}_i \otimes \mathbf{e}_i$$

where  $\{\mathbf{e}_i\}$  is an orthonormal basis for  $\mathcal{U}$  consisting exclusively of eigenvectors of  $\mathbf{T}$  and  $\lambda_i$  are the corresponding eigenvalues. The above is called the *spectral representation* or *spectral decomposition* of tensor  $\mathbf{T}$ .

Next we consider the case of the three dimensional space and study the characteristic equation of a tensor  $\mathbf{T}$ . In this case, the characteristic equation has the following representation:

$$\det(\mathbf{T} - \lambda\mathbf{I}) = -\lambda^3 + \lambda^2 I_1 - \lambda I_2 + I_3$$

Where  $I_1, I_2$  and  $I_3$  are three principal invariants of the tensor  $\mathbf{T}$  and are defined as follows:

$$I_1(\mathbf{T}) = \text{tr}\mathbf{T} = T_{ii}$$

$$I_2(\mathbf{T}) = \frac{1}{2}[(\text{tr}\mathbf{T})^2 - \text{tr}(\mathbf{T}^2)] = \frac{1}{2}(T_{ii}T_{jj} - T_{ij}T_{ji})$$

$$I_3(\mathbf{T}) = \det\mathbf{T} = \frac{1}{6}[(\text{tr}\mathbf{T})^3 - 3\text{tr}(\mathbf{T})\text{tr}(\mathbf{T}^2) + 2\text{tr}(\mathbf{T}^3)]$$

### 1.3. Higher-Order Tensors

Up to this point, we have studied operations and relations involving scalars that can be considered as *zero-order tensors*, vectors classed as *first-order tensors* and also *second-order tensors* which are linear operators on vectors. In continuum mechanics and especially in constitutive stress-strain relations, linear operators of higher order are employed. These operators are called *higher-order tensors*. Here we introduce some basic definitions and operations involving higher order tensor.

A very useful *third-order tensor* that is thoroughly used is the *alternating tensor*. It is a linear operator that maps vectors into skew symmetric tensors. It can be represented as:

$$\boldsymbol{\epsilon} = \epsilon_{ijk} \mathbf{e}_i \otimes \mathbf{e}_j \otimes \mathbf{e}_k$$

With components:

$$\epsilon_{ijk} = \begin{cases} +1 & \text{if } \{i, j, k\} \text{ is an even permutation of } \{1, 2, 3\} \\ -1 & \text{if } \{i, j, k\} \text{ is an odd permutation of } \{1, 2, 3\} \\ 0 & \text{if at least two indices coincide} \end{cases}$$

The tensor product of three vectors, is defined as the operator that satisfies:

$$(\mathbf{a} \otimes \mathbf{b} \otimes \mathbf{c}) \mathbf{d} = (\mathbf{c} \cdot \mathbf{d})(\mathbf{a} \otimes \mathbf{b}),$$

for arbitrary vectors  $\mathbf{a}, \mathbf{b}, \mathbf{c}, \mathbf{d}$ .

The multiplication of the alternating tensor by a vector  $\mathbf{v}$  yields the skew-symmetric second-order tensor also written in component form:

$$\boldsymbol{\epsilon} \mathbf{v} = \epsilon_{ijk} v_k \mathbf{e}_i \otimes \mathbf{e}_j$$

#### 1.3.1. Fourth-Order Tensors and Symmetry

A general *fourth-order tensor*  $\mathbf{T}$ , is a linear transformation that maps second-order tensors into second-order tensors. It also maps vectors into third-order tensors and third-order tensors into vectors. It can be represented as:

$$\mathbf{T} = T_{ijkl} \mathbf{e}_i \otimes \mathbf{e}_j \otimes \mathbf{e}_k \otimes \mathbf{e}_l$$

where the tensor product between four vectors  $\mathbf{a}, \mathbf{b}, \mathbf{c}, \mathbf{d}$  satisfies:

$$(\mathbf{a} \otimes \mathbf{b} \otimes \mathbf{c} \otimes \mathbf{d}) \mathbf{e} = (\mathbf{e} \cdot \mathbf{d})(\mathbf{a} \otimes \mathbf{b} \otimes \mathbf{c})$$

Any fourth-order tensor  $\mathbf{T}$  which satisfies the following:

$$\mathbf{S} : \mathbf{T} : \mathbf{U} = (\mathbf{T} : \mathbf{S}) : \mathbf{U}$$

for any second-order tensors  $\mathbf{S}$  and  $\mathbf{U}$  is called *symmetric*. In component form, the major symmetries are satisfied:

$$T_{ijkl} = T_{klij}$$

Other symmetries are also possible when considering fourth-order tensors. If symmetry occurs in the last two indices:

$$T_{ijkl} = T_{ijlk}$$

Then the following relation holds for any second-order tensor :

$$\mathbf{T}:\mathbf{S} = \mathbf{T}:\mathbf{S}^T \quad \text{and} \quad \mathbf{S}:\mathbf{T} = (\mathbf{S}:\mathbf{T})^T$$

while symmetry in the first two indices i.e. :

$$T_{ijkl} = T_{jikl}$$

implies:

$$\mathbf{T}:\mathbf{S} = (\mathbf{T}:\mathbf{S})^T \quad \text{and} \quad \mathbf{S}:\mathbf{T} = \mathbf{S}^T:\mathbf{T}$$

### 1.3.2. Change of Basis for Fourth-Order Tensors

As in the case of second-order tensors, if we consider the two Cartesian orthonormal bases  $\{\mathbf{e}_i\}$  and  $\{\mathbf{e}'_i\}$  of  $\mathcal{U}$  which are related via a proper orthogonal tensor  $\mathbf{R}$  (a rotation) by:

$$\mathbf{e}'_i = \mathbf{R}\mathbf{e}_i, \quad \text{for } i = 1, 2, \dots, n$$

Then, the components of a fourth-order tensor  $\mathbf{T}$  relative to the basis  $\{\mathbf{e}'_i\}$  are given by:

$$T_{ijkl} = R_{mi}R_{nj}R_{pk}R_{ql}T_{mnpq}$$

Where  $T_{mnpq}$  are the components of  $\mathbf{T}$  relative to the first basis  $\{\mathbf{e}_i\}$ .

### 1.4. Isotropic Tensors

A tensor is said to be *isotropic*, if its components remain unchanged under any arbitrary transformation of Cartesian basis (subject to right-handedness being maintained).

A second-order tensor  $\mathbf{T}$  if the matrix of its components relative to a Cartesian basis, remain unchanged under any rotation  $\mathbf{R}$ :

$$[\mathbf{T}] = [\mathbf{R}][\mathbf{T}][\mathbf{R}]^T$$

The only isotropic second-order tensors, are scalar multiples of the identity second-order tensor  $\mathbf{I}$  and are called *spherical* tensors:

$$\alpha \mathbf{I}$$

As in the case of second-order tensors a fourth-order tensor  $\mathbf{T}$  if its components remain unchanged under any rotation:

$$T_{ijkl} = R_{mi}R_{nj}R_{pk}R_{ql}T_{mnpq}.$$

Any isotropic fourth-order tensor can be represented as a linear combination of three basic isotropic fourth order tensors:

$$\mathbf{U} = \alpha \mathbf{I} + \beta \mathbf{I}_T + \gamma (\mathbf{I} \otimes \mathbf{I})$$

where  $\alpha, \beta, \gamma$  are scalars and the fourth order tensors included above are special fourth-order tensors and are explained in the following.

The tensor  $\mathbf{I}$  is called the *fourth-order identity*, and its components are given by:

$$I_{ijkl} = \delta_{ik}\delta_{jl}.$$

For any fourth-order tensor  $\mathbf{T}$ , the following relation involving the fourth-order identity holds:

$$\mathbf{I} : \mathbf{T} = \mathbf{T} : \mathbf{I} = \mathbf{T}.$$

Whereas for any second-order tensor :

$$\mathbf{I} : \mathbf{T} = \mathbf{T} : \mathbf{I} = \mathbf{T}.$$

The tensor  $\mathbf{I}_T$  is the *transposition* vector. It is a fourth-order tensor which through contraction, it maps any second-order tensor  $\mathbf{S}$  to its transpose:

$$\mathbf{I}_T : \mathbf{S} = \mathbf{S} : \mathbf{I}_T = \mathbf{S}^T$$

and its components are given by:

$$(\mathbf{I}_T)_{ijkl} = \delta_{il}\delta_{jk}.$$

Finally the tensor  $\mathbf{I} \otimes \mathbf{I}$  is a fourth-order tensors which when multiplied with any second order tensor  $\mathbf{T}$  gives:

$$(\mathbf{I} \otimes \mathbf{I}) : \mathbf{T} = (tr \mathbf{T}) \mathbf{I}$$

and has components:

$$(\mathbf{I} \otimes \mathbf{I})_{ijkl} = \delta_{ij}\delta_{kl}.$$

Another very important identity that is going to be used in subsequent chapters is the tensor defined as:

$$\mathbf{I}_S = \frac{1}{2} (\mathbf{I} + \mathbf{I}_T).$$

It is referred as the *symmetric projection* or *symmetric identity* tensor. It is a fourth-order tensor that maps any second-order tensor  $\mathbf{T}$  into its symmetric part:

$$\mathbf{I}_S : \mathbf{T} = \mathbf{T} : \mathbf{I}_S = \text{sym}(\mathbf{T}).$$

It is obvious that for any symmetric second-order tensor  $\mathbf{S}$ , this tensor maps  $\mathbf{S}$  to itself:

$$\mathbf{I}_S : \mathbf{S} = \mathbf{S}.$$

Its components can be retrieved by the following expression:

$$(\mathbf{I}_S)_{ijkl} = \frac{1}{2}(\delta_{ik}\delta_{jl} + \delta_{il}\delta_{jk}).$$

## ***Chapter 2: Theory of Rate-Independent Plasticity – Classical Yield Criteria***

### **The Mathematical Theory of Plasticity**

The term *inelasticity*, is used to describe any constitutive behaviour other than elastic. Generally, the inelastic behaviour includes viscoelastic, viscoplastic and elastoplastic behaviour.

Throughout this thesis, only the elastoplastic behaviour is studied. In particular the theory of plasticity is concerned with solids which when subjected to a loading program, may sustain permanent deformations when completely unloaded. The assumption that these permanent (plastic) deformations do not depend on the rate of the application of loads, leads to the theory of *rate-independent plasticity*. The materials that can be adequately described by this theory are called *plastic* or *rate-independent plastic*.

The adjective “plastic” comes from the Greek work “πλάσσειν”, meaning “to shape”. A large number of engineering materials such as metals, soils, rocks can be modeled as plastic in a wide range of applications. This is true despite the materials’ different nature and constitution.

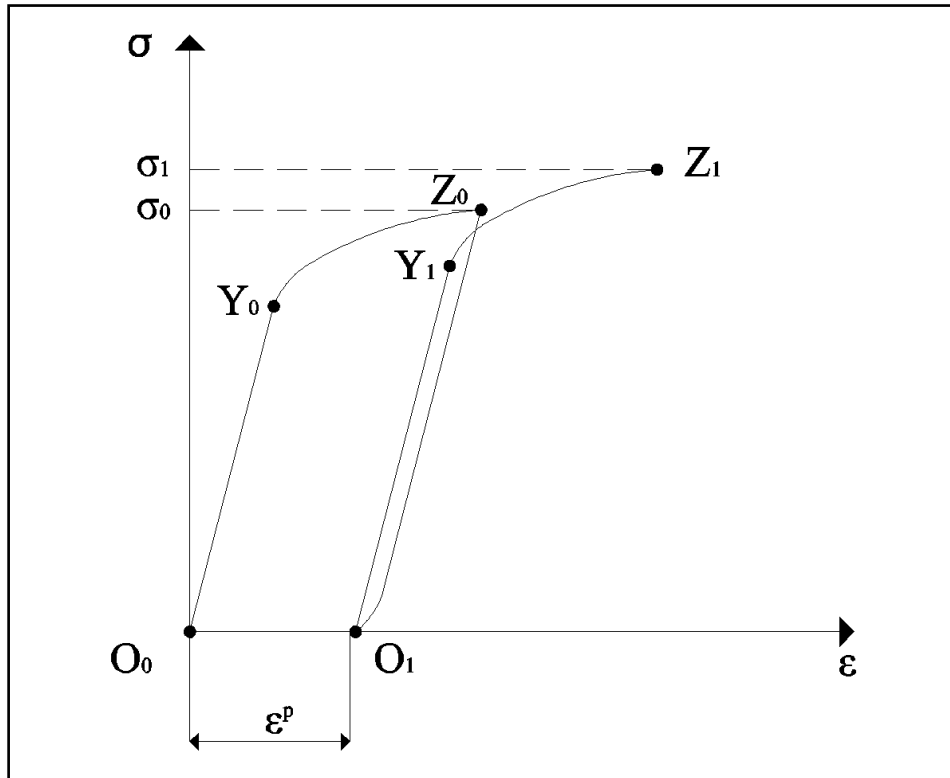
In this chapter, the mathematical theory of rate-independent plasticity is introduced. Plasticity theory is a very large topic and clearly cannot be covered in a single chapter of a master thesis. Thus, this brief review is restricted to infinitesimal deformations and aims to provide a solid basis for the numerical simulation of elastoplastic solids.

### **2.1. Phenomenological Aspects**

As already mentioned, in spite of their qualitatively distinct mechanical characteristics, materials as contrasting as metals and soils share some common features of their phenomenological behaviour that make them amenable to modeling by means of the theory of plasticity. To illustrate all those common features, we begin by discussing a uniaxial tension experiment of a metallic bar. The uniaxial tension test although it may appear simple, it introduces some very important aspects of the plasticity theory.

“Of all mechanical tests for structural materials, the tension test is the most common. This is true primarily because it is a relatively rapid test and requires simple apparatus. It is not as simple to interpret the data it gives, however, as might appear at first sight.” J.J Gilman [1969].

The immediate result of a tension test is a relation between the axial force and either the change in length (elongation) of a gage portion of the specimen or a representative value of longitudinal strain as measured by one or more strain gages. This relation is usually changed to one between the stress (force  $F$  divided by cross-sectional area) and the strain (elongation divided by gage length or strain-gage output) and is plotted as the stress-strain diagram. Uniaxial tension tests of ductile metals, produce stress-strain curves of the type illustrated in the following figure.



Uniaxial tension experiment of a ductile metal.

The metallic bar, is subjected to the following loading program. Firstly, it is loaded monotonically from zero to a prescribed load value  $\sigma_0$ . The bar is then unloaded to unstressed state and it is subsequently loaded up to stress  $\sigma_1$ . The stress-strain curve follows the path  $O_0Y_0Z_0O_1Y_1Z_1$  easily identified in the above figure.

The initial line segment  $O_0Y_0$  is virtually straight and any unloading of the bar at this stage would follow the same straight path and would lead to stress point  $O_0$ . Thus, in this segment the behaviour of the material is regarded as *linear elastic*. By increasing the stress beyond  $Y_0$  (in this case up to point  $Z_0$ ) the slope of the stress-strain curve decreases dramatically. An unloading of the bar to an unstressed state, follows the path  $Z_0O_1$ . The difference from the unstressed state  $O_0$  is the permanent change in the shape of the bar. This permanent shape change is represented in the graph by the permanent axial plastic strain  $\epsilon^p$ . Similarly to the loading path  $O_0Y_0$ , monotonic reloading of the bar to a stress level  $Y_1$  will now follow the path  $O_1Y_1Z_1$ . The portion  $O_1Y_1$  of this path is virtually straight, and similarly to  $O_0Y_0$  linear elastic. Any unloading of the bar before reaching point  $Y_1$  will follow the same straight path and lead to point  $O_1$  without further increase of plastic strain. Again loading beyond the *elastic limit*  $Y_1$  will cause further increase in plastic axial strain.

The important phenomenological properties identified in the above uniaxial test are enumerated below:

1. The existence of an *elastic domain*, i.e. a range of stresses within which the behaviour of the material can be considered as purely elastic. No evolution of permanent

deformation (axial strain in this case) is possible when the material is subjected to stresses lying within the elastic domain. This domain is delimited by the so-called *yield stress* which in the uniaxial experiment, correspond to points  $Y_0$  and  $Y_1$  for segments  $O_0Y_0$  and  $O_1Y_1$  respectively.

2. If the material is further loaded at the yield stress, then *plastic yielding* also denoted as *plastic flow* takes place which leads to evolution of plastic strains.
3. The evolution of plastic strain during plastic flow is accompanied by the evolution of the yield stress as well. This phenomenon known as *hardening*, can be identified by the different yield stresses corresponding to points  $Y_0$  and  $Y_1$  of the stress-strain curve.

It is emphasized that the properties identified above, can be observed not only in metals but also in a wide variety of materials such as concrete, rocks, soils and many others. The underlying mechanisms that give rise to these phenomenological characteristics can be completely distinct and different for each type of material. It is also crucial to understand that materials such as soils need other experimental procedures in order to verify their distinct properties. A typical example is the *triaxial shear test* which is widely used when dealing with materials such as soils which typically cannot resist tensile stresses.

The object of plasticity theory is to provide continuum constitutive models capable of describe this kind of phenomenological behaviour for a variety of different materials that possess the characteristics described and identified in the uniaxial tension test.

## 2.2. One-dimensional Constitutive Model

A simple mathematical model of the uniaxial tension experiment studied in the previous section is formulated in what follows. As mentioned previously, the uniaxial experiment, despite its simplicity, contains all the essential features that form the basis of the mathematical theory of plasticity.

The uniaxial stress-strain curve illustrated in the previous section is approximated by an idealized version shown in a following figure. The assumptions involved in the approximation, are summarized as follows:

1. The difference between unloading and reloading curves (segments  $Z_0O_1$  and  $O_1Y_1$  respectively in the stress-strain curve of the uniaxial experiment) is ignored and points  $Z_0$  and  $Y_1$ , which correspond to the beginning of unloading and the beginning of the plastic yielding of subsequent reloading coincide.
2. The transition between the elastic region and the elastoplastic region is now clearly marked by a non-smooth change of slope (points  $Y_0$  and  $Y_1$ ).

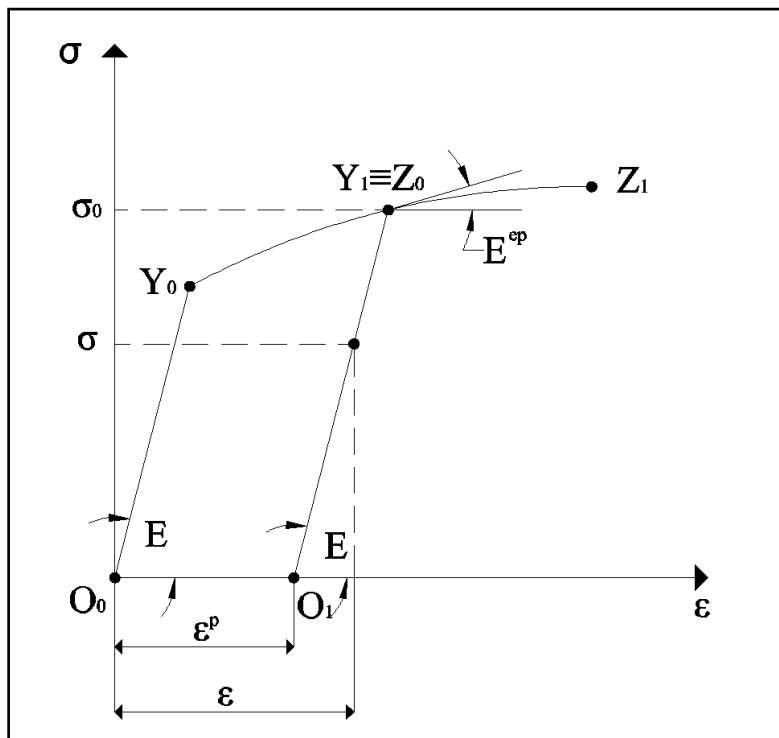


3. During plastic yielding, the stress-strain curve always follows the path  $O_0Y_0Y_1Z_1$  which is referred as the virgin curve and is obtained when the material is subjected to a continuous monotonic loading from the initial unstressed state  $O_0$ .

Under the assumptions enumerated above, after being monotonically loaded from the initial unstressed state to stress level  $\sigma_0$ , the behaviour of the metallic bar, between  $O_1$  and  $Y_1$  is considered to be linear elastic with constant plastic strain  $\varepsilon^p$  and yield limit  $\sigma_0$ . The uniaxial stress corresponding to a configuration between  $O_1$  and  $Y_1$  with *total* strain  $\varepsilon$  is given by:

$$\sigma = E(\varepsilon - \varepsilon^p)$$

Where  $E$  denotes the Young's modulus of the material. One very important aspect is that the difference between the total strain and the plastic strain which appears at the right hand of the above expression is fully *reversible*. This motivates the additive decomposition of the axial strain described in the following section. The idealized mathematical model discussed is illustrated in the following figure.



Uniaxial tension experiment. Mathematical model.

### 2.2.1. Elastoplastic Decomposition of the Axial Strain

One of the chief hypotheses underlying the small strain theory of plasticity is the decomposition of the *total strain*  $\varepsilon$ , into the sum of a fully reversible *elastic* component  $\varepsilon^e$  and a *plastic* permanent component  $\varepsilon^p$ . Mathematically, the additive decomposition of the total strain is expressed in the following relation:

$$\varepsilon = \varepsilon^e + \varepsilon^p$$

where the elastic component  $\varepsilon^e$  is defined as:

$$\varepsilon^e = \varepsilon - \varepsilon^p .$$

### 2.2.2. The Elastic Uniaxial Constitutive Law

The definition of the elastic axial strain was given above. The constitutive law which relates the elastic axial strain with the axial stress can be expressed as:

$$\sigma = E\varepsilon^e .$$

The next step in the definition of the axial constitutive law is to derive formulae that express mathematically the three phenomenological aspects which were enumerated for the one-dimensional constitutive model. A *yield criterion* as well as a *plastic flow rule* must be formulated, combined with a *hardening law* which describes the evolution of the yield limit.

### 2.2.3. The Yield Function and the Yield Criterion

The existence of an elastic domain delimited by a yield stress has been mentioned when studying uniaxial stress-strain curve. Mathematically, by introducing a yield function  $\Phi$ , of the form:

$$\Phi(\sigma, \sigma_y) = |\sigma| - \sigma_y$$

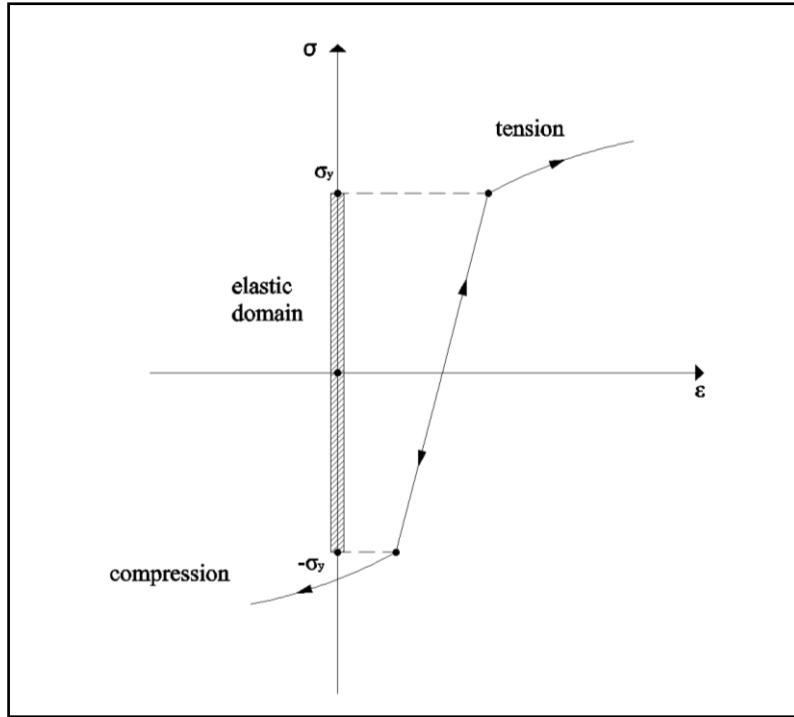
the *elastic domain* at a state with uniaxial yield stress  $\sigma_y$  can be defined in the one-dimensional plasticity model as the set of stresses satisfying:

$$\mathcal{E} = \{\sigma | \Phi(\sigma, \sigma_y) < 0\}$$

or equivalently by using the definition of the yield function as the set of stresses that satisfy:

$$|\sigma| - \sigma_y < 0$$

Generalizing the results of the uniaxial stress, it has been assumed that the yield stress in compression is identical to that in tension. The following figure, illustrates the idealized elastic domain.



Idealized elastic domain for the uniaxial model.

It should be noted that, at any stage, no stress level is allowed to exceed the current yield stress. The so-called *plastically admissible stresses* lie either within the elastic domain or on its boundary (the yield limit). In yield function terms, any plastically admissible stress must satisfy:

$$\Phi(\sigma, \sigma_y) \leq 0$$

For stresses within the elastic domain, only elastic straining may occur whereas on its boundary, either *plastic yielding* (plastic loading) or *elastic unloading* takes place. This yield criterion can be expressed in terms of yield function and plastic strain rate (denoted by a dot above the strain symbol):

$$\text{If } \Phi(\sigma, \sigma_y) < 0 \Rightarrow \dot{\epsilon}^p = 0,$$

$$\text{If } \Phi(\sigma, \sigma_y) = 0 \Rightarrow \begin{cases} \dot{\epsilon}^p = 0 & \text{for elastic unloading} \\ \dot{\epsilon}^p \neq 0 & \text{for plastic loading} \end{cases}$$

#### 2.2.4. The Plastic Flow Rule. Loading/Unloading Conditions

The above expressions define a criterion for plastic yielding. Upon plastic loading, the plastic strain rate is positive under tension and negative under compression. Thus the plastic flow rule can be mathematically established as:

$$\dot{\epsilon}^p = \dot{\gamma} \text{sign}(\sigma)$$

where sign is the *signum* function defined as:

$$\text{sign}(\alpha) \Rightarrow \begin{cases} +1 & , & \text{if } \alpha \geq 0 \\ -1 & , & \text{if } \alpha < 0 \end{cases}$$

for any scalar  $\alpha$  and the other scalar  $\dot{\gamma}$  is the *plastic multiplier*. The plastic multiplier is non-negative:

$$\dot{\gamma} \geq 0$$

and satisfies the *complementarity condition*:

$$\Phi \dot{\gamma} = 0 .$$

All the above constitutive equations imply that the plastic strain rate vanishes within the elastic domain:

$$\Phi < 0 \Rightarrow \dot{\gamma} = 0 \Rightarrow \dot{\varepsilon}^p = 0$$

and plastic flow occurs only when the stress level coincides with the elastic domain boundary i.e. the current yield stress:

$$|\sigma| = \sigma_y \Rightarrow \Phi = 0 \Rightarrow \dot{\gamma} \geq 0$$

Summarizing, the set of the following constraints, define the so-called *loading/unloading conditions* of the elastoplastic model and establish when plastic flow may occur:

$$\Phi \leq 0, \quad \dot{\gamma} \geq 0, \quad \dot{\gamma} \Phi = 0 .$$

### 2.2.5. The Hardening Law

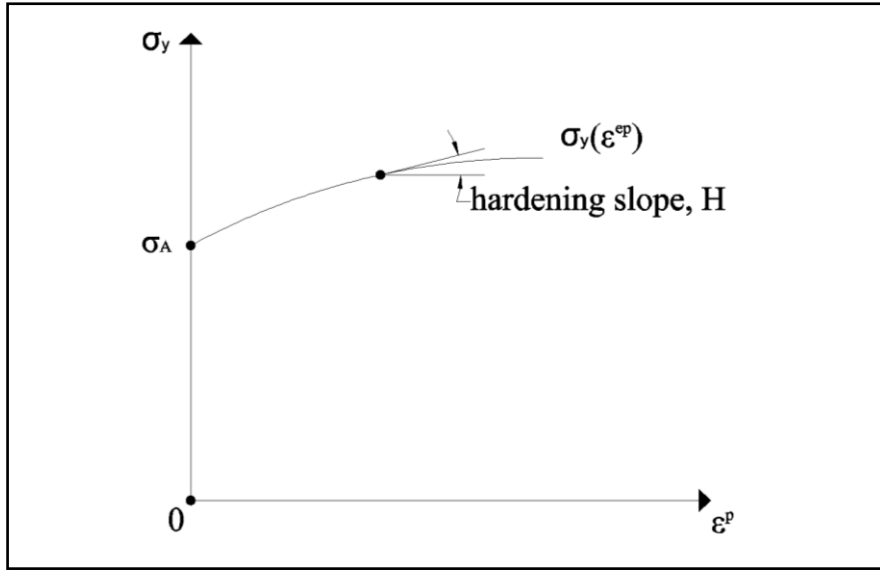
In order to completely characterize the uniaxial model, an additional component must be introduced. By observing the uniaxial experiment, an evolution of the yield stress during plastic yielding can be easily identified. This phenomenon is known as *hardening*. The corresponding *hardening law* describes the relation between the evolution of the yield stress and the accompanying plastic strain. The hardening phenomenon can be easily incorporated to the uniaxial model by assuming that the yield stress is a given function:

$$\sigma_y = \sigma_y(\bar{\varepsilon}^p)$$

Where  $\bar{\varepsilon}^p$  is the *accumulated plastic strain*. It is defined as:

$$\bar{\varepsilon}^p = \int_0^t |\dot{\varepsilon}^p| dt$$

The absolute value, ensure that both tensile and compressive plastic strains contribute to the accumulated plastic strain. The curve defined by the hardening function introduced above is usually referred as the *hardening curve* and it's illustrated in the following figure.



Hardening Curve for the uniaxial model

From the definition of the accumulated plastic strain  $\bar{\epsilon}^p$ , it follows that its evolution law is given by:

$$\dot{\bar{\epsilon}}^p = |\dot{\epsilon}^p|$$

which can be expressed in terms of the plastic multiplier  $\dot{\gamma}$  as:

$$\dot{\bar{\epsilon}}^p = \dot{\gamma}.$$

### 2.2.6. Determination of the Plastic Multiplier

So far, all the essential components of the uniaxial plasticity have been described. Nevertheless, the value of the plastic multiplier  $\dot{\gamma}$  which is assumed to be non-negative during plastic yielding is left undetermined. In the following, this indetermination will be eliminated by making use of the relations and conditions of the uniaxial plasticity model.

First of all, during plastic yielding the value of the yield function remains constant and equal to zero:

$$\Phi = 0$$

Also the additional complementarity condition is satisfied:

$$\Phi \dot{\gamma} = 0$$

which implies that during plastic yielding the rate of change of the yield function becomes zero since the plastic multiplier is strictly positive:

$$\dot{\Phi} = 0$$

while the rate  $\dot{\Phi}$  can take any value during elastic straining. The above condition, is called the *consistency condition*. Now, by taking the time derivative of the yield function, we obtain the following relation:

$$\dot{\Phi}(\sigma, \sigma_y) = |\dot{\sigma}| - \dot{\sigma}_y = \text{sign}(\sigma)\dot{\sigma} - H\dot{\varepsilon}^p$$

where  $H$  is the *hardening modulus* or *hardening slope*. The hardening modulus is tangent to the hardening curve and is defined as:

$$H = \frac{d\sigma_y}{d\varepsilon^p}$$

As mentioned earlier, during plastic yielding, the rate of the yield function vanishes, so:

$$\text{sign}(\sigma)\dot{\sigma} = H\dot{\varepsilon}^p$$

From the elastic law and the decomposition of the strain, it follows:

$$\dot{\sigma} = E(\dot{\varepsilon} - \dot{\varepsilon}^p)$$

Finally, by combining the two previous relations, the plastic multiplier can be uniquely determined:

$$\dot{\gamma} = \frac{E}{E + H} \text{sign}(\sigma)\dot{\varepsilon} = \frac{E}{E + H} |\dot{\varepsilon}|$$

### 2.2.7. The Elastoplastic Tangent Modulus

The final crucial component of the uniaxial model is the tangent relation between strain and stress during plastic flow at a generic yield limit. This relation, can be established by making use of the *elastoplastic tangent modulus*  $E^{ep}$  as follows:

$$\dot{\sigma} = E^{ep}\dot{\varepsilon}$$

The elastoplastic tangent modulus can be calculated by the following relation which is obtained by combining the flow rule, the above relation and the elastic law:

$$E^{ep} = \frac{EH}{E + H}$$

The hardening modulus can be expressed by the above relation as:

$$H = \frac{E^{ep}}{1 - E^{ep}/E}$$

## 2.3. General Elastoplastic Constitutive Model

In the previous section the mathematical model of a uniaxial experiment with a ductile metal has been presented and analyzed. This model contains all the essential components needed to describe a general elastoplastic constitutive model. In this section, the generalization of the concepts of the theory of plasticity will be described for two- and three-dimensional cases.

### 2.3.1. Additive Decomposition of the Strain Tensor

In the uniaxial case we have seen that axial strain can be decomposed into two parts i.e the elastic and the plastic components. This holds for the multidimensional case as well but now the corresponding decomposition is obtained by splitting the strain tensor  $\boldsymbol{\varepsilon}$  into the sum of an elastic component  $\boldsymbol{\varepsilon}^e$  and a plastic component  $\boldsymbol{\varepsilon}^p$ . That is:

$$\boldsymbol{\varepsilon} = \boldsymbol{\varepsilon}^e + \boldsymbol{\varepsilon}^p$$

The above tensors are known as the *elastic strain tensor* and the *plastic strain tensor* respectively and the above relation can be written in rate form:

$$\dot{\boldsymbol{\varepsilon}} = \dot{\boldsymbol{\varepsilon}}^e + \dot{\boldsymbol{\varepsilon}}^p$$

### 2.3.2. The Free Energy Potential and the Elastic Law

The starting assumption for the plasticity theory treated in this thesis, is that the *free energy*,  $\psi$ , is a function:

$$\psi(\boldsymbol{\varepsilon}, \boldsymbol{\varepsilon}^p, \boldsymbol{\alpha})$$

of the total strain tensor, the plastic strain tensor which is considered as an internal variable and a set  $\boldsymbol{\alpha}$  of internal variables, associated with the phenomenon of hardening. By taking into account the additive decomposition of the strain tensor, the free energy can be split as:

$$\begin{aligned} \psi(\boldsymbol{\varepsilon}, \boldsymbol{\varepsilon}^p, \boldsymbol{\alpha}) &= \psi^e(\boldsymbol{\varepsilon} - \boldsymbol{\varepsilon}^p) + \psi^p(\boldsymbol{\alpha}) \\ &= \psi^e(\boldsymbol{\varepsilon}^e) + \psi^p(\boldsymbol{\alpha}) \end{aligned}$$

which is the sum of an elastic contribution,  $\psi^e$ , which depends only on the elastic strain and a contribution due to hardening,  $\psi^p$ .

Now the Clausius-Duhem inequality reads:

$$\left( \boldsymbol{\sigma} - \bar{\rho} \frac{\partial \psi^e}{\partial \boldsymbol{\varepsilon}^e} \right) : \dot{\boldsymbol{\varepsilon}}^e + \boldsymbol{\sigma} : \dot{\boldsymbol{\varepsilon}}^p - \mathbf{A} * \dot{\boldsymbol{\alpha}} \geq 0$$

where

$$\mathbf{A} \equiv \bar{\rho} \frac{\partial \psi^p}{\partial \boldsymbol{\alpha}}$$

is the *hardening thermodynamical force* and the symbol  $*$  indicates the appropriate product between  $\mathbf{A}$  and  $\dot{\boldsymbol{\alpha}}$ . The above inequality implies a general elastic law of the form:

$$\boldsymbol{\sigma} = \bar{\rho} \frac{\partial \psi^e}{\partial \boldsymbol{\varepsilon}^e}$$

so the requirements for non-negative dissipation can be reduced to:

$$\Upsilon^p(\boldsymbol{\sigma}, \mathbf{A}; \dot{\boldsymbol{\varepsilon}}^p, \dot{\boldsymbol{\alpha}}) \geq 0$$

where  $\Upsilon^p$  is called *the plastic dissipation function* and it is defined by:

$$\Upsilon^p(\boldsymbol{\sigma}, \mathbf{A}; \dot{\boldsymbol{\varepsilon}}^p, \dot{\boldsymbol{\alpha}}) \equiv \boldsymbol{\sigma} : \dot{\boldsymbol{\varepsilon}}^p - \mathbf{A} * \dot{\boldsymbol{\alpha}}.$$

In this thesis, the elastic behaviour of the materials treated is assumed to be *linear* and *isotropic*. In this case, the elastic contribution to the free energy is given by the following relation:

$$\begin{aligned} \bar{\rho} \psi^e(\boldsymbol{\varepsilon}^e) &= \frac{1}{2} \boldsymbol{\varepsilon}^e : \mathbf{D}^e : \boldsymbol{\varepsilon}^e \\ &= G \boldsymbol{\varepsilon}_d^e : \boldsymbol{\varepsilon}_d^e + \frac{1}{2} K (\varepsilon_v^e)^2 \end{aligned}$$

As a result, the elastic law between the elastic strain tensor and the corresponding stress tensor can be described via the following relation:

$$\begin{aligned} \boldsymbol{\sigma} &= \mathbf{D}^e : \boldsymbol{\varepsilon}^e \\ &= 2G \boldsymbol{\varepsilon}_d^e + K \varepsilon_v^e \mathbf{I} \end{aligned}$$

where  $G$  and  $K$  are the shear and bulk moduli. The tensor  $\boldsymbol{\varepsilon}_d^e$  is the deviatoric component of the elastic strain tensor and the scalar  $\varepsilon_v^e = tr(\boldsymbol{\varepsilon}^e)$  is the volumetric elastic strain. Finally  $\mathbf{D}^e$  is the standard fourth-order isotropic elasticity tensor which has the general format:

$$\mathbf{D}^e = 2G \mathbf{I}_S + A \left( K - \frac{2}{3} G \right) \mathbf{I} \otimes \mathbf{I}$$

where  $A = 1$  for three-dimensional, plane strain and axisymmetric analyses, whereas in plane stress:

$$A = \frac{2G}{K + \frac{4}{3}G}.$$



### 2.3.3. Yield Criterion and Yield Surface

In the uniaxial yield criterion discussed previously in this section, it is clear that plastic flow may occur when the uniaxial stress reaches a critical value, the uniaxial yield stress. This principle was expressed by the use of a yield function whose value is negative when the stress lies in the elastic region and becomes zero during plastic flow. This concept of yield function can be extended for two and three-dimensional cases. The scalar yield function  $\Phi$  is now a function of the stress tensor  $\boldsymbol{\sigma}$  and a set  $\mathbf{A}$  of hardening thermodynamical forces. Analogously to the uniaxial case the *elastic domain* is defined as the set satisfying:

$$\mathcal{E} = \{\boldsymbol{\sigma} | \Phi(\boldsymbol{\sigma}, \mathbf{A}) < 0\}$$

Plastic yielding is impossible when the stress tensor of the material is in the elastic domain. Again, the set of plastically admissible stresses is a set that includes the stresses lying in the elastic domain or on its boundary:

$$\bar{\mathcal{E}} = \{\boldsymbol{\sigma} | \Phi(\boldsymbol{\sigma}, \mathbf{A}) \leq 0\}.$$

The set of stresses which is termed as *yield locus* and for which plastic flow may occur is the boundary of the elastic domain, where the value of the yield function  $\Phi$  becomes zero. This yield locus can be represented by a hypersurface in the space of stresses which is known as *yield surface*. The graphical representation of the yield surface is possible only in the principal stress space.

### 2.3.4. Plastic Flow Rule and Hardening Law

The next step for a characterization of a plasticity model requires the definition of the evolution laws for the internal variables which are associated with the dissipative phenomena. In this case, the internal variables consist of the plastic strain tensor and the set  $\boldsymbol{\alpha}$  of hardening variables. The following plastic flow rule and hardening law are then postulated:

$$\dot{\boldsymbol{\epsilon}}^p = \dot{\gamma} \mathbf{N},$$

$$\dot{\boldsymbol{\alpha}} = \dot{\gamma} \mathbf{H}$$

where the tensor:

$$\mathbf{N} = \mathbf{N}(\boldsymbol{\sigma}, \mathbf{A})$$

is termed the *flow vector* in plasticity and the function:

$$\mathbf{H} = \mathbf{H}(\boldsymbol{\sigma}, \mathbf{A})$$

is the *generalized hardening modulus* which is the generalization of the hardening modulus defined in the uniaxial case. It defines the evolution of the hardening variables.

Finally, the *loading/unloading conditions* defined for the uniaxial model hold in the general case as well:

$$\Phi \leq 0, \quad \dot{\gamma} \geq 0, \quad \dot{\gamma}\Phi = 0$$

and define when evolution of plastic strains and internal variables may occur.

### 2.3.5. Flow Rules Defined from a Flow Potential

In multidimensional plasticity models, it is convenient to define the flow rule in terms of a *flow potential* (the term *plastic potential* is also used). This approach begins by postulating a flow potential with general form:

$$\Psi = \Psi(\boldsymbol{\sigma}, \mathbf{A})$$

from which the flow vector  $\mathbf{N}$  can be obtained by differentiation by:

$$\mathbf{N} \equiv \frac{\partial \Psi}{\partial \boldsymbol{\sigma}}$$

If the hardening rule is assumed to be derived from the same potential, then we have in addition:

$$\mathbf{H} \equiv -\frac{\partial \Psi}{\partial \mathbf{A}}$$

The plastic potential, is required to be a non-negative convex function of both  $\boldsymbol{\sigma}$  and  $\mathbf{A}$  which is zero-valued at the origin:

$$\Psi(\mathbf{0}, \mathbf{0}) = 0$$

In many plasticity models, the yield function can be used itself as a flow potential:

$$\Psi \equiv \Phi$$

Such models are called *associative* or *associated* plasticity models. When this is not the case the models are called *non-associative*. In this thesis, only associative plasticity models are studied.

### 2.3.6. The Plastic Multiplier

As in the uniaxial case the procedure for determination of the plastic multiplier  $\dot{\gamma}$  begins by taking into consideration the complementarity condition:

$$\dot{\Phi}\dot{\gamma} = 0$$

which implies the consistency condition:

$$\dot{\Phi} = 0$$

during plastic yielding. By differentiating the yield function with respect to time, the following expression can be obtained:

$$\dot{\Phi} = \frac{\partial \Phi}{\partial \boldsymbol{\sigma}} : \dot{\boldsymbol{\sigma}} + \frac{\partial \Phi}{\partial \mathbf{A}} * \dot{\mathbf{A}}$$

Now by taking into account the additive decomposition of the strain tensor, the elastic law and the flow rule, we substitute into the above expression and we obtain:

$$\dot{\boldsymbol{\sigma}} = \mathbf{D}^e : (\dot{\boldsymbol{\varepsilon}}^e - \dot{\boldsymbol{\varepsilon}}^p) = \mathbf{D}^e : (\dot{\boldsymbol{\varepsilon}} - \dot{\gamma} \mathbf{N})$$

By using the definition of the hardening thermodynamical force  $\mathbf{A}$  in terms of the free energy potential which was derived in an earlier section and also by taking into consideration the evolution law:

$$\dot{\boldsymbol{\alpha}} = \dot{\gamma} \mathbf{H}$$

the rate of the yield function can be written in the form:

$$\begin{aligned} \dot{\Phi} &= \frac{\partial \Phi}{\partial \boldsymbol{\sigma}} : \mathbf{D}^e : (\dot{\boldsymbol{\varepsilon}}^e - \dot{\boldsymbol{\varepsilon}}^p) + \frac{\partial \Phi}{\partial \mathbf{A}} * \bar{\rho} \frac{\partial^2 \psi^p}{\partial \boldsymbol{\alpha}^2} * \dot{\boldsymbol{\alpha}} \\ &= \frac{\partial \Phi}{\partial \boldsymbol{\sigma}} : \mathbf{D}^e : (\dot{\boldsymbol{\varepsilon}} - \dot{\gamma} \mathbf{N}) + \dot{\gamma} \frac{\partial \Phi}{\partial \mathbf{A}} * \bar{\rho} \frac{\partial^2 \psi^p}{\partial \boldsymbol{\alpha}^2} * \mathbf{H} \end{aligned}$$

From the above and the consistency conditions which says that the rate of the yield function during plastic yielding becomes zero, the plastic multiplier  $\dot{\gamma}$  can be obtained by the following formula:

$$\dot{\gamma} = \frac{\frac{\partial \Phi}{\partial \boldsymbol{\sigma}} : \mathbf{D}^e : (\dot{\boldsymbol{\varepsilon}})}{\frac{\partial \Phi}{\partial \boldsymbol{\sigma}} : \mathbf{D}^e : \mathbf{N} - \frac{\partial \Phi}{\partial \mathbf{A}} * \bar{\rho} \frac{\partial^2 \psi^p}{\partial \boldsymbol{\alpha}^2} * \mathbf{H}}$$

### 2.3.7. Rate Form and the Elastoplastic Tangent Operator

In the elastic region, the rate constitutive equation reads:

$$\dot{\boldsymbol{\sigma}} = \mathbf{D}^e : \dot{\boldsymbol{\varepsilon}}$$

while during plastic flow the corresponding equation reads:

$$\dot{\boldsymbol{\sigma}} = \mathbf{D}^{ep} : \dot{\boldsymbol{\varepsilon}}$$

where  $\mathbf{D}^{ep}$  is the *elastoplastic tangent modulus* given by:

$$\mathbf{D}^{ep} = \mathbf{D}^e - \frac{(\mathbf{D}^e : \mathbf{N}) \otimes \left( \mathbf{D}^e : \frac{\partial \Phi}{\partial \boldsymbol{\sigma}} \right)}{\frac{\partial \Phi}{\partial \boldsymbol{\sigma}} : \mathbf{D}^e : \mathbf{N} - \frac{\partial \Phi}{\partial \mathbf{A}} * \bar{\rho} \frac{\partial^2 \psi^p}{\partial \boldsymbol{\alpha}^2} * \mathbf{H}}$$

The elastoplastic tangent modulus  $\mathbf{D}^{ep}$  is a fourth-order tensor and it is the multidimensional equivalent of the elastoplastic scalar modulus  $E^{ep}$  introduced for the uniaxial model.

If the flow rule is associative, then  $\mathbf{D}^{ep}$  is symmetric, while form models with non-associative plastic flow  $\mathbf{D}^{ep}$  is generally unsymmetric.

## 2.4. Classical Yield Criteria

In this section, some of the most common yield criteria used in engineering applications are described in detail. Namely the von Mises, Mohr-Coulomb and Drucker-Prager criteria are examined. Their basic characteristics are presented and various representations of the according yield functions are established. In addition, the graphical representation of each criterion in three dimensional principal stress space is shown.

### 2.4.1. Von Mises Yield-Criterion

The von Mises yield criterion was proposed by von Mises (1913) in order to describe plastic yielding in metals. One of its main advantages is the absence of singularities in the yield function which when present as in the case of the Tresca yield criterion, cause problems when analytical solutions to simple boundary problems are sought. In addition it offers a number of attractive features with respect to numerical integration of rate equations. Finally the von Mises criterion due to its lack of corners in its graphical representation allows the simple calculation of the differentials of the yield and plastic potential functions required in order to obtain the elastoplastic modulus.

According to the von Mises criterion, plastic yielding begins when the  $J_2$  stress deviator invariant reaches a critical value. The yield surface constitutes of an infinite circular cylinder in principal stress space with the principal diagonal (hydrostatic axis) as center axis. It is easily understood that only the deviatoric stress tensor takes part in the definition of the von Mises criterion. The pressure component of the stress tensor does not influence the plastic yielding and that's the reason why this criterion is characterized as a pressure-independent. Mathematically, the yield function can be expresses in a number of ways:

$$\Phi(\boldsymbol{\sigma}) = \sqrt{3J_2(\mathbf{s}(\boldsymbol{\sigma}))} - \sigma_y$$

$$\Phi(\boldsymbol{\sigma}) = q(\boldsymbol{\sigma}) - \sigma_y.$$

In the above relation,  $\Phi$  is used to describe the yield function,  $\sigma_y$  is the uniaxial yield stress and  $q$  is the so-called von Mises effective or equivalent stress. The von Mises effective stress is calculated from the expression:

$$q(\boldsymbol{\sigma}) = \sqrt{3J_2(\mathbf{s}(\boldsymbol{\sigma}))}$$

where  $\mathbf{s}$  denotes the stress deviator. In terms of principal deviatoric stresses  $s_i$ , the above relation can be written as:

$$q(\boldsymbol{\sigma})^2 = \frac{3}{2}(s_1s_1 + s_2s_2 + s_3s_3)$$

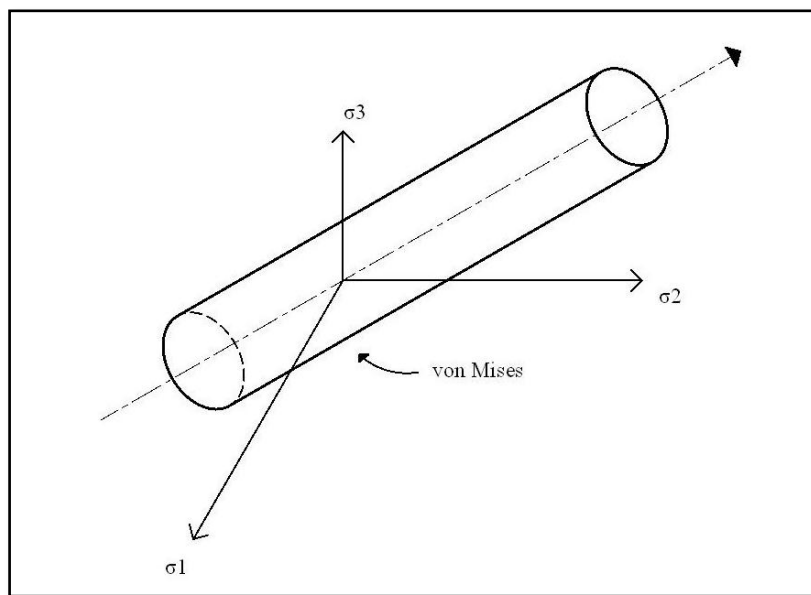
Additionally, the yield function can be expressed in terms of a shear yield stress  $\tau_y$  :

$$\Phi(\boldsymbol{\sigma}) = \sqrt{J_2(\mathbf{s}(\boldsymbol{\sigma}))} - \tau_y$$

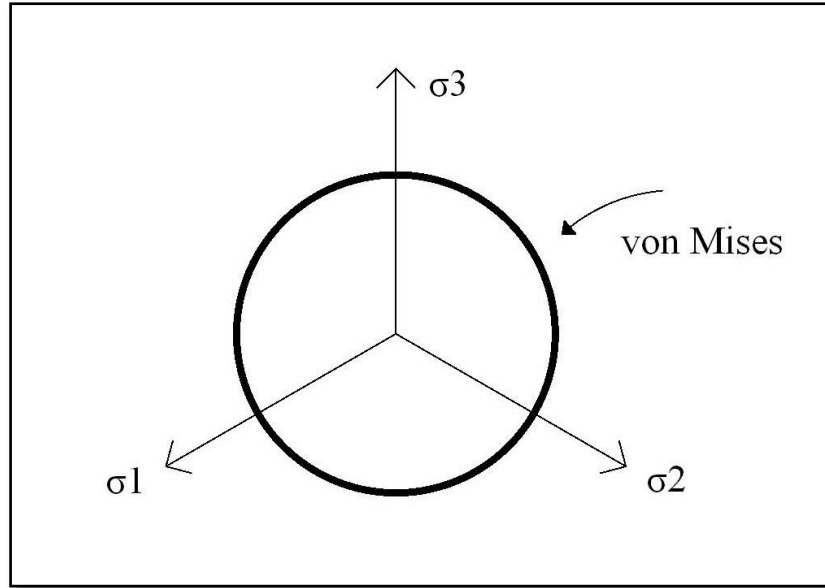
The shear yield stress and the uniaxial yield stress for the von Mises yield criterion are related via the following relation:

$$\sigma_y = \sqrt{3}\tau_y$$

The following picture demonstrates the shape of the yield surface in principal stress space:



The von Mises yield surface in principal stress space.



The  $\pi$ -plane representation of the von Mises yield surface.

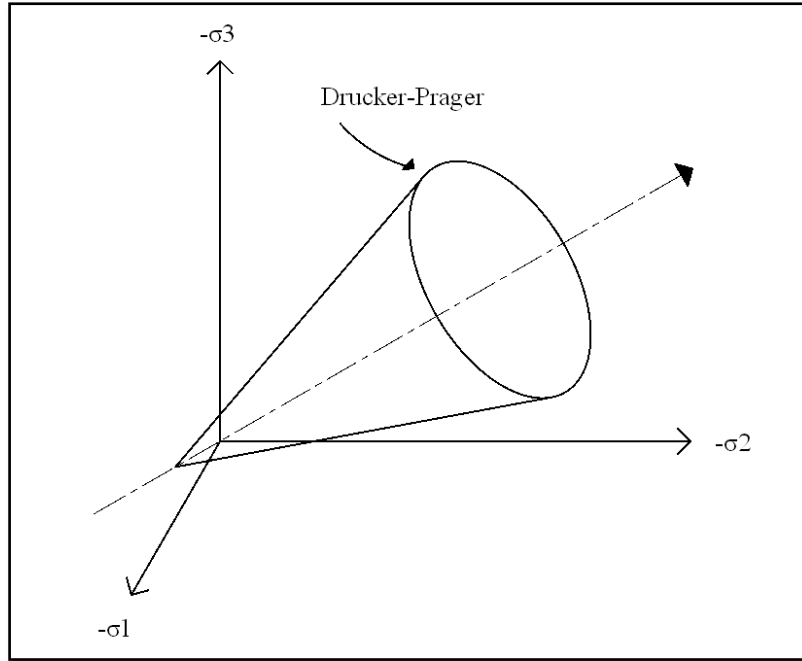
#### 2.4.2. Drucker-Prager Yield-Criterion

As with the Tresca yield criterion, the Mohr-Coulomb yield function has corners when plotted in principal stress space. This requires special treatment of the integration of rate equations and calculation of the elastoplastic tangent. To overcome this difficulties, Drucker and Prager(1952) proposed the Drucker-Prager yield criterion as a smooth approximation to the Mohr-Coulomb law. It consists of a modification of the von Mises model described earlier in which an extra term is included in order to introduce pressure-sensitivity. Due to the addition of this extra term the Drucker-Prager yield function is also known as extended von Mises yield function. The pressure-sensitivity incorporation in the model is crucial so that materials such as soil, rock and concrete, which are characterized by a strong dependence of their yield limit on the hydrostatic pressure, are accurately modeled.

The Drucker-Prager criterion states that plastic yielding begins when the  $J_2$  invariant of the deviatoric stress tensor and the hydrostatic pressure  $p$ , reach a critical combination. The yield function is given by the following relation:

$$\Phi(\boldsymbol{\sigma}, c) = \sqrt{J_2(\boldsymbol{s}(\boldsymbol{\sigma}))} + \eta p(\boldsymbol{\sigma}) - \xi c$$

Where  $c$  is the cohesion and the parameters  $\eta$  and  $\xi$  are chosen according to the desired approximation of the Mohr-Coulomb model. Represented in the principal stress space, the yield locus of this criterion is a circular cone whose axis coincides with the hydrostatic line. The Drucker-Prager cone is illustrated in the following figure:



The Drucker-Prager yield surface in principal stress space.

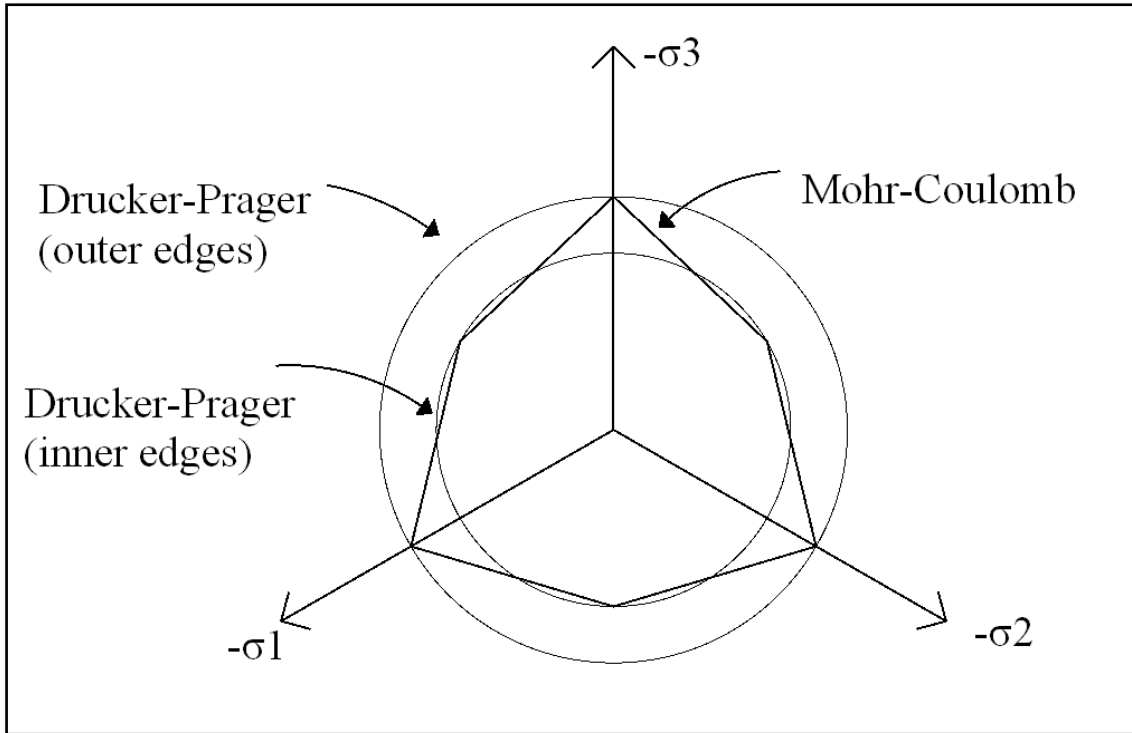
The two most common approximations to the Mohr-Coulomb yield surface by the Drucker-Prager criterion, are obtained by making the yield surface of the latter coincident at the outer or inner surface of the Mohr-Coulomb yield function. The desired coincidence is achieved by the appropriate selection of the  $\eta$  and  $\xi$  parameters. Thus, for coincidence at the outer edges,  $\eta$  and  $\xi$  are given by the following relations:

$$\eta = \frac{6\sin(\varphi)}{\sqrt{3}(3 - \sin(\varphi))} , \quad \xi = \frac{6\cos(\varphi)}{\sqrt{3}(3 - \sin(\varphi))}$$

Whereas, coincidence at the inner edges is given by the following relations:

$$\eta = \frac{6\sin(\varphi)}{\sqrt{3}(3 + \sin(\varphi))} , \quad \xi = \frac{6\cos(\varphi)}{\sqrt{3}(3 + \sin(\varphi))}$$

The outer and inner cones are known respectively, as the compression cone and the extension cone. The inner cone matches the Mohr-Coulomb criterion in uniaxial tension and biaxial compression. The outer edge approximation matches the Mohr-Coulomb surface in uniaxial compression and biaxial extension. The  $\pi$ -plane section of both surfaces is shown in the following figure.



Drucker-Prager approximations of the Mohr-Coulomb yield surface.

Another useful approximation is obtained by forcing both criteria to predict identical collapse loads under plane strain conditions. In this case which is used in the subsequent application section the Drucker-Prager parameters are derived from the following relations:

$$\eta = \frac{3 \tan(\varphi)}{\sqrt{9 + 12 \tan^2 \varphi}} \quad , \quad \xi = \frac{3}{\sqrt{9 + 12 \tan^2 \varphi}}$$

In all three approximations described above, the apex of the approximating Drucker-Prager cone coincides with the apex of the corresponding Mohr-Coulomb surface.





## ***Chapter 3: Numerical Solution of the Elastoplastic Constitutive Initial Value Problem with the Finite Element Method***

### **3.1. The Incremental Finite Element Solution for Path-Dependent Materials**

When dealing with elastoplastic materials, the constitutive equations are path-dependent. This means that the stress tensor cannot be calculated from the instantaneous value of the infinitesimal strain tensor only. The whole *history* of strains to which the solid of interest has been subjected needs to be known. The stress tensor is the solution of the constitutive initial value problem whose general form is the following:

*Given the initial values of the internal variables  $\mathbf{a}(t_0)$  and the history of the infinitesimal strain tensor,*

$$\boldsymbol{\varepsilon}(t), \quad t \in [t_0, T],$$

*find the functions  $\boldsymbol{\sigma}(t)$  and  $\mathbf{a}(t)$ , for the stress tensor and the set of internal variables, such that the constitutive equations*

$$\boldsymbol{\sigma}(t) = \bar{\rho} \left. \frac{\partial \psi}{\partial \boldsymbol{\varepsilon}} \right|_t,$$

$$\dot{\mathbf{a}}(t) = f(\boldsymbol{\varepsilon}(t), \mathbf{a}(t))$$

*are satisfied for every  $t \in [t_0, T]$ .*

#### **3.1.1. The Incremental Constitutive Function**

For a generic path-dependent material model, the solution of the above constitutive initial value problem for a given set of initial conditions is usually not known for complex strain paths  $\boldsymbol{\varepsilon}(t)$ . Therefore, the use of an appropriate numerical algorithm for integration of the rate constitutive equations is an essential requirement in the finite element simulations of models including path-dependent materials. The choice of the particular integration technique depends on the characteristics and of each specific material model. In general, some kind of time or pseudo-time discretization is adopted along with some hypothesis on the deformation path between adjacent time stations. Within the context of purely mechanical theory, considering the time increment  $[t_n, t_{n+1}]$  and by having the set  $\mathbf{a}_n$  of internal variables at time  $t_n$ , then the strain tensor  $\boldsymbol{\varepsilon}_{n+1}$  at time  $t_{n+1}$  must uniquely determine the strain tensor  $\boldsymbol{\sigma}_{n+1}$  through the integration algorithm. An approximate *incremental constitutive function*  $\hat{\boldsymbol{\sigma}}$  for the stress tensor is defined:

$$\boldsymbol{\sigma}_{n+1} = \hat{\boldsymbol{\sigma}}(\mathbf{a}_n, \boldsymbol{\varepsilon}_{n+1})$$

whose outcome  $\boldsymbol{\sigma}_{n+1}$ , is expected to converge to the actual solution of the evolution problem as the strain increments are reduced.

The numerical constitutive law is generally nonlinear and is path-dependent within one increment. Within each increment  $\boldsymbol{\sigma}_{n+1}$  is a function of  $\boldsymbol{\varepsilon}_{n+1}$  alone. The integration algorithm also defines a similar incremental constitutive function for the internal variables of the model:

$$\mathbf{a}_{n+1} = \hat{\mathbf{a}}(\mathbf{a}_n, \boldsymbol{\varepsilon}_{n+1})$$

In the context of elastoplasticity the procedure of elastic predictor/return-mapping algorithms is the numerical integration scheme which is going to be used in this thesis.

### 3.1.2. The Incremental Boundary Value Problem

Having defined the generic incremental constitutive law in the previous section, we can now state the incremental or time-discrete version of the initial boundary problem:

*Given the set  $\mathbf{a}_n$  of the internal variables at time  $t_n$ , find a displacement field  $\mathbf{u}_{n+1} \in \mathcal{K}_{n+1}$  such that*

$$\int_{\Omega} [\hat{\boldsymbol{\sigma}}(\mathbf{a}_n, \nabla^s \mathbf{u}_{n+1}) : \nabla^s \boldsymbol{\eta} - \mathbf{b}_{n+1} \cdot \boldsymbol{\eta}] dv - \int_{\partial\Omega_t} \mathbf{t}_{n+1} \cdot \boldsymbol{\eta} da = 0$$

*for any  $\boldsymbol{\eta} \in \mathcal{V}$ , where  $\mathbf{b}_{n+1}$  and  $\mathbf{t}_{n+1}$  are the body forces and surface traction fields prescribed at time  $t_{n+1}$ . The set  $\mathcal{K}_{n+1}$  is defined as:*

$$\mathcal{K}_{n+1} = \{\mathbf{u} : \Omega \rightarrow \mathcal{U} \mid \mathbf{u} = \bar{\mathbf{u}}_{n+1} \text{ on } \partial\Omega_u\},$$

*where  $\bar{\mathbf{u}}_{n+1}$  are the prescribed boundary displacements at  $t_{n+1}$ .*

### 3.1.3. The Nonlinear Incremental Finite Element Equation

After the standard finite element discretization of the incremental boundary value problem introduced in the previous section, the problem is reduced to the following.

Find the nodal displacement vector  $\mathbf{u}_{n+1}$  at time  $t_{n+1}$  such that the incremental finite element equilibrium equation

$$\mathbf{r}(\mathbf{u}_{n+1}) \equiv \mathbf{f}^{int}(\mathbf{u}_{n+1}) - \mathbf{f}_{n+1}^{ext} = \mathbf{0}$$

is satisfied, where  $\mathbf{f}^{int}(\mathbf{u}_{n+1})$  and  $\mathbf{f}_{n+1}^{ext}$  are assembled from the element vectors

$$\begin{aligned} \mathbf{f}_{(e)}^{int} &= \int_{\Omega^{(e)}} \mathbf{B}^T \hat{\boldsymbol{\sigma}}(\mathbf{a}_n, \boldsymbol{\varepsilon}(\mathbf{u}_{n+1})) dv \\ \mathbf{f}_{(e)}^{ext} &= \int_{\Omega^{(e)}} \mathbf{N}^T \mathbf{b}_{n+1} dv + \int_{\partial\Omega_t^{(e)}} \mathbf{N}^T \mathbf{t}_{n+1} da. \end{aligned}$$

The equilibrium equation is generally nonlinear. The source of nonlinearity is the nonlinearity of the incremental constitutive function that takes part in the definition of the element internal force vector.

In our case the use of *proportional loading* is used in the incremental finite element scheme. Proportional loading is characterized by body force and surface traction fields given at an arbitrary time instant  $t_{n+1}$ , by:

$$\begin{aligned}\mathbf{b}_{n+1} &= \lambda_{n+1} \tilde{\mathbf{b}} \\ \mathbf{t}_{n+1} &= \lambda_{n+1} \tilde{\mathbf{t}}\end{aligned}$$

where  $\lambda_{n+1}$  is the prescribed *load factor* at  $t_{n+1}$  and  $\tilde{\mathbf{b}}$ ,  $\tilde{\mathbf{t}}$  are prescribed, constant in time fields. In this case, the global external force vector reduces to

$$\mathbf{f}_{n+1}^{ext} = \lambda_{n+1} \bar{\mathbf{f}}^{ext},$$

where  $\bar{\mathbf{f}}^{ext}$  is computed only once at the beginning of the incremental procedure as the assembly of element vectors

$$\bar{\mathbf{f}}_{(e)}^{ext} = \int_{\Omega^{(e)}} \mathbf{N}^T \tilde{\mathbf{b}} dv + \int_{\partial\Omega_t^{(e)}} \mathbf{N}^T \tilde{\mathbf{t}} da.$$

### 3.1.4. Nonlinear Solution. The Newton-Raphson Scheme

The Newton-Raphson algorithm is particularly attractive for the solution of the nonlinear incremental equilibrium equation. Due to the quadratic rates of asymptotic convergence it offers, the Newton-Raphson method produces relatively robust and efficient incremental nonlinear finite element schemes and is adopted in our case.

Each iteration of the Newton-Raphson scheme, comprises the solution of the linearized version of the discretized incremental equilibrium equation.

At a state defined by the global displacement vector  $\mathbf{u}_{n+1}^{(k-1)}$ , the typical iteration ( $k$ ) of the Newton-Raphson scheme, consists of solving the linear system of equations

$$\mathbf{K}_T \delta \mathbf{u}^{(k)} = -\mathbf{r}^{(k-1)}$$

for  $\mathbf{u}^{(k)}$ , where we have defined the *residual* or *out-of balance force* vector

$$\mathbf{r}^{(k-1)} \equiv \mathbf{f}^{int}(\mathbf{u}_{n+1}^{(k-1)}) - \mathbf{f}_{n+1}^{ext}$$

and  $\mathbf{K}_T$  is the *global tangent stiffness matrix*:

$$\mathbf{K}_T \equiv \int_{h_\Omega} (\mathbf{B}^g)^T \mathbf{D} \mathbf{B}^g dv = \left. \frac{\partial \mathbf{r}}{\partial \mathbf{u}_{n+1}} \right|_{\mathbf{u}_{n+1}^{(k-1)}}.$$

With the solution  $\delta \mathbf{u}^{(k)}$  at hand, we apply the Newton correction to the global displacement

$$\mathbf{u}_{n+1}^{(k)} = \mathbf{u}_{n+1}^{(k-1)} + \delta \mathbf{u}^{(k)},$$

or in terms of displacement *increments*,

$$\mathbf{u}_{n+1}^{(k)} = \mathbf{u}_n + \Delta \mathbf{u}^{(k)}$$

where  $\Delta \mathbf{u}^{(k)}$  is the *incremental displacement vector*:

$$\Delta \mathbf{u}^{(k)} = \Delta \mathbf{u}^{(k-1)} + \delta \mathbf{u}^{(k)}.$$

The Newton-Raphson iterations are repeated until after some iteration ( $m$ ), the following *convergence criterion* is satisfied:

$$\frac{|\mathbf{r}^{(m)}|}{|\mathbf{f}_{n+1}^{ext}|} \leq \varepsilon_{tol},$$

where  $\varepsilon_{tol}$  is a sufficiently small specified *equilibrium convergence tolerance*. The corresponding displacement vector,  $\mathbf{u}_{n+1}^{(m)}$ , is then accepted as sufficiently small to the solution of the incremental equilibrium equation:

$$\mathbf{u}_{n+1} := \mathbf{u}_{n+1}^{(m)}.$$

At the start of the Newton-Raphson iterations, we need an initial guess,  $\mathbf{u}_{n+1}^{(0)}$ . This initial guess is usually taken as the converged equilibrium displacement vector of the previous increment,

$$\mathbf{u}_{n+1}^{(0)} = \mathbf{u}_n \quad \text{or} \quad \Delta \mathbf{u}_{n+1}^{(0)} = 0$$

### 3.1.5. The Consistent Tangent Modulus

The global tangent stiffness is the assembly of the element tangent stiffness matrices:

$$\mathbf{K}_T^{(e)} = \int_{\Omega^{(e)}} \mathbf{B}^T \mathbf{D} \mathbf{B} dv$$

where  $\mathbf{D}$  is the *consistent tangent matrix* – the matrix form of the fourth-order *consistent tangent operator*

$$\mathbf{D} \equiv \left. \frac{\partial \hat{\boldsymbol{\sigma}}}{\partial \boldsymbol{\varepsilon}_{n+1}} \right|_{\boldsymbol{\varepsilon}_{n+1}^{(k-1)}}.$$

This tensor possesses the symmetries:

$$\mathcal{D}_{ijkl} = \mathcal{D}_{jikl} = \mathcal{D}_{ijlk}.$$

The consistent tangent operator is the derivative of the incremental constitutive function  $\hat{\sigma}$ . This *generally implicit* function is typically defined by some numerical algorithm for integration of the rate constitutive equations of the model. The derivation of this operator consistent with the numerical integration used for the material model, is discussed thoroughly in a following section in the context of elastoplasticity.

### 3.2. Preliminary Implementation Aspects for the Elastoplastic Constitutive Initial Value Problem

The numerical procedure necessary for the implicit finite element solution of small strain plasticity problems within the finite element framework presented in the previous sections can be summarized into two most fundamental operations specific for every material model.

1. The *state update procedure* which, in the case of elastoplastic materials, requires the formulation of a scheme for numerical integration of the rate elastoplastic evolution equations. Within a pseudo-time increment  $[t_n, t_{n+1}]$ , the state update procedure gives the stresses  $\boldsymbol{\sigma}_{n+1}$  and the internal variables  $\mathbf{a}_{n+1}$  at the end of the increment as a function of the internal variables  $\mathbf{a}_n$  at the beginning of the increment and the strains  $\boldsymbol{\varepsilon}_{n+1}$  at the end of the increment:

$$\boldsymbol{\sigma}_{n+1} = \hat{\sigma}(\mathbf{a}_n, \boldsymbol{\varepsilon}_{n+1}),$$

$$\mathbf{a}_{n+1} = \hat{\mathbf{a}}(\mathbf{a}_n, \boldsymbol{\varepsilon}_{n+1}).$$

The incremental constitutive functions  $\hat{\sigma}$  and  $\hat{\mathbf{a}}$  are defined by the integration algorithm adopted and the stress delivered by  $\hat{\sigma}$  is used to assemble the internal force vector

$$\mathbf{f}_e^{int} = \sum_{n=1}^{nGaussp} j_i w_i \mathbf{B}_i^T \boldsymbol{\sigma}_{n+1}|_i.$$

2. The computation of the associated *consistent tangent modulus*

$$\mathbf{D} = \frac{\partial \hat{\sigma}}{\partial \boldsymbol{\varepsilon}_{n+1}},$$

to be used for the evaluation of a new tangent stiffness matrix whenever the Newton-Raphson scheme requires for solution of the nonlinear finite element equilibrium equations. The element tangent stiffness matrix is computed as

$$\mathbf{K}_T^{(e)} = \sum_{n=1}^{nGaussp} w_i j_i \mathbf{B}_i^T \mathbf{D}_i \mathbf{B}_i.$$

### 3.2.1 The Elastoplastic Constitutive Initial Value Problem

Let us consider a point  $\mathbf{p}$  of a solid body  $\mathcal{B}$  with constitutive behaviour described by the general elastoplastic model. Assume that at a given pseudo-time  $t_0$  the elastic strain  $\boldsymbol{\varepsilon}^e(t_0)$ , the plastic strain tensor  $\boldsymbol{\varepsilon}^p(t_0)$  and all the elements of the set  $\mathbf{a}(t_0)$  of hardening internal variables are known at point  $\mathbf{p}$ . Furthermore, let the motion of  $\mathcal{B}$  be prescribed between  $t_0$  and a subsequent instant,  $T$ . The prescribed motion, defines the history of the strain tensor,  $\boldsymbol{\varepsilon}(t)$ , at the material point of interest between the time instants  $t_0$  and  $T$ . The basic elastoplastic constitutive initial value problem at point  $\mathbf{p}$  is stated as follows.

*Given the initial values  $\boldsymbol{\varepsilon}^e(t_0)$  and  $\mathbf{a}(t_0)$  and the given history of the strain tensor,  $\boldsymbol{\varepsilon}(t)$ ,  $t \in [t_0, T]$ , find the functions  $\boldsymbol{\varepsilon}^e(t)$ ,  $\mathbf{a}(t)$  and  $\dot{\gamma}(t)$  for the elastic strain tensor, hardening internal variables set and plastic multiplier respectively that satisfy the reduced general elastoplastic constitutive equations*

$$\dot{\boldsymbol{\varepsilon}}^e(t) = \dot{\boldsymbol{\varepsilon}}(t) - \dot{\gamma}(t)\mathbf{N}(\boldsymbol{\sigma}(t), \mathbf{A}(t))$$

$$\dot{\mathbf{a}}(t) = \dot{\gamma}(t)\mathbf{H}(\boldsymbol{\sigma}(t), \mathbf{A}(t))$$

$$\dot{\gamma}(t) \geq 0, \quad \Phi(\boldsymbol{\sigma}(t), \mathbf{A}(t)) \leq 0, \quad \dot{\gamma}(t)\Phi(\boldsymbol{\sigma}(t), \mathbf{A}(t)) = 0$$

for each instant  $t \in [t_0, T]$ , with

$$\boldsymbol{\sigma}(t) = \bar{\rho} \left. \frac{\partial \psi}{\partial \boldsymbol{\varepsilon}^e} \right|_t, \quad \mathbf{A}(t) = \bar{\rho} \left. \frac{\partial \psi}{\partial \mathbf{a}} \right|_t.$$

The above system of equation is *reduced* because the plastic flow equation has been incorporated into the additive strain rate decomposition. Therefore the plastic strain tensor does not appear explicitly in the above equations. The only unknowns are the elastic strain tensor, the set of hardening variables and the plastic multiplier. With the solution  $\boldsymbol{\varepsilon}^e(t)$  at hand, we can easily determine the history of the plastic strain tensor from the trivial relation

$$\boldsymbol{\varepsilon}^p(t) = \boldsymbol{\varepsilon}(t) - \boldsymbol{\varepsilon}^e(t).$$

As already mentioned, the solution of the above problem is generally unknown for complex strain paths. Therefore the adoption of a numerical technique to find an approximate solution becomes absolutely essential. A general framework for the above constitutive initial value problem of elastoplasticity is described in the following section.

### 3.2.2. Euler Discretization: The Incremental Constitutive Problem

The starting point here is the adoption of an *Euler scheme* to discretize the equations of the elastoplastic constitutive initial value problem. Here the *backward or fully implicit Euler scheme* is chosen. Accordingly for integration within a generic pseudo-time interval  $[t_n, t_{n+1}]$ , we replace all the rate quantities with corresponding incremental values within the considered time interval and the functions  $\mathbf{N}$ ,  $\mathbf{H}$  and  $\Phi$  with their values at the end of the time

interval,  $t_{n+1}$ . The resulting discrete version of the elastoplastic constitutive problem is states as follows.

Given the values  $\boldsymbol{\varepsilon}_n^e$  and  $\mathbf{a}_n$  of the elastic strain tensor and the internal variables set at the beginning of the pseudo-time interval  $[t_n, t_{n+1}]$  and given the prescribed incremental strain  $\Delta\boldsymbol{\varepsilon}$  for this interval, solve the following system of algebraic equations

$$\boldsymbol{\varepsilon}_{n+1}^e = \boldsymbol{\varepsilon}_n^e + \Delta\boldsymbol{\varepsilon} - \Delta\gamma\mathbf{N}(\boldsymbol{\sigma}_{n+1}, \mathbf{A}_{n+1})$$

$$\mathbf{a}_{n+1} = \mathbf{a}_n + \Delta\gamma\mathbf{H}(\boldsymbol{\sigma}_{n+1}, \mathbf{A}_{n+1})$$

for the unknowns  $\boldsymbol{\varepsilon}_{n+1}^e$ ,  $\mathbf{a}_{n+1}$  and  $\Delta\gamma$ , subjected to the constraints

$$\Delta\gamma \geq 0, \quad \Phi(\boldsymbol{\sigma}_{n+1}, \mathbf{A}_{n+1}) \leq 0, \quad \Delta\gamma\Phi(\boldsymbol{\sigma}_{n+1}, \mathbf{A}_{n+1}) = 0$$

where

$$\boldsymbol{\sigma}_{n+1} = \bar{\rho} \left. \frac{\partial\psi}{\partial\boldsymbol{\varepsilon}^e} \right|_{n+1}, \quad \mathbf{A}_{n+1} = \bar{\rho} \left. \frac{\partial\psi}{\partial\mathbf{a}} \right|_{n+1}.$$

In the above, we have adopted the notation

$$\Delta(\cdot) = (\cdot)_{n+1} - (\cdot)_n,$$

with  $(\cdot)_n$  and  $(\cdot)_{n+1}$  denoting the value of  $(\cdot)$  respectively at times  $t_n$  and  $t_{n+1}$ . The increment  $\Delta\gamma$  is called the *incremental plastic multiplier*. Once the solution  $\boldsymbol{\varepsilon}_{n+1}^e$  has been obtained, the plastic strain tensor at  $t_{n+1}$  can be calculated as

$$\boldsymbol{\varepsilon}_{n+1}^p = \boldsymbol{\varepsilon}_n^p + \Delta\boldsymbol{\varepsilon} - \Delta\boldsymbol{\varepsilon}^e,$$

so that all variables of the model are known at the end of the interval  $[t_n, t_{n+1}]$ .

### 3.2.3. Solution of the incremental problem

Due to the presence of the complementarity condition

$$\Delta\gamma \geq 0, \quad \Phi(\boldsymbol{\sigma}_{n+1}, \mathbf{A}_{n+1}) \leq 0, \quad \Delta\gamma\Phi(\boldsymbol{\sigma}_{n+1}, \mathbf{A}_{n+1}) = 0$$

the solution of the incremental elastoplastic problem presented in the previous section, does not follow directly the conventional procedure for standard initial value problems. The complementarity condition, gives rise to a two-step algorithm derived in the following.

First of all, it must be noted that the constraint  $\Delta\gamma \geq 0$ , allows only for two mutually exclusive possibilities enumerated below:

1. Null incremental plastic multiplier,



$$\Delta\gamma = 0.$$

In this case there is no plastic flow or evolution of internal variables within the considered time interval  $[t_n, t_{n+1}]$  and the process is purely elastic. The third constrain of the complementarity condition is automatically satisfied and  $\boldsymbol{\varepsilon}_{n+1}^e, \mathbf{a}_{n+1}$  are given by:

$$\boldsymbol{\varepsilon}_{n+1}^e = \boldsymbol{\varepsilon}_n^e + \Delta\boldsymbol{\varepsilon}$$

$$\mathbf{a}_{n+1} = \mathbf{a}_n.$$

In addition, the constraint

$$\Phi(\boldsymbol{\sigma}_{n+1}, \mathbf{A}_{n+1}) \leq 0$$

must hold, where  $\boldsymbol{\sigma}_{n+1}$  and  $\mathbf{A}_{n+1}$  are functions of  $\boldsymbol{\varepsilon}_{n+1}^e$  and are defined through the potential relations

$$\boldsymbol{\sigma}_{n+1} = \bar{\rho} \left. \frac{\partial \psi}{\partial \boldsymbol{\varepsilon}^e} \right|_{n+1}, \quad \mathbf{A}_{n+1} = \bar{\rho} \left. \frac{\partial \psi}{\partial \mathbf{a}} \right|_{n+1}$$

2. Strictly positive plastic multiplier,

$$\Delta\gamma > 0.$$

In this case,  $\boldsymbol{\varepsilon}_{n+1}^e, \mathbf{a}_{n+1}$  and  $\Delta\gamma$  satisfy

$$\boldsymbol{\varepsilon}_{n+1}^e = \boldsymbol{\varepsilon}_n^e + \Delta\boldsymbol{\varepsilon} - \Delta\gamma \mathbf{N}(\boldsymbol{\sigma}_{n+1}, \mathbf{A}_{n+1})$$

$$\mathbf{a}_{n+1} = \mathbf{a}_n + \Delta\gamma \mathbf{H}(\boldsymbol{\sigma}_{n+1}, \mathbf{A}_{n+1})$$

and the second and third equations of the complementarity condition combined, result in the constraint

$$\Phi(\boldsymbol{\sigma}_{n+1}, \mathbf{A}_{n+1}) = 0$$

Finally the procedure which selects which one of the above cases holds and solves the required equations is described in the next section.

### 3.2.4. The Elastic Predictor/Plastic Corrector Algorithm

The nature of the above problem motivates the establishment of a two-step algorithm in which the two possible sets of equations are employed sequentially and the final solution is selected as the only valid one. The strategy adopted is the following:

- a) *The Elastic Trial Step.*

Firstly we assume that the null incremental plastic multiplier situation ( $\Delta\gamma = 0$ ) occurs. In other words, we assume that the step  $[t_n, t_{n+1}]$  is purely elastic. This

solution which is not necessarily the actual solution of the problem is called the *elastic trial solution*. According to the elastic trial solution:

$$\boldsymbol{\varepsilon}_{n+1}^{e\ trial} = \boldsymbol{\varepsilon}_n^e + \Delta \boldsymbol{\varepsilon}$$

$$\mathbf{a}_{n+1}^{trial} = \mathbf{a}_n .$$

The corresponding stress and hardening force are called the *elastic trial stress* and the *elastic trial hardening force* and are given by the known potential relations:

$$\boldsymbol{\sigma}_{n+1}^{trial} = \bar{\rho} \left. \frac{\partial \psi}{\partial \boldsymbol{\varepsilon}^e} \right|_{n+1}^{trial} , \quad \mathbf{A}_{n+1}^{trial} = \bar{\rho} \left. \frac{\partial \psi}{\partial \mathbf{a}} \right|_{n+1}^{trial}$$

The above variables are collectively called the *elastic trial state*. If the elastic trial state is indeed the solution of the problem, then it must also satisfy the constraint:

$$\Phi(\boldsymbol{\sigma}_{n+1}^{trial}, \mathbf{A}_{n+1}^{trial}) \leq 0$$

which means that the elastic trial stress state, lies within the elastic domain or on its boundary which is the yield surface. Therefore, if the constraint is satisfied the state variables are updated as:

$$(\cdot)_{n+1} := (\cdot)_{n+1}^{trial}$$

and the algorithm is terminated. Otherwise the elastic trial state is not plastically admissible and the solution must be obtained from the plastic corrector step described next.

b) *The Plastic Corrector Step or Return-Mapping Algorithm.*

Since this step is applied only if the elastic trial step is not plastically admissible, the only option left is to solve the system of algebraic equations:

$$\boldsymbol{\varepsilon}_{n+1}^e = \boldsymbol{\varepsilon}_{n+1}^{e\ trial} - \Delta \gamma \mathbf{N}(\boldsymbol{\sigma}_{n+1}, \mathbf{A}_{n+1})$$

$$\mathbf{a}_{n+1} = \mathbf{a}_{n+1}^{trial} + \Delta \gamma \mathbf{H}(\boldsymbol{\sigma}_{n+1}, \mathbf{A}_{n+1})$$

$$\Phi(\boldsymbol{\sigma}_{n+1}, \mathbf{A}_{n+1}) = 0$$

which are of course complemented with the potential relations

$$\boldsymbol{\sigma}_{n+1} = \bar{\rho} \left. \frac{\partial \psi}{\partial \boldsymbol{\varepsilon}^e} \right|_{n+1} , \quad \mathbf{A}_{n+1} = \bar{\rho} \left. \frac{\partial \psi}{\partial \mathbf{a}} \right|_{n+1}$$

The solution of the above system must satisfy

$$\Delta \gamma > 0 .$$



## Chapter 4: Numerical Implementation of Classical Elastoplastic Models

### 4.1. The von Mises Plasticity Model

Firstly, the basic points of the implemented von Mises plasticity model are summarized below. The model that we are going to analyze adopts the fully implicit algorithm and comprises:

1. A linear elastic law

$$\boldsymbol{\sigma} = \mathbf{D}^e : \boldsymbol{\varepsilon}^e ,$$

where  $\mathbf{D}^e$  is the standard isotropic elasticity tensor.

2. A yield function of the form

$$\Phi(\boldsymbol{\sigma}, \sigma_y) = \sqrt{3J_2(\mathbf{s}(\boldsymbol{\sigma}))} - \sigma_y ,$$

where

$$\sigma_y = \sigma_y(\bar{\varepsilon}^p)$$

is the uniaxial yield stress – a function of the accumulated plastic strain,  $\bar{\varepsilon}^p$ .

3. A standard associative flow rule

$$\dot{\boldsymbol{\varepsilon}}^p = \dot{\gamma} \mathbf{N} = \dot{\gamma} \frac{\partial \Phi}{\partial \boldsymbol{\sigma}} ,$$

with the (Prandtl-Reuss) flow vector,  $\mathbf{N}$ , explicitly given by

$$\mathbf{N} \equiv \frac{\partial \Phi}{\partial \boldsymbol{\sigma}} = \sqrt{\frac{3}{2}} \frac{\mathbf{s}}{\|\mathbf{s}\|} .$$

4. An associative hardening rule, with the evolution for the hardening internal variable given by

$$\dot{\bar{\varepsilon}}^p = \sqrt{\frac{2}{3}} \|\dot{\boldsymbol{\varepsilon}}^p\| = \dot{\gamma} .$$

### 4.1.1 The Implicit Elastic Predictor/Return Mapping Scheme

Given the strain increment

$$\Delta \boldsymbol{\varepsilon} = \boldsymbol{\varepsilon}_{n+1} - \boldsymbol{\varepsilon}_n ,$$

corresponding to a typical pseudo-time increment  $[t_n, t_{n+1}]$  , and given the state variables  $\{\boldsymbol{\varepsilon}_n^e, \bar{\boldsymbol{\varepsilon}}_n^p\}$  at  $t_n$  , the elastic trial strain and trial accumulated plastic strain are given by

$$\boldsymbol{\varepsilon}_{n+1}^{e \text{ trial}} = \boldsymbol{\varepsilon}_n^e + \Delta \boldsymbol{\varepsilon}$$

$$\bar{\boldsymbol{\varepsilon}}_{n+1}^{p \text{ trial}} = \bar{\boldsymbol{\varepsilon}}_n^p .$$

The corresponding trial stress is computed as:

$$\boldsymbol{\sigma}_{n+1}^{trial} = \mathbf{D}^e : \boldsymbol{\varepsilon}_{n+1}^{e \text{ trial}} ,$$

or, equivalently, by applying the hydrostatic/deviatoric decomposition

$$\mathbf{s}_{n+1}^{trial} = 2G \boldsymbol{\varepsilon}_{d \ n+1}^{e \text{ trial}} , \quad p_{n+1}^{trial} = K \boldsymbol{\varepsilon}_{v \ n+1}^{e \text{ trial}} ,$$

Where  $\mathbf{s}$  and  $p$  , denote, respectively, the deviatoric and hydrostatic stresses,  $G$  and  $K$  are, respectively, the shear and bulk moduli and the subscripts  $d$  and  $v$  in the elastic trial strain denote, respectively, the deviatoric and volumetric components. The trial yield stress is simply

$$\sigma_{y \ n+1}^{trial} = \sigma_y(\bar{\boldsymbol{\varepsilon}}_n^p) = \sigma_{y_n} .$$

Having computed the elastic trial state, the next step in the algorithm is to check whether  $\boldsymbol{\sigma}_{n+1}^{trial}$  lies inside or outside of the trial yield surface:

- If  $\boldsymbol{\sigma}_{n+1}^{trial}$  lies inside the yield surface, i.e. if

$$\Phi(\boldsymbol{\sigma}_{n+1}^{trial}, \sigma_{y_n}) \leq 0 ,$$

then the process within the interval  $[t_n, t_{n+1}]$  is purely elastic and the elastic trial state itself is valid and itself is the solution to the integration problem. In this case,

$$\boldsymbol{\varepsilon}_{n+1}^e = \boldsymbol{\varepsilon}_{n+1}^{e \text{ trial}} ,$$

$$\boldsymbol{\sigma}_{n+1} = \boldsymbol{\sigma}_{n+1}^{trial} ,$$

$$\bar{\boldsymbol{\varepsilon}}_{n+1}^p = \bar{\boldsymbol{\varepsilon}}_{n+1}^{p \text{ trial}} = \bar{\boldsymbol{\varepsilon}}_n^p ,$$

$$\sigma_{y \ n+1} = \sigma_{y \ n+1}^{trial} = \sigma_{y_n}$$

is updated.

- Otherwise, the process is elastoplastic within the interval  $[t_n, t_{n+1}]$  and the *return-mapping* procedure which is going to be described in the following section has to be applied.

The fully implicit return-mapping equations for the von Mises model consists of the following set of nonlinear equations:

$$\boldsymbol{\varepsilon}_{n+1}^e = \boldsymbol{\varepsilon}_{n+1}^{e \text{ trial}} - \Delta\gamma \sqrt{\frac{3}{2}} \frac{\mathbf{s}_{n+1}}{\|\mathbf{s}_{n+1}\|}$$

$$\bar{\boldsymbol{\varepsilon}}_{n+1}^p = \bar{\boldsymbol{\varepsilon}}_n^p + \Delta\gamma$$

$$\sqrt{3J_2(\mathbf{s}_{n+1})} - \sigma_y(\bar{\boldsymbol{\varepsilon}}_{n+1}^p) = 0$$

which has to be solved for  $\boldsymbol{\varepsilon}_{n+1}^e$ ,  $\bar{\boldsymbol{\varepsilon}}_{n+1}^p$  and  $\Delta\gamma$  and where

$$\mathbf{s}_{n+1} = \mathbf{s}_{n+1}(\boldsymbol{\varepsilon}_{n+1}^e) = 2Gdev[\boldsymbol{\varepsilon}_{n+1}^e].$$

After the solution of the above system, the plastic strain tensor can be updated according to the following formula:

$$\boldsymbol{\varepsilon}_{n+1}^p = \boldsymbol{\varepsilon}_n^p + \Delta\gamma \sqrt{\frac{3}{2}} \frac{\mathbf{s}_{n+1}}{\|\mathbf{s}_{n+1}\|}.$$

#### 4.1.2. Single-equation return-mapping

The above system can be substantially simplified. In fact, it can be reduced to a single nonlinear equation that has the incremental plastic multiplier  $\Delta\gamma$  as the only unknown. For this simplification to be achieved, it should be noted firstly that the von Mises flow vector is *purely deviatoric* so that the deviatoric/volumetric split gives:

$$\boldsymbol{\varepsilon}_{v n+1}^e = \boldsymbol{\varepsilon}_{v n+1}^{e \text{ trial}}$$

$$\boldsymbol{\varepsilon}_{d n+1}^e = \boldsymbol{\varepsilon}_{d n+1}^{e \text{ trial}} - \Delta\gamma \sqrt{\frac{3}{2}} \frac{\mathbf{s}_{n+1}}{\|\mathbf{s}_{n+1}\|}.$$

Equivalently, in stresses terms we have:

$$p_{n+1} = p_{n+1}^{trial}$$

$$\mathbf{s}_{n+1} = \mathbf{s}_{n+1}^{trial} - \Delta\gamma 2G \sqrt{\frac{3}{2}} \frac{\mathbf{s}_{n+1}}{\|\mathbf{s}_{n+1}\|},$$

which means that the return-mapping affects only the deviatoric stress component. The hydrostatic pressure  $p_{n+1}$ , has its value computed at the predictor state and can, therefore, be eliminated from the system of equations. Rearranging of the deviatoric stress-update formula gives:

$$\left(1 + \sqrt{\frac{3}{2}} \frac{\Delta\gamma 2G}{\|\mathbf{s}_{n+1}\|}\right) \mathbf{s}_{n+1} = \mathbf{s}_{n+1}^{trial}.$$

From the above relation, it becomes clear that the trial and the updated deviatoric stresses are *co-linear*. This implies that

$$\frac{\mathbf{s}_{n+1}}{\|\mathbf{s}_{n+1}\|} = \frac{\mathbf{s}_{n+1}^{trial}}{\|\mathbf{s}_{n+1}^{trial}\|}.$$

Substitution of the above identity into the deviatoric stress-update formula gives

$$\begin{aligned} \mathbf{s}_{n+1} &= \left(1 - \sqrt{\frac{3}{2}} \frac{\Delta\gamma 2G}{\|\mathbf{s}_{n+1}^{trial}\|}\right) \mathbf{s}_{n+1}^{trial} \\ &= \left(1 - \frac{\Delta\gamma 3G}{q_{n+1}^{trial}}\right) \mathbf{s}_{n+1}^{trial}, \end{aligned}$$

where

$$q_{n+1}^{trial} = \sqrt{3J_2(\mathbf{s}_{n+1}^{trial})},$$

is the elastic trial von Mises effective stress. It is important to note that as  $\mathbf{s}_{n+1}^{trial}$  is a constant tensor during the return-mapping procedure, the updated deviatoric stress tensor  $\mathbf{s}_{n+1}$  is a linear function of  $\Delta\gamma$  only. Also the fully implicit return-mapping derived above, implies that the updated deviatoric stress tensor is obtained by scaling down the trial deviatoric stress by the factor  $(1 - \Delta\gamma 3G/q_{n+1}^{trial})$ . Finally, substitution of the above relation in the plastic consistency condition produces the generally nonlinear scalar equation, having  $\Delta\gamma$  as the only unknown:

$$\bar{\Phi}(\Delta\gamma) \equiv q_{n+1}^{trial} - 3G\Delta\gamma - \sigma_y(\bar{\varepsilon}_n^p + \Delta\gamma) = 0.$$

With the solution of the above equation and  $\Delta\gamma$  at hand, the state variables are updated as follows:

$$\begin{aligned}\mathbf{s}_{n+1} &= \left(1 - \frac{\Delta\gamma 3G}{q_{n+1}^{trial}}\right) \mathbf{s}_{n+1}^{trial}, \\ \boldsymbol{\sigma}_{n+1} &= \mathbf{s}_{n+1} + p_{n+1}^{trial} \mathbf{I}, \\ \boldsymbol{\varepsilon}_{n+1}^e &= [\mathbf{D}^e]^{-1} : \boldsymbol{\sigma}_{n+1} = \frac{1}{2G} \mathbf{s}_{n+1} + \frac{1}{3} \varepsilon_{v n+1}^{e trial}, \\ \bar{\varepsilon}_{n+1}^p &= \bar{\varepsilon}_n^p + \Delta\gamma.\end{aligned}$$

### 4.1.3. Linear Isotropic Hardening and Perfect Plasticity: The Closed-Form Return Mapping

It should be noted that the main source of nonlinearity in the von Mises return-mapping equation is the *hardening curve*, defined by the given function  $\sigma_y = \sigma_y(\bar{\varepsilon}^p)$ . For *linear hardening* materials, this function is linear and is expressed as:

$$\sigma_y = \sigma_0 + H \bar{\varepsilon}^p,$$

where  $\sigma_0$  is the initial yield stress and  $H$  is the constant hardening modulus. In such cases, the plastic consistency condition reads:

$$\bar{\Phi}(\Delta\gamma) \equiv q_{n+1}^{trial} - 3G\Delta\gamma - [\sigma_0 + (\bar{\varepsilon}_n^p + \Delta\gamma)H] = 0$$

and the incremental plastic multiplier can be obtained in *closed form* as

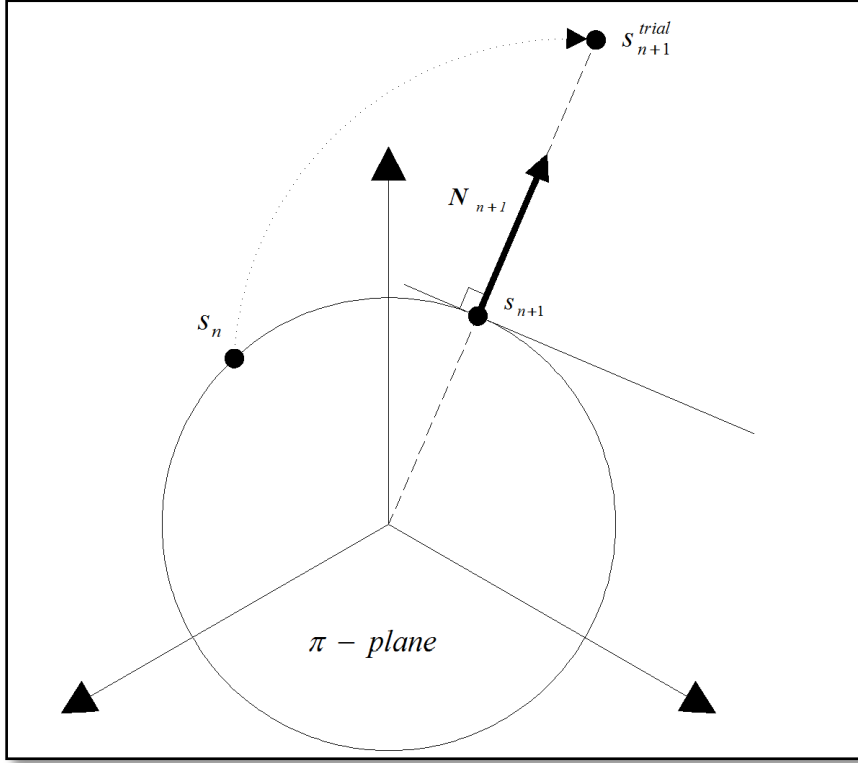
$$\Delta\gamma = \frac{\Phi^{trial}}{3G + H}$$

and the Newton-Raphson algorithm is not needed. In the case of *perfect plasticity*  $H = 0$  the above expression reads:

$$\Delta\gamma = \frac{\Phi^{trial}}{3G}$$

In this case, the updated stress is simply the projection of the elastic trial stress onto the fixed yield surface along its *radial direction*. It is the *closest point projection* of the trial stress onto the yield surface. The return mapping for this case is illustrated in the following figure.





The perfectly plastic von Mises model. Geometric representation of the implicit return-mapping scheme as the closest point projection algorithm.

#### 4.1.4. The Elastoplastic Consistent Tangent for the Von Mises Model with Isotropic Hardening

In the previous sections, the implicit return-mapping algorithm for the von Mises model has been described. In this section, the elastoplastic tangent operator consistent with the von Mises implicit return mapping is derived step by step.

We start by using the update formula for  $\sigma_{n+1}$  under plastic flow when the return-mapping procedure is used:

$$\sigma_{n+1} = \left[ \mathbf{D}^e - \frac{\Delta\gamma 6G^2}{q_{n+1}^{trial}} \mathbf{I}_d \right] : \boldsymbol{\varepsilon}_{n+1}^{e\,trial},$$

where  $\Delta\gamma$  is the solution of the return-mapping equation:

$$\bar{\Phi}(\Delta\gamma) \equiv q_{n+1}^{trial} - 3G\Delta\gamma - \sigma_y(\bar{\varepsilon}_n^p + \Delta\gamma) = 0.$$

The elastoplastic consistent tangent is obtained by differentiation of the stress-update formula given above:

$$\frac{\partial \sigma_{n+1}}{\partial \boldsymbol{\varepsilon}_{n+1}^{e\,trial}} = \mathbf{D}^e - \frac{\Delta\gamma 6G^2}{q_{n+1}^{trial}} \mathbf{I}_d - \frac{6G^2}{q_{n+1}^{trial}} \boldsymbol{\varepsilon}_{d+1}^{e\,trial} \otimes \frac{\partial \Delta\gamma}{\partial \boldsymbol{\varepsilon}_{n+1}^{e\,trial}} + \frac{\Delta\gamma 6G^2}{(q_{n+1}^{trial})^2} \boldsymbol{\varepsilon}_{d+1}^{e\,trial} \otimes \frac{\partial q_{n+1}^{trial}}{\partial \boldsymbol{\varepsilon}_{n+1}^{e\,trial}}$$

By the definition of  $q_{n+1}^{trial}$  and using some tensor calculus, we obtain:

$$\frac{\partial q_{n+1}^{trial}}{\partial \boldsymbol{\varepsilon}_{n+1}^{e\ trial}} = 2G \sqrt{\frac{3}{2}} \bar{\mathbf{N}}_{n+1}$$

where the unit flow vector  $\bar{\mathbf{N}}_{n+1}$  is defined as:

$$\bar{\mathbf{N}}_{n+1} = \sqrt{\frac{2}{3}} \mathbf{N}_{n+1} = \frac{\mathbf{s}_{n+1}^{trial}}{\|\mathbf{s}_{n+1}^{trial}\|} = \frac{\boldsymbol{\varepsilon}_{d+1}^{e\ trial}}{\|\boldsymbol{\varepsilon}_{d+1}^{e\ trial}\|}.$$

In addition, the differentiation of the implicit return mapping equation gives:

$$\frac{\partial \Delta\gamma}{\partial \boldsymbol{\varepsilon}_{n+1}^{e\ trial}} = \frac{1}{3G + H} \frac{\partial q_{n+1}^{trial}}{\partial \boldsymbol{\varepsilon}_{n+1}^{e\ trial}} = \frac{2G}{3G + H} \sqrt{\frac{3}{2}} \bar{\mathbf{N}}_{n+1}$$

where  $H$  is the slope of the hardening curve:

$$H \equiv \left. \frac{d\sigma_y}{d\varepsilon^p} \right|_{\bar{\varepsilon}_n^p + \Delta\gamma}$$

By combining all the above expressions, the following implicit expression for the elastoplastic tangent operator consistent with the implicit return-mapping for the isotropically hardening von Mises model is obtained:

$$\begin{aligned} \mathbf{D}^{ep} &= \mathbf{D}^e - \frac{\Delta\gamma 6G^2}{q_{n+1}^{trial}} \mathbf{I}_d + 6G^2 \left( \frac{\Delta\gamma}{q_{n+1}^{trial}} - \frac{1}{3G + H} \right) \bar{\mathbf{N}}_{n+1} \otimes \bar{\mathbf{N}}_{n+1} \\ &= 2G \left( 1 - \frac{\Delta\gamma 3G}{q_{n+1}^{trial}} \right) \mathbf{I}_d + 6G^2 \left( \frac{\Delta\gamma}{q_{n+1}^{trial}} - \frac{1}{3G + H} \right) \bar{\mathbf{N}}_{n+1} \otimes \bar{\mathbf{N}}_{n+1} + KI \otimes \mathbf{I}. \end{aligned}$$

Finally, it should be noted that the operator  $\mathbf{D}^{ep}$  in the present case and for this particular model and numerical integration algorithm is *symmetric*.

## 4.2. The Drucker-Prager Model

In this section, we focus on the implementation of the Drucker-Prager model with isotropic hardening

### 4.2.1. The Drucker-Prager constitutive equations

The Drucker-Prager yield surface is defined by means of the yield function:

$$\Phi(\boldsymbol{\sigma}, c) = \sqrt{J_2(s(\boldsymbol{\sigma}))} + \eta p(\boldsymbol{\sigma}) - \xi c ,$$

where:

$$J_2 = \frac{1}{2} \mathbf{s} : \mathbf{s} , \quad \mathbf{s} = \boldsymbol{\sigma} - p(\boldsymbol{\sigma}) \mathbf{I} , \quad p = \frac{1}{3} \text{tr}[\boldsymbol{\sigma}]$$

In the above relations  $p$  is the hydrostatic pressure and  $c$  is the cohesion. The constants  $\eta$  and  $\xi$  are calculated according to the required approximation to the Mohr-Coulomb criterion.

The general non-associative flow rule will be adopted but only the associative case will be studied. The flow potential for the non-associative model is:

$$\Psi(\boldsymbol{\sigma}, c) = \sqrt{J_2(s(\boldsymbol{\sigma}))} + \bar{\eta} p(\boldsymbol{\sigma})$$

where the constant  $\bar{\eta}$  depends on the dilatancy angle  $\psi$  and is calculated according to the required approximation to the Mohr-Coulomb law by replacing the frictional angle  $\varphi$  with  $\psi$  in the relations that give  $\eta$  and where given in an earlier chapter. The flow rule reads:

$$\dot{\boldsymbol{\varepsilon}}^p = \dot{\gamma} \mathbf{N} ,$$

where for the smooth portion of the yield surface, the flow vector is given by:

$$\mathbf{N} = \frac{\partial \Psi}{\partial \boldsymbol{\sigma}} = \frac{1}{2\sqrt{J_2(s)}} + \frac{\bar{\eta}}{3} \mathbf{I}$$

while at the cone apex the flow vector  $\mathbf{N}$  is a subgradient of  $\Psi$ .

A general associative isotropic strain hardening is adopted for the Drucker-Prager model. The associative evolution equation for the *accumulated plastic strain* is:

$$\dot{\bar{\varepsilon}}^p = \dot{\gamma} \bar{\xi}$$

while at the apex of the Drucker-Prager cone:

$$\dot{\boldsymbol{\varepsilon}}^p = \frac{\bar{\xi}}{\bar{\eta}} \dot{\bar{\varepsilon}}^p$$

### 4.2.2. Integration Algorithm for the Drucker-Prager model

The Drucker-Prager material model has two main features. Firstly, only one singularity exists on the yield surface, at the apex of the cone. Secondly, the Drucker-Prager yield surface as well as the resulting flow vector field resulting from the generally non-associative flow potential, are fully symmetric about the hydrostatic axis.

For materials with linear elastic law, the general return-mapping update formula for the stress tensor is:

$$\boldsymbol{\sigma}_{n+1} = \boldsymbol{\sigma}_{n+1}^{trial} - \Delta\gamma \mathbf{D}^e : \mathbf{N}_{n+1}$$

where  $-\Delta\gamma \mathbf{D}^e : \mathbf{N}_{n+1}$  is the *return vector*. As a consequence of the symmetry about the hydrostatic axis, whenever the above formula is applied, regardless of whether  $\boldsymbol{\sigma}_{n+1}$  lies on the smooth portion of the cone or on its apex, the return vector is always parallel to the plane that contains  $\boldsymbol{\sigma}_{n+1}^{trial}$  and the hydrostatic axis. Thus the return-mapping algorithm can be completely formulated in such a plane of stress space. Since the corresponding flow vector  $\mathbf{N}_{n+1}$  differs for the smooth portion of the cone and its apex, two possible explicit forms exist for the return-mapping algorithm. They are treated separately in the following section.

### 4.2.3. Return to the smooth portion of the cone

In a previous section, the flow vector for the smooth portion of the cone was defined by:

$$\mathbf{N} = \frac{\partial \Psi}{\partial \boldsymbol{\sigma}} = \frac{1}{2\sqrt{J_2(\mathbf{s})}} + \frac{\bar{\eta}}{3} \mathbf{I}.$$

The corresponding increment of plastic strain reads:

$$\Delta \boldsymbol{\varepsilon}^p = \Delta\gamma \mathbf{N}_{n+1} = \Delta\gamma \left( \frac{1}{\sqrt{J_2(\mathbf{s})}} \mathbf{s}_{n+1} + \frac{\bar{\eta}}{3} \mathbf{I} \right).$$

The corresponding stress-update formula is:

$$\begin{aligned} \boldsymbol{\sigma}_{n+1} &= \boldsymbol{\sigma}_{n+1}^{trial} - \Delta\gamma [2G(\mathbf{N}_d)_{n+1} + K(\mathbf{N}_v)_{n+1}] \\ &= \boldsymbol{\sigma}_{n+1}^{trial} - \Delta\gamma \left( \frac{G}{\sqrt{J_2(\mathbf{s})}} \mathbf{s}_{n+1} + \frac{K\bar{\eta}}{3} \mathbf{I} \right). \end{aligned}$$

Simplification of the above expression can be obtained by noting that, due to the definition of  $J_2$ , the following identity holds:

$$\frac{\mathbf{s}_{n+1}}{J_2(\mathbf{s}_{n+1})} = \frac{\mathbf{s}_{n+1}^{trial}}{J_2(\mathbf{s}_{n+1}^{trial})}.$$

Substitution of the above identity into the stress-update formula, gives:

$$\boldsymbol{\sigma}_{n+1} = \boldsymbol{\sigma}_{n+1}^{trial} - \Delta\gamma \left( \frac{G}{\sqrt{J_2(\mathbf{s}_{n+1}^{trial})}} \mathbf{s}_{n+1}^{trial} + \frac{K\bar{\eta}}{3} \mathbf{I} \right).$$

which can be equivalently written in terms of deviatoric and hydrostatic components:

$$\mathbf{s}_{n+1} = \left( 1 - \frac{G\Delta\gamma}{\sqrt{J_2(\mathbf{s}_{n+1}^{trial})}} \right) \mathbf{s}_{n+1}^{trial},$$

$$p_{n+1} = p_{n+1}^{trial} - K\bar{\eta}\Delta\gamma.$$

The consistency condition in the present case is given by:

$$\Phi_{n+1} \equiv J_2(\mathbf{s}_{n+1}) + \eta p_{n+1} - \xi c(\bar{\varepsilon}_{n+1}^p) = 0.$$

The updated accumulated plastic strain is obtained from:

$$\bar{\varepsilon}_{n+1}^p = \bar{\varepsilon}_n^p + \Delta\bar{\varepsilon}^p,$$

with

$$\Delta\bar{\varepsilon}^p = \xi\Delta\gamma$$

Finally, the substitution of the two above expressions in the consistency condition, results in the following (generally nonlinear) equation for the incremental plastic multiplier  $\Delta\gamma$ .

$$\Phi(\Delta\gamma) = \sqrt{J_2(\mathbf{s}_{n+1}^{trial})} - G\Delta\gamma + \eta(p_{n+1}^{trial} - K\bar{\eta}\Delta\gamma) - \xi c(\bar{\varepsilon}_n^p + \xi\Delta\gamma) = 0$$

#### 4.2.4. Return to the apex

At the apex, the return vector must be contained in the complementary cone of the yield surface. The consistency condition in this case is reduced to:

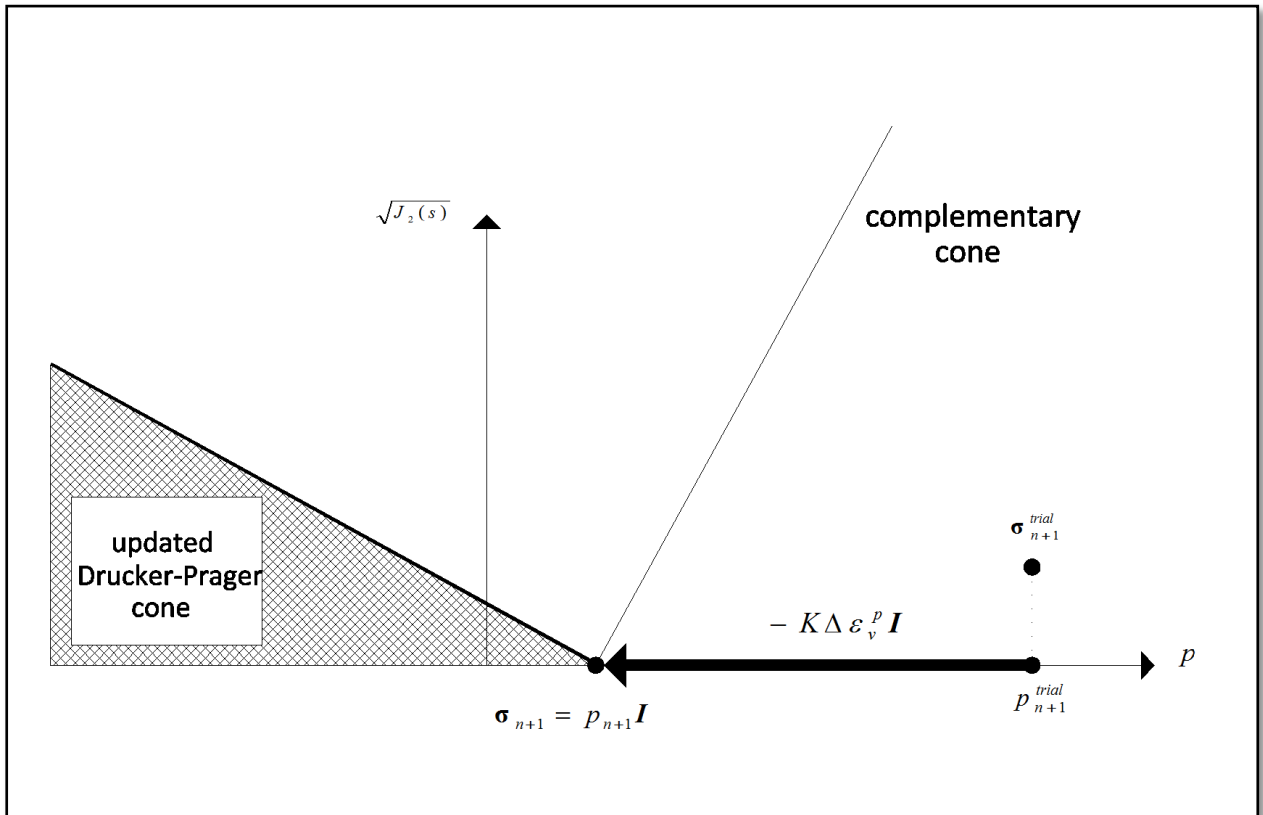
$$c(\bar{\varepsilon}_n^p + \Delta\bar{\varepsilon}^p) \frac{\xi}{\bar{\eta}} - p_{n+1}^{trial} + K\Delta\varepsilon_v^p = 0.$$

By introducing the discretised form of the accumulated plastic strain the final return-mapping equation for the Drucker-Prager apex is obtained:

$$r(\Delta\varepsilon_v^p) \equiv c(\bar{\varepsilon}_n^p + \alpha\Delta\varepsilon_v^p)\beta - p_{n+1}^{trial} + K\Delta\varepsilon_v^p = 0,$$

$$\alpha = \frac{\xi}{\bar{\eta}}, \quad \beta = \frac{\xi}{\bar{\eta}}$$

The geometrical representation of the above return mapping to the apex, is illustrated in the following figure.



Return mapping to apex for the Drucker-Prager model.

After the solution of the return mapping equation for  $\Delta \varepsilon_v^p$  we apply the updates:

$$\bar{\varepsilon}_{n+1}^p = \bar{\varepsilon}_n^p + a \Delta \varepsilon_v^p,$$

$$\sigma_{n+1} := (p_{n+1}^{trial} + K \Delta \varepsilon_v^p) \mathbf{I}$$

In the case of non-dilatant flow ( $\bar{\eta} = 0$ ), the return to the apex does not make sense since now volumetric plastic flow takes place.

One crucial remark is that for perfectly plastic materials, cohesion  $c$  is constant and for linearly hardening models where the hardening function reads  $c(\bar{\varepsilon}^p) = c_0 + H \bar{\varepsilon}^p$  where  $H$  is the hardening modulus. In these cases, the return-mapping equations for both the smooth portion of the cone and the apex become linear and  $\Delta \gamma, \Delta \varepsilon_v^p$  respectively are computed in closed form.

#### 4.2.5. Selection of the appropriate return-mapping

In the previous section, we have derived the two possible forms of the return-mapping algorithm for the Drucker-Prager model. Here we are going to describe the strategy for selection of the appropriate one necessary in order to completely define the integration algorithm.

The selection strategy is quite simple. There are only two possible return-mappings. If the application of one of them generates a contradiction then the other one is valid. The following steps describe the selection procedure:

- First we apply the return-mapping to the smooth portion of the cone. The corresponding deviatoric stress-update formula gives:

$$\sqrt{J_2(\mathbf{s}_{n+1})} = \sqrt{J_2(\mathbf{s}_{n+1}^{trial})} - G\Delta\gamma$$

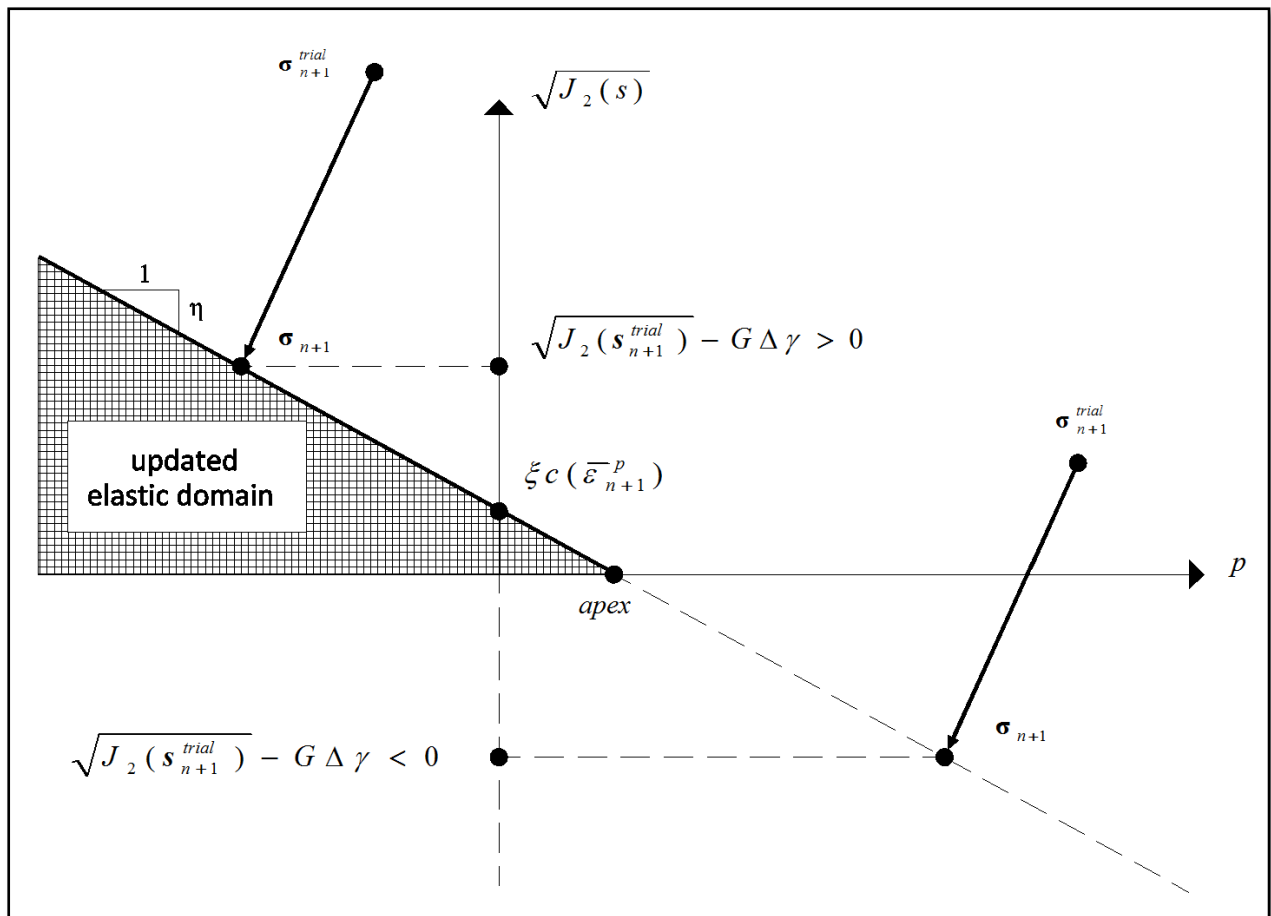
If after the determination of the related consistency condition, the following is satisfied

$$a^{cone} = \sqrt{J_2(\mathbf{s}_{n+1}^{trial})} - G\Delta\gamma \geq 0,$$

then the returned stress indeed lies on the Drucker-Prager cone and the return-mapping is validated.

- Otherwise the returned stress lies outside the updated elastic domain and it is not admissible. In this case, the return mapping to the apex must be applied.

The following figure illustrates the above procedure



Selection of the appropriate return-mapping for the Drucker-Prager model.

#### 4.2.6. Consistent Tangent Operator for the Drucker-Prager Model

The final step for the Drucker-Prager model, is the calculation of the elastoplastic tangent associated with the integration algorithm described in the previous sections. The difference between the Drucker-Prager model and the von Mises model described earlier is that there are two possible return-mapping schemes i.e. the return-mapping to the smooth portion of cone and the return-mapping to the apex. As a result two explicit forms of the elastoplastic tangent exist. The actual elastoplastic tangent chosen in order to assemble the tangent stiffness matrix is the one consistent with the last application of the return-mapping procedure at each Gauss point.



#### 4.2.6.1. Tangent consistent with the smooth portion return

Firstly, we have the deviatoric stress-update formula of the return-mapping to the smooth part of the cone:

$$\mathbf{s}_{n+1} = \left(1 - \frac{G\Delta\gamma}{\sqrt{J_2(\mathbf{s}^{trial})}}\right) \mathbf{s}_{n+1}^{trial} = 2G \left(1 - \frac{\Delta\gamma}{\sqrt{2}\|\boldsymbol{\varepsilon}_{d\,n+1}^{e\,trial}\|}\right) \boldsymbol{\varepsilon}_{d\,n+1}^{e\,trial}.$$

By differentiating the above expression:

$$d\mathbf{s}_{n+1} = 2G \left[ \left(1 - \frac{\Delta\gamma}{\sqrt{2}\|\boldsymbol{\varepsilon}_{d\,n+1}^{e\,trial}\|}\right) d\boldsymbol{\varepsilon}_{d\,n+1}^{e\,trial} + \frac{\Delta\gamma}{\sqrt{2}\|\boldsymbol{\varepsilon}_{d\,n+1}^{e\,trial}\|} \mathbf{D} \otimes \mathbf{D} : d\boldsymbol{\varepsilon}_{d\,n+1}^{e\,trial} - \frac{1}{\sqrt{2}} d\Delta\gamma \mathbf{D} \right],$$

where the second-order tensor  $\mathbf{D}$  is the unit tensor parallel to  $\boldsymbol{\varepsilon}_{d\,n+1}^{e\,trial}$ :

$$\mathbf{D} = \frac{\boldsymbol{\varepsilon}_{d\,n+1}^{e\,trial}}{\|\boldsymbol{\varepsilon}_{d\,n+1}^{e\,trial}\|}$$

Next we have the update formula form the hydrostatic pressure:

$$p_{n+1} = p_{n+1}^{trial} - K\bar{\eta}\Delta\gamma = K(\varepsilon_{v\,n+1}^{e\,trial} - \bar{\eta}\Delta\gamma).$$

Differentiation gives:

$$dp_{n+1} = K(d\varepsilon_{v\,n+1}^{e\,trial} - \bar{\eta}d\Delta\gamma)$$

Now by linearizing the consistency conditions and using the elastic relation, we can obtain the expression relating  $d\Delta\gamma$  and the differentials of trial strains:

$$d\bar{\Phi} = \sqrt{2}G\mathbf{D} : d\boldsymbol{\varepsilon}_{d\,n+1}^{e\,trial} + K\eta d\varepsilon_{v\,n+1}^{e\,trial} - (G + K\eta\bar{\eta} + \xi^2 H)d\Delta\gamma = 0,$$

which results in the identity:

$$d\Delta\gamma = \frac{1}{G + K\eta\bar{\eta} + \xi^2 H} (\sqrt{2}G\mathbf{D} : d\boldsymbol{\varepsilon}_{d\,n+1}^{e\,trial} + K\eta d\varepsilon_{v\,n+1}^{e\,trial})$$

Finally by substitution of the above relation to the differentiated version of the stress-update expression, and by using the identity:

$$\mathbf{D}^{ep} = \frac{d\boldsymbol{\sigma}_{n+1}}{d\boldsymbol{\varepsilon}_{n+1}^{e\,trial}} = \frac{d\mathbf{s}_{n+1}}{d\boldsymbol{\varepsilon}_{n+1}^{e\,trial}} + \mathbf{I} \otimes \frac{dp_{n+1}}{d\boldsymbol{\varepsilon}_{n+1}^{e\,trial}}$$

the explicit expression for the elastoplastic tangent consistent with the one-vector return is obtained after some manipulation as:

$$\begin{aligned} \mathbf{D}^{ep} = & 2G \left(1 - \frac{\Delta\gamma}{\sqrt{2}\|\boldsymbol{\varepsilon}_{d\,n+1}^{e\,trial}\|}\right) \mathbf{I}_d + 2G \left(\frac{\Delta\gamma}{\sqrt{2}\|\boldsymbol{\varepsilon}_{d\,n+1}^{e\,trial}\|} - GA\right) \mathbf{D} \otimes \mathbf{D} \\ & - \sqrt{2}GAK(\eta\mathbf{D} \otimes \mathbf{I} + \bar{\eta}\mathbf{I} \otimes \mathbf{D}) + K(1 - K\eta\bar{\eta}A)\mathbf{I} \otimes \mathbf{I}, \end{aligned}$$

where  $\mathbf{l}_d$  is the deviatoric projection vector and  $A$  is defined as:

$$A = \frac{1}{G + K\eta\bar{\eta} + \xi^2 H}$$

#### 4.2.6.2. Tangent consistent with the return-mapping to the apex

The key point in this case is that the stress deviator  $\mathbf{s}_{n+1}$  vanishes. The differential of the updated stress is simply:

$$d\boldsymbol{\sigma}_{n+1} = dp_{n+1}\mathbf{I}.$$

The associated elastoplastic tangent modulus is given by:

$$\mathbf{D}^{ep} = \frac{d\boldsymbol{\sigma}_{n+1}}{d\boldsymbol{\varepsilon}_{n+1}^{e\,trial}} = \mathbf{I} \otimes \frac{dp_{n+1}}{d\varepsilon_{n+1}^{e\,trial}}.$$

Now, recalling the hydrostatic pressure update formula:

$$p_{n+1} = p_{n+1}^{trial} - K\Delta\varepsilon_v^p,$$

we can differentiate and obtain:

$$dp_{n+1} = K\mathbf{I}:\boldsymbol{\varepsilon}_{n+1}^{e\,trial} - Kd\Delta\varepsilon_v^p.$$

Differentiating the residual equation of the return-mapping to the apex it is possible to obtain the explicit expression that gives  $d\Delta\varepsilon_v^p$ :

$$dr = (K + \alpha\beta H)d\Delta\varepsilon_v^p - K\mathbf{I}:d\boldsymbol{\varepsilon}_{n+1}^{e\,trial} = \mathbf{0}$$

$$\rightarrow d\Delta\varepsilon_v^p = \left(\frac{K}{K + \alpha\beta H}\right)\mathbf{I}:d\boldsymbol{\varepsilon}_{n+1}^{e\,trial}.$$

Finally, substituting the formula into the hydrostatic pressure update expression and also making use of the elastoplastic tangent modulus identity we obtain the explicit expression for the tangent operator consistent with the return to the apex return-mapping:

$$\mathbf{D}^{ep} = K\left(1 - \frac{K}{K + \alpha\beta H}\right)\mathbf{I} \otimes \mathbf{I}$$

which vanishes if the hardening modulus  $H = 0$ .

### 4.3. The Plane Stress-Projected von Mises Model

First of all, it is convenient to explain the meaning of *plane stress-projected* models. A plane stress-projected plasticity model, is defined by a set of evolution equations that:

- Involve only in-plane stress and strain components
- Are equivalent to the three-dimensional model with the added plane stress constraints defined for plane stress-conditions.

As a result, the in-plane stress/strain components are the primary variables which are determined by the solution of the rate evolution equations. The out of plane strain component is a dependent variable and can be calculated as a function of the in-plane strain components. In the situation of linear elasticity being studied, the plane stress-projected elastic constitutive equation can be written in complete analogy to the plane stress linear elasticity. So we can write the stress-strain relations in matrix-vector form as follows:

$$\begin{Bmatrix} \sigma_{11} \\ \sigma_{22} \\ \sigma_{12} \end{Bmatrix} = \frac{E}{1-\nu^2} \begin{bmatrix} 1 & \nu & 0 \\ \nu & 1 & 0 \\ 0 & 0 & \frac{1-\nu}{2} \end{bmatrix} \begin{Bmatrix} \varepsilon_{11} \\ \varepsilon_{22} \\ 2\varepsilon_{12} \end{Bmatrix}$$

The out-of-plane axial strain can be calculated by:

$$\varepsilon_{33} = -\frac{\nu}{1-\nu}(\varepsilon_{11} + \varepsilon_{22})$$

Obviously plane stress conditions require:

$$\sigma_{13} = \sigma_{31} = \sigma_{23} = \sigma_{32} = \sigma_{33} = 0,$$

$$\varepsilon_{13} = \varepsilon_{31} = \varepsilon_{23} = \varepsilon_{32} = 0$$

The general three-dimensional von Mises model with isotropic hardening is defined by the following set of equations rewritten for consistency:

$$\dot{\boldsymbol{\varepsilon}} = \dot{\boldsymbol{\varepsilon}}^e + \dot{\boldsymbol{\varepsilon}}^p,$$

$$\boldsymbol{\sigma} = \mathbf{D}^e : \boldsymbol{\varepsilon}^e,$$

$$\Phi = \sqrt{3J_2(\boldsymbol{s})} - \sigma_y(\bar{\boldsymbol{\varepsilon}}^p),$$

$$\dot{\boldsymbol{\varepsilon}}^p = \dot{\gamma} \frac{\partial \Phi}{\partial \boldsymbol{\sigma}} = \dot{\gamma} \sqrt{\frac{3}{2}} \frac{\boldsymbol{s}}{\|\boldsymbol{s}\|},$$

$$\dot{\bar{\boldsymbol{\varepsilon}}}^p = \dot{\gamma},$$

$$\dot{\gamma} \geq 0, \quad \Phi \leq 0, \quad \dot{\gamma} \Phi = 0$$

Whereas in plane stress conditions the following constraints are added:

$$\sigma_{13}(\boldsymbol{\varepsilon}^e) = \sigma_{31}(\boldsymbol{\varepsilon}^e) = 0 , \quad \sigma_{23}(\boldsymbol{\varepsilon}^e) = \sigma_{32}(\boldsymbol{\varepsilon}^e) = 0 , \quad \sigma_{33}(\boldsymbol{\varepsilon}^e) = 0.$$

### 4.3.1 The plane stress-projected equations

In order to obtain the plane stress-projected von Mises equations, firstly we need to derive explicit expressions which relate the dependent out-of-plane elastic and plastic strain components to the in-plane components. We start by taking into considerations that, as the elastic behaviour is linear and isotropic, the plane stress constraints for the out-of-stress components are equivalent to:

$$\varepsilon_{13}^e = \varepsilon_{31}^e = 0 , \quad \varepsilon_{23}^e = \varepsilon_{32}^e = 0 , \quad \varepsilon_{33}^e = -\frac{\nu}{1-\nu}(\varepsilon_{11}^e + \varepsilon_{22}^e).$$

In addition, the plastic incompressibility that follows from the flow rule, gives:

$$\varepsilon_{33}^p = -(\varepsilon_{11}^p + \varepsilon_{22}^p)$$

Moreover, as the out of plane components of the stress deviator vanish under plane stress conditions, it also follows from the flow rule that:

$$\varepsilon_{13}^p = \varepsilon_{31}^p = \varepsilon_{23}^p = \varepsilon_{32}^p = 0.$$

Summarizing, the history of the out-of-plane strain components is automatically prescribed as:

$$\begin{aligned} \varepsilon_{13}(t) &= \varepsilon_{31}(t) = \varepsilon_{13}^e(t) + \varepsilon_{13}^p(t) = 0 \\ \varepsilon_{23}(t) &= \varepsilon_{32}(t) = \varepsilon_{23}^e(t) + \varepsilon_{23}^p(t) = 0 \\ \varepsilon_{33}(t) &= -\left[ \frac{\nu}{1+\nu}(\varepsilon_{11}^e(t) + \varepsilon_{22}^e(t)) + \varepsilon_{11}^p(t) + \varepsilon_{22}^p(t) \right]. \end{aligned}$$

With the history of the out-of-plane strain components completely prescribed, we can now eliminate them from the original set of equations of the general von Mises plasticity model. This results in the *plane stress-projected* set of equations which, in component form, is given by:

$$\begin{aligned} \dot{\varepsilon}_{\alpha\beta} &= \dot{\varepsilon}_{\alpha\beta}^e + \dot{\varepsilon}_{\alpha\beta}^p , \\ \sigma_{\alpha\beta} &= \bar{D}_{\alpha\beta\gamma\delta}^e \varepsilon_{\gamma\delta}^e , \\ \Phi &= \sqrt{\frac{3}{2} \sigma_{\alpha\beta} \sigma_{\alpha\beta} - \frac{1}{3} (\sigma_{\alpha\alpha})^2} - \sigma_y(\bar{\varepsilon}^p) , \\ \dot{\varepsilon}_{\alpha\beta}^p &= \dot{\gamma} \sqrt{\frac{3}{2} \frac{s_{\alpha\beta}}{\sqrt{\sigma_{\gamma\delta} \sigma_{\gamma\delta} - \frac{1}{3} (\sigma_{\gamma\gamma})^2}}} , \end{aligned}$$

$$\dot{\boldsymbol{\varepsilon}}^p = \dot{\gamma} ,$$

$$\dot{\gamma} \geq 0 , \quad \Phi \leq 0 , \quad \dot{\gamma}\Phi = 0$$

where  $\bar{D}_{\alpha\beta\gamma\delta}^e$  denote the components of the plane stress elasticity tensor.

In order to derive the third and fourth equations above, we have made use of the identity:

$$\|\mathbf{s}\| = \sqrt{\sigma_{\gamma\delta}\sigma_{\gamma\delta} - \frac{1}{3}(\sigma_{\gamma\gamma})^2}$$

which is obtained by introducing the plane stress constraints into the definition of the deviatoric stress tensor and the Euclidean norm of a tensor:

$$\mathbf{s} \equiv \boldsymbol{\sigma} - \frac{1}{3}tr[\boldsymbol{\sigma}]\mathbf{I} , \quad \|\mathbf{s}\| = \sqrt{\mathbf{s}:\mathbf{s}} .$$

### 4.3.2. Matrix Notation

A compact representation of tensor quantities involved in plane stress-projected equations for the von Mises model can be obtained by making use of the following matrix and vector notations:

$$\boldsymbol{\sigma} = [\sigma_{11} \quad \sigma_{22} \quad \sigma_{12}]^T , \quad \mathbf{s} = [s_{11} \quad s_{22} \quad s_{12}]^T$$

$$\boldsymbol{\varepsilon} = [\varepsilon_{11} \quad \varepsilon_{22} \quad \varepsilon_{12}]^T , \quad \boldsymbol{\varepsilon}^e = [\varepsilon_{11}^e \quad \varepsilon_{22}^e \quad 2\varepsilon_{12}^e]^T$$

$$\boldsymbol{\varepsilon}^p = [\varepsilon_{11}^p \quad \varepsilon_{22}^p \quad 2\varepsilon_{12}^p]^T .$$

Also we introduce a special matrix denoted by  $\mathbf{P}$  which gives the deviatoric stress vector when multiplied by the stress vector:

$$\mathbf{s} = \mathbf{P}\boldsymbol{\sigma}$$

and it has the components:

$$\mathbf{P} = \frac{1}{3} \begin{bmatrix} 2 & -1 & 0 \\ -1 & 2 & 0 \\ 0 & 0 & 6 \end{bmatrix}$$

With the above matrix/vector notation and by using matrix  $\mathbf{P}$ , the plane stress-projected equations can be written in compact form:

$$\dot{\boldsymbol{\varepsilon}} = \dot{\boldsymbol{\varepsilon}}^e + \dot{\boldsymbol{\varepsilon}}^p ,$$

$$\boldsymbol{\sigma} = \mathbf{D}^e \boldsymbol{\varepsilon}^e ,$$

$$\Phi = \sqrt{\frac{3}{2} \boldsymbol{\sigma}^T \mathbf{P} \boldsymbol{\sigma} - \sigma_y(\bar{\boldsymbol{\varepsilon}}^p)},$$

$$\dot{\boldsymbol{\varepsilon}}^p = \dot{\gamma} \frac{\partial \Phi}{\partial \boldsymbol{\sigma}} = \dot{\gamma} \sqrt{\frac{3}{2}} \frac{\mathbf{P} \boldsymbol{\sigma}}{\sqrt{\boldsymbol{\sigma}^T \mathbf{P} \boldsymbol{\sigma}}},$$

$$\dot{\bar{\boldsymbol{\varepsilon}}}^p = \dot{\gamma},$$

$$\dot{\gamma} \geq 0, \quad \Phi \leq 0, \quad \dot{\gamma} \Phi = 0$$

where now,  $\mathbf{D}^e$  denotes the plane stress elasticity matrix. In the following section we are deriving the integration algorithm. In order to accomplish it, the squared form of the yield function will be introduced. The third, fourth and fifth equations above are written in squared form:

$$\Phi = \frac{1}{2} \boldsymbol{\sigma}^T \mathbf{P} \boldsymbol{\sigma} - \frac{1}{3} \sigma_y^2(\bar{\boldsymbol{\varepsilon}}^p),$$

$$\dot{\boldsymbol{\varepsilon}}^p = \dot{\gamma} \frac{\partial \Phi}{\partial \boldsymbol{\sigma}} = \dot{\gamma} \mathbf{P} \boldsymbol{\sigma},$$

$$\dot{\bar{\boldsymbol{\varepsilon}}}^p = \dot{\gamma} \sqrt{\frac{2}{3} \boldsymbol{\sigma}^T \mathbf{P} \boldsymbol{\sigma}}$$

### 4.3.3. The Plane Stress-Projected Integration Algorithm

Within the framework of general elastic predictor/return-mapping schemes described in the previous chapter and taking  $[t_n, t_{n+1}]$  as the underlying pseudo-time interval, we start by computing the predictor state:

$$\boldsymbol{\varepsilon}_{n+1}^{e \text{ trial}} = \boldsymbol{\varepsilon}_n^e + \Delta \boldsymbol{\varepsilon},$$

$$\boldsymbol{\sigma}_{n+1}^{trial} = \mathbf{D}^e \boldsymbol{\varepsilon}_{n+1}^{e \text{ trial}},$$

$$\bar{\boldsymbol{\varepsilon}}_{n+1}^{p \text{ trial}} = \bar{\boldsymbol{\varepsilon}}_n^p$$

where  $\Delta \boldsymbol{\varepsilon}$  is the vector of in-plane incremental strains within the considered interval  $[t_n, t_{n+1}]$ :

$$\Delta \boldsymbol{\varepsilon} = \boldsymbol{\varepsilon}_{n+1}^e - \boldsymbol{\varepsilon}_n^e$$

The next step is to check for plastic admissibility of the elastic trial state. We then compute the (using the squared form of the yield function):

$$\Phi^{trial} = \frac{1}{2} (\boldsymbol{\sigma}_{n+1}^{trial})^T \mathbf{P} \boldsymbol{\sigma}_{n+1}^{trial} - \frac{1}{3} \sigma_y^2(\bar{\boldsymbol{\varepsilon}}_{n+1}^{p \text{ trial}})$$

If the trial state is admissible, i.e. if:

$$\Phi^{\text{trial}} \leq 0$$

then the process is elastic within the time interval  $[t_n, t_{n+1}]$  and we update:

$$(\cdot)_{n+1} = (\cdot)_{n+1}^{\text{trial}}$$

Otherwise, the return mapping algorithm must be applied and is described in the following section.

#### 4.3.4. The plane stress-projected return mapping

The implicit return mapping in the present case consists of solving the following system of algebraic equations:

$$\begin{aligned} \boldsymbol{\varepsilon}_{n+1}^e &= \boldsymbol{\varepsilon}_{n+1}^{e \text{ trial}} - \Delta\gamma \mathbf{P} \boldsymbol{\sigma}_{n+1} , \\ \bar{\varepsilon}_{n+1}^p &= \bar{\varepsilon}_n^p + \Delta\gamma \sqrt{\frac{2}{3}} (\boldsymbol{\sigma}_{n+1})^T \mathbf{P} \boldsymbol{\sigma}_{n+1} , \\ \frac{1}{2} (\boldsymbol{\sigma}_{n+1})^T \mathbf{P} \boldsymbol{\sigma}_{n+1} - \frac{1}{3} \sigma_y^2 (\bar{\varepsilon}_{n+1}^p) &= 0 \end{aligned}$$

for  $\boldsymbol{\varepsilon}_{n+1}^e, \bar{\varepsilon}_{n+1}^p$  and  $\Delta\gamma$  where  $\boldsymbol{\sigma}_{n+1}$  is a function of  $\boldsymbol{\varepsilon}_{n+1}^e$  defined by the elastic law.

In complete analogy to the three-dimensional von Mises model, the number of unknowns of the plane stress-projected return-mapping equations can be reduced. So the above set of equations can be reduced to a single equation having the incremental plastic multiplier  $\Delta\gamma$  as the only unknown. This can be achieved by substituting the second equation to the third and by rearranging the first equation, using the inverse of the elastic law:

$$\begin{aligned} \boldsymbol{\sigma}_{n+1} &= [\mathbf{C} + \Delta\gamma \mathbf{P}]^{-1} \mathbf{C} \boldsymbol{\sigma}_{n+1}^{\text{trial}} , \\ \frac{1}{2} (\boldsymbol{\sigma}_{n+1})^T \mathbf{P} \boldsymbol{\sigma}_{n+1} - \frac{1}{3} \sigma_y^2 \left( \bar{\varepsilon}_n^p + \Delta\gamma \sqrt{\frac{2}{3}} (\boldsymbol{\sigma}_{n+1})^T \mathbf{P} \boldsymbol{\sigma}_{n+1} \right) &= 0 \end{aligned}$$

where the unknowns now are the stress vector,  $\boldsymbol{\sigma}_{n+1}$  and the incremental plastic multiplier  $\Delta\gamma$  and  $\mathbf{C}$  is the inverse of the elastic matrix:

$$\mathbf{C} = (\mathbf{D}^e)^{-1}.$$

Finally, by substituting the first equation to the second equations which represents the consistency condition, the return-mapping for the plane stress-projected von Mises plasticity model is reduced to the following *scalar* nonlinear equation having the incremental plastic multiplier  $\Delta\gamma$  as the only unknown:

$$\bar{\Phi}(\Delta\gamma) = \frac{1}{2}\xi(\Delta\gamma) - \frac{1}{3}\sigma_y^2 \left( \bar{\varepsilon}_n^p + \Delta\gamma \sqrt{\frac{2}{3}\xi(\Delta\gamma)} \right) = 0$$

In order to keep the notation as compact as possible, we have conveniently defined:

$$\xi(\Delta\gamma) = (\boldsymbol{\sigma}_{n+1}^{trial})^T \mathbf{A}^T(\Delta\gamma) \mathbf{P} \mathbf{A}(\Delta\gamma) \boldsymbol{\sigma}_{n+1}^{trial} ,$$

Where matrix  $\mathbf{A}(\Delta\gamma)$  is defined as:

$$\mathbf{A}(\Delta\gamma) \equiv [\mathbf{C} + \Delta\gamma \mathbf{P}]^{-1} \mathbf{C} .$$

Thus the return mapping is carried out as follows. Firstly we solve the consistency condition using the Newton-Raphson algorithm. Then with the incremental plastic multiplier  $\Delta\gamma$  known, we update the other variables:

$$\begin{aligned} \boldsymbol{\sigma}_{n+1} &= \mathbf{A}(\Delta\gamma) \boldsymbol{\sigma}_{n+1}^{trial} , \\ \boldsymbol{\varepsilon}_{n+1}^e &= \mathbf{C} \boldsymbol{\sigma}_{n+1} , \\ \bar{\varepsilon}_{n+1}^p &= \bar{\varepsilon}_n^p + \Delta\gamma \sqrt{\frac{2}{3}\xi(\Delta\gamma)} . \end{aligned}$$

The in-plane plastic stresses can also be updated if necessary by:

$$\boldsymbol{\varepsilon}_{n+1}^p = \boldsymbol{\varepsilon}_n^p + \Delta\gamma \mathbf{P} \boldsymbol{\sigma}_{n+1}$$

One very crucial remark regarding the plane stress-projected return-mapping algorithm of the von Mises plasticity model, is that is always *nonlinear* in  $\Delta\gamma$  , regardless of the prescribed function  $\sigma_\gamma$ . This is in contrast with its three-dimensional counterpart whose main source of nonlinearity is the hardening curve and which becomes linear for perfectly plastic and linearly hardening models.

#### 4.3.5. Newton-Raphson return-mapping solution

In the present case where the elastic behaviour is *isotropic* the explicit expression for the solution of the consistency condition, as well as the calculation of matrix  $\mathbf{A}(\Delta\gamma)$  can be significantly simplified. The key point is the fact that matrices  $\mathbf{P}$  and  $\mathbf{D}^e$  share the same eigenvectors so that they both have a diagonal representation on the same basis. The same fact holds for matrices  $\mathbf{C}$  and  $\mathbf{A}$ . So by applying the orthogonal transformation  $\mathbf{Q}$ :

$$\mathbf{Q} = \begin{bmatrix} \frac{1}{\sqrt{2}} & -\frac{1}{\sqrt{2}} & 0 \\ -\frac{1}{\sqrt{2}} & \frac{1}{\sqrt{2}} & 0 \\ 0 & 0 & 1 \end{bmatrix}$$



to  $\mathbf{P}$  and  $\mathbf{D}^e$  we obtain their diagonal representations:

$$\mathbf{P}^* = \mathbf{Q}\mathbf{P}\mathbf{Q}^T = \begin{bmatrix} \frac{1}{3} & 0 & 0 \\ 0 & 1 & 0 \\ 0 & 0 & 2 \end{bmatrix},$$

$$\mathbf{D}^{e*} = \mathbf{Q}\mathbf{D}^e\mathbf{Q}^T = \begin{bmatrix} \frac{E}{1-\nu} & 0 & 0 \\ 0 & 2G & 0 \\ 0 & 0 & G \end{bmatrix}$$

On the same basis, the matrix  $\mathbf{A}(\Delta\gamma)$  has the diagonal representation:

$$\mathbf{A}^*(\Delta\gamma) \equiv [\mathbf{C}^* + \Delta\gamma\mathbf{P}^*]^{-1}\mathbf{C}^*$$

$$= \begin{bmatrix} \frac{3(1-\nu)}{3(1-\nu) + E\Delta\gamma} & 0 & 0 \\ 0 & \frac{1}{1 + 2G\Delta\gamma} & 0 \\ 0 & 0 & \frac{1}{1 + 2G\Delta\gamma} \end{bmatrix}$$

Where  $\mathbf{C}^* = [\mathbf{D}^{e*}]^{-1}$ . The corresponding representation of the elastic trial stress vector is:

$$\boldsymbol{\sigma}_{n+1}^{trial*} \equiv \mathbf{Q}\boldsymbol{\sigma}_{n+1}^{trial} = \begin{bmatrix} \frac{1}{\sqrt{2}}(\sigma_{11}^{trial} + \sigma_{22}^{trial}) \\ \frac{1}{\sqrt{2}}(\sigma_{22}^{trial} - \sigma_{11}^{trial}) \\ \sigma_{12}^{trial} \end{bmatrix}$$

With all the transformed variables at hand, the expression that gives  $\xi(\Delta\gamma)$  can be written in the simpler form:

$$\begin{aligned} \xi(\Delta\gamma) &= (\boldsymbol{\sigma}_{n+1}^{trial})^T \mathbf{A}^T(\Delta\gamma) \mathbf{P} \mathbf{A}(\Delta\gamma) \boldsymbol{\sigma}_{n+1}^{trial} \\ &= (\boldsymbol{\sigma}_{n+1}^{trial*})^T (\mathbf{A}^*(\Delta\gamma))^2 \mathbf{P}^* \boldsymbol{\sigma}_{n+1}^{trial*} \\ &= \frac{(\sigma_{11}^{trial} + \sigma_{22}^{trial})^2}{6 \left[1 + \frac{E\Delta\gamma}{3(1-\nu)}\right]^2} + \frac{\frac{1}{2}(\sigma_{22}^{trial} - \sigma_{11}^{trial})^2 + 2(\sigma_{12}^{trial})^2}{(1 + 2G\Delta\gamma)^2} \end{aligned}$$

Finally, using the orthogonal transformation  $\mathbf{Q}$  we can calculate the matrix  $\mathbf{A}(\Delta\gamma)$  which takes part in the stress update formula:

$$\mathbf{A}(\Delta\gamma) = \mathbf{Q}^T \mathbf{A}^*(\Delta\gamma) \mathbf{Q}$$

which leads to the explicit form:

$$\mathbf{A}(\Delta\gamma) = \begin{bmatrix} \frac{1}{2}(A_{11}^* + A_{22}^*) & \frac{1}{2}(A_{11}^* - A_{22}^*) & 0 \\ \frac{1}{2}(A_{11}^* - A_{22}^*) & \frac{1}{2}(A_{11}^* + A_{22}^*) & 0 \\ 0 & 0 & A_{33}^* \end{bmatrix}$$

with  $A_{11}^*$ ,  $A_{22}^*$ ,  $A_{33}^*$  representing the diagonal terms of matrix  $\mathbf{A}^*$  (the diagonal representation of  $\mathbf{A}$  which are given here for consistency:

$$A_{11}^* = \frac{3(1-\nu)}{3(1-\nu) + E\Delta\gamma}, \quad A_{22}^* = \frac{1}{1 + 2G\Delta\gamma}, \quad A_{33}^* = A_{22}^*$$

### 4.3.6. The Elastoplastic Consistent Tangent Operator

With the matrix/vector notation adopted throughout the preceding derivations, the elastoplastic tangent matrix is defined as:

$$\mathbf{D}^{ep} = \frac{d\boldsymbol{\sigma}_{n+1}}{d\boldsymbol{\varepsilon}_{n+1}} = \frac{d\boldsymbol{\sigma}_{n+1}}{d\boldsymbol{\varepsilon}_{n+1}^{trial}}$$

The explicit expression for the elastoplastic tangent matrix is derived in the same way as its three-dimensional counterpart. We start by combining the following equations:

$$\boldsymbol{\varepsilon}_{n+1}^e = \boldsymbol{\varepsilon}_{n+1}^{e\,trial} - \Delta\gamma \mathbf{P} \boldsymbol{\sigma}_{n+1},$$

$$\boldsymbol{\sigma}_{n+1} = [\mathbf{C} + \Delta\gamma \mathbf{P}]^{-1} \mathbf{C} \boldsymbol{\sigma}_{n+1}^{trial},$$

Beginning with the first equation:

$$\boldsymbol{\varepsilon}_{n+1}^e = \boldsymbol{\varepsilon}_{n+1}^{e\,trial} - \Delta\gamma \mathbf{P} \boldsymbol{\sigma}_{n+1} \rightarrow \mathbf{C} \boldsymbol{\sigma}_{n+1}^{trial} = \boldsymbol{\varepsilon}_{n+1}^{e\,trial} - \Delta\gamma \mathbf{P} \boldsymbol{\sigma}_{n+1}$$

$$\rightarrow [\mathbf{C} + \Delta\gamma \mathbf{P}] \boldsymbol{\sigma}_{n+1} = \boldsymbol{\varepsilon}_{n+1}^{e\,trial} - \Delta\gamma \mathbf{P} \boldsymbol{\sigma}_{n+1} \rightarrow \boldsymbol{\sigma}_{n+1} = [\mathbf{C} + \Delta\gamma \mathbf{P}]^{-1} [\boldsymbol{\varepsilon}_{n+1}^{e\,trial} - \Delta\gamma \mathbf{P} \boldsymbol{\sigma}_{n+1}]$$

$$\rightarrow \boldsymbol{\sigma}_{n+1} = \mathbf{E} [\boldsymbol{\varepsilon}_{n+1}^{e\,trial} - \Delta\gamma \mathbf{P} \boldsymbol{\sigma}_{n+1}]$$

where the matrix  $\mathbf{E}$  is defined as:

$$\mathbf{E} \equiv [\mathbf{C} + \Delta\gamma \mathbf{P}]^{-1}$$

We continue by differentiating the derived equation:

$$d\boldsymbol{\sigma}_{n+1} = \mathbf{E} [d\boldsymbol{\varepsilon}_{n+1}^{e\,trial} - d\Delta\gamma \mathbf{P} \boldsymbol{\sigma}_{n+1}]$$

The plastic consistency condition is:

$$\bar{\Phi}(\Delta\gamma) = \frac{1}{2}\xi(\Delta\gamma) - \frac{1}{3}\sigma_y^2 \left( \bar{\epsilon}_n^p + \Delta\gamma \sqrt{\frac{2}{3}\xi(\Delta\gamma)} \right) = 0$$

So by differentiating it we obtain the following:

$$\begin{aligned} d\bar{\Phi} &= \frac{1}{2}d\xi - \frac{2}{3}\sigma_y H \sqrt{\frac{2}{3}} \left( d\Delta\gamma \sqrt{\xi} + \frac{\Delta\gamma}{2\sqrt{\xi}} d\xi \right) \\ &= \frac{1}{2}d\xi - \frac{2}{3} \left( H\xi d\Delta\gamma + \frac{1}{2}\Delta\gamma d\xi \right) = 0 \end{aligned}$$

In the above, we have used the identity  $\sigma_y = \sqrt{\frac{3}{2}\xi}$ , which holds during plastic flow. From the above equation, solving with respect to  $d\Delta\gamma$  we have:

$$d\Delta\gamma = \frac{3}{4H\xi} \left( 1 - \frac{2}{3}H\Delta\gamma \right) d\xi.$$

By making use of the elastic law,  $\xi$  can now be defined in terms of matrix  $\mathbf{E}$  as:

$$\xi = (\boldsymbol{\epsilon}_{n+1}^{trial})^T \mathbf{E} \mathbf{P} \mathbf{E} \boldsymbol{\epsilon}_{n+1}^{trial}.$$

At this point, we can remind the useful relation which gives the differential of the inverse of a matrix:

$$d(\mathbf{M}^{-1}) = -\mathbf{M}^{-1}d\mathbf{M}\mathbf{M}^{-1}$$

for any invertible matrix  $\mathbf{M}$ .

By using the above relation, we can calculate the differential of the matrix :

$$\begin{aligned} \mathbf{E} &= [\mathbf{C} + \Delta\gamma\mathbf{P}]^{-1} \rightarrow d\mathbf{E} = d([\mathbf{C} + \Delta\gamma\mathbf{P}]^{-1}) = -[\mathbf{C} + \Delta\gamma\mathbf{P}]^{-1}d(\mathbf{C} + \Delta\gamma\mathbf{P})[\mathbf{C} + \Delta\gamma\mathbf{P}]^{-1} \\ &= -\mathbf{E} d\Delta\gamma\mathbf{P} \mathbf{E} \rightarrow d\mathbf{E} = -\mathbf{E} \mathbf{P} \mathbf{E} d\Delta\gamma. \end{aligned}$$

Direct differentiation of the expression between  $\xi$  and the matrix , gives:

$$\begin{aligned} d\xi &= 2(\boldsymbol{\epsilon}_{n+1}^{trial})^T \mathbf{E} \mathbf{P} \mathbf{E} d\boldsymbol{\epsilon}_{n+1}^{trial} + 2(\boldsymbol{\epsilon}_{n+1}^{trial})^T d\mathbf{E} \mathbf{P} \mathbf{E} \boldsymbol{\epsilon}_{n+1}^{trial} \\ &= 2(\boldsymbol{\sigma}_{n+1}^T \mathbf{P} \mathbf{E} d\boldsymbol{\epsilon}_{n+1}^{trial} - \boldsymbol{\sigma}_{n+1}^T \mathbf{P} \mathbf{E} \boldsymbol{\sigma}_{n+1} d\Delta\gamma). \end{aligned}$$

It has been proved that:

$$\begin{aligned} d\Delta\gamma &= \frac{3}{4H\xi} \left( 1 - \frac{2}{3}H\Delta\gamma \right) d\xi \rightarrow \\ d\Delta\gamma &= \frac{3}{4H\xi} \left( 1 - \frac{2}{3}H\Delta\gamma \right) 2(\boldsymbol{\sigma}_{n+1}^T \mathbf{P} \mathbf{E} d\boldsymbol{\epsilon}_{n+1}^{trial} - \boldsymbol{\sigma}_{n+1}^T \mathbf{P} \mathbf{E} \boldsymbol{\sigma}_{n+1} d\Delta\gamma) \end{aligned}$$

Solving with respect to  $d\Delta\gamma$  and substituting in the following:

$$d\boldsymbol{\sigma}_{n+1} = \mathbf{E}[d\boldsymbol{\varepsilon}_{n+1}^{e\ trial} - d\Delta\gamma\mathbf{P}\boldsymbol{\sigma}_{n+1}]$$

results to the following relation:

$$d\boldsymbol{\sigma}_{n+1} = [\mathbf{E} - \alpha(\mathbf{E}\mathbf{P}\boldsymbol{\sigma}_{n+1})\otimes(\mathbf{E}\mathbf{P}\boldsymbol{\sigma}_{n+1})]d\boldsymbol{\varepsilon}_{n+1}^{e\ trial}$$

where the scalar  $\alpha$  is defined as:

$$a = \frac{1}{\boldsymbol{\sigma}_{n+1}^T \mathbf{P} \mathbf{E} \mathbf{P} \boldsymbol{\sigma}_{n+1} + \frac{2\xi H}{3 - 2\xi H \Delta\gamma}}$$

Finally we can write the explicit expression for the calculation of the elastoplastic consistent tangent operator:

$$\mathbf{D}^{ep} = \mathbf{E} - \alpha(\mathbf{E}\mathbf{P}\boldsymbol{\sigma}_{n+1})\otimes(\mathbf{E}\mathbf{P}\boldsymbol{\sigma}_{n+1})$$

The same procedure used to calculate matrix  $\mathbf{A}$  used for the update of the stress vector, can be used in order to derive an explicit formula for matrix  $\mathbf{E}$ . So we arrive at the following:

$$\mathbf{E}(\Delta\gamma) = \begin{bmatrix} \frac{1}{2}(E_{11}^* + E_{22}^*) & \frac{1}{2}(E_{11}^* - E_{22}^*) & 0 \\ \frac{1}{2}(E_{11}^* - E_{22}^*) & \frac{1}{2}(E_{11}^* + E_{22}^*) & 0 \\ 0 & 0 & E_{33}^* \end{bmatrix}$$

with:

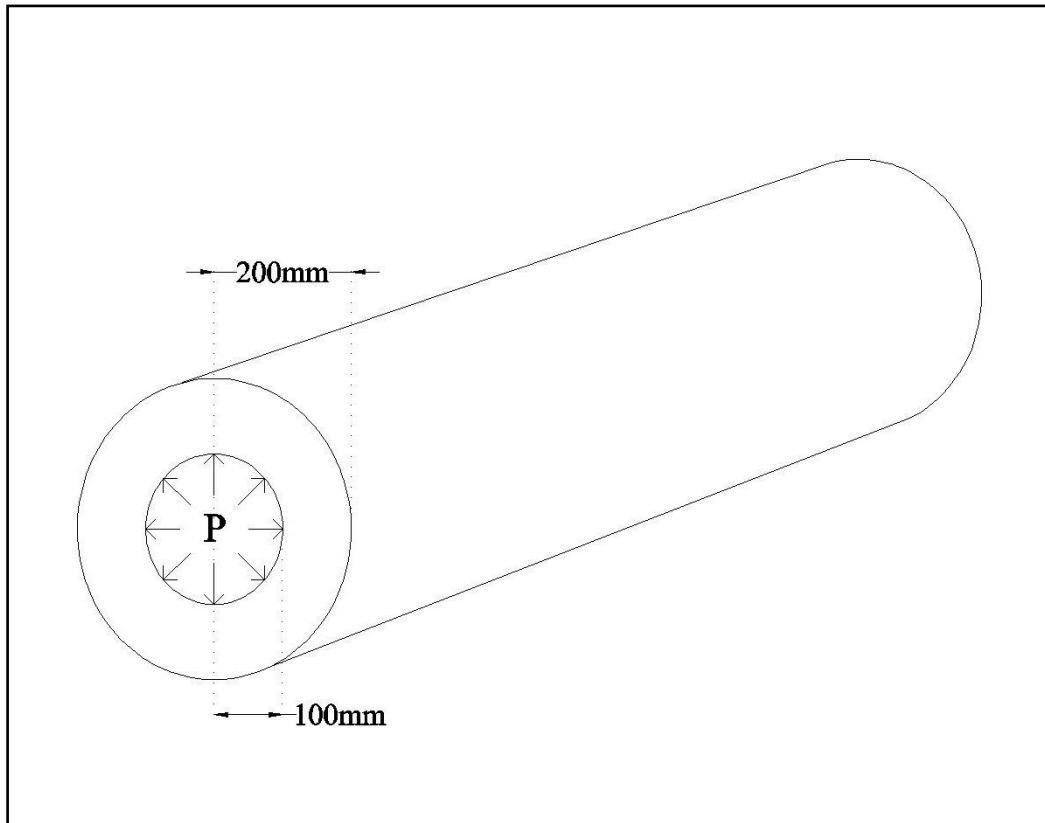
$$E_{11}^* = \frac{3E}{3(1-\nu) + E\Delta\gamma} , \quad E_{22}^* = \frac{2G}{1 + 2G\Delta\gamma} , \quad A_{33}^* = \frac{E_{22}^*}{2} .$$



## Chapter 5: Applications

### 5.1. Internally pressurized thick-walled cylinder

In this application, we investigate the behaviour of a long metallic thick-walled cylinder, subjected to internal pressure. The geometry and the dimensions of the cylinder are illustrated in the following figure.



Geometry and dimensions of the internally pressurized cylinder.

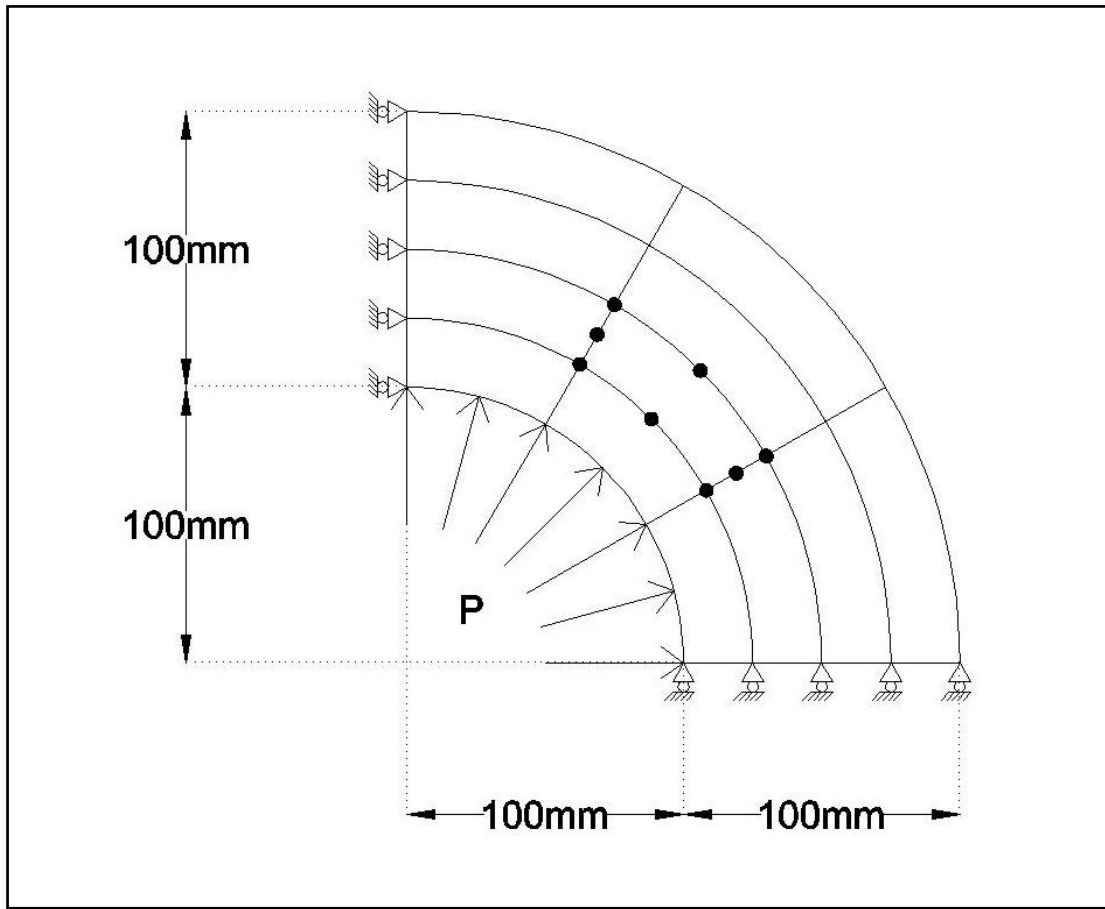
The material used for the metallic cylinder is an elastic-perfectly plastic von Mises material with associated flow rule. The material properties are the following:

Young's Modulus	$E = 210\text{GPa}$
Poisson's Ratio	$\nu = 0.3$
Uniaxial yield stress	$\sigma_y = 0.24\text{Gpa}$

The length of the cylinder is large compared to the other two dimensions. This fact allows us to perform the analysis assuming plane strain conditions.

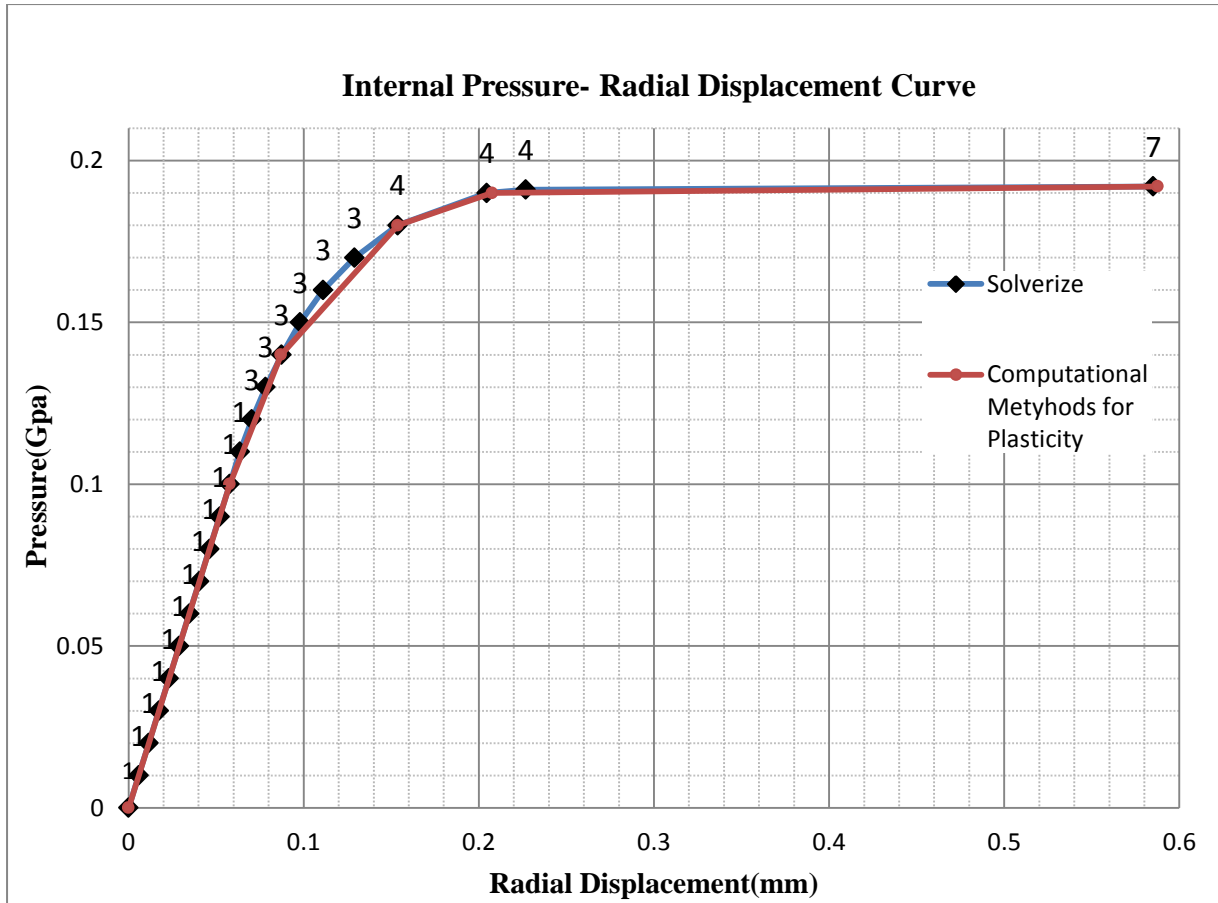
By taking into account the symmetry of the problem it is possible to analyze only one quarter of the cross-section of the cylinder, by applying the required symmetry boundary conditions

imposed on the edge nodes of the model. For the finite element mesh, isoparametric 8-noded quadrilateral elements are used with Gauss numerical integration (Gauss 3x3). The final model which is used in the analysis of the problem is illustrated in the following figure.



Cylinder cross-section finite element model.

The internal pressure  $P$ , is applied as consistent nodal loading at each node of the internal surface of the model. This pressure, is gradually increased until the collapse load is. The following graph shows the evolution of the internal pressure versus the radial displacement of the external surface of the cylinder. For comparison the curve for the analysis of the same model taken from the book “Computational Methods for Plasticity” which is included in the references:



Above each equilibrium point, the total number of iterations required for convergence of the Newton-Raphson nonlinear procedure is plotted.

Collapse of the model is takes place when for a relatively small load increment the increment of the radial displacement is large and the nonlinear procedure cannot. For this particular problem the analytical collapse load proposed by Hill is given by the following relation:

$$P_{lim} = \frac{2\sigma_y}{\sqrt{3}} \ln(b/a)$$

where  $b$  and  $a$  are the external and internal radius of the cylinder. For the geometrical dimensions of the particular problem, the above relation gives collapse pressure:

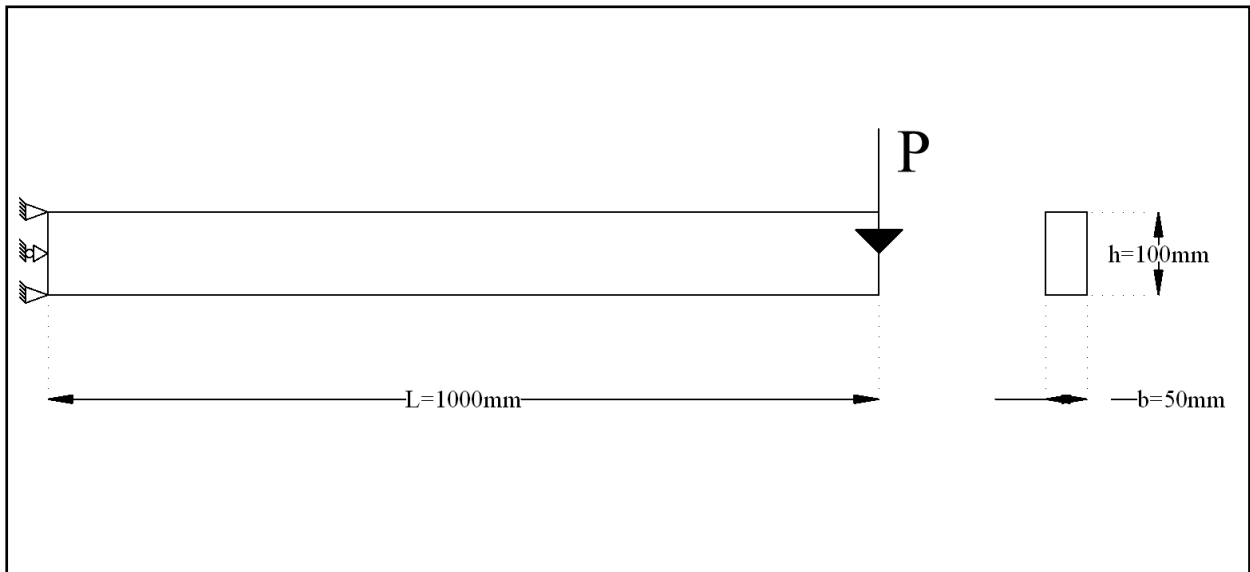
$$P_{lim} \approx 0.19209GPa$$

The limit load  $P = 0.192Gpa$  calculated from the analysis with program *Solverize* is practically identical to the analytical pressure proposed by Hill and the limit pressure obtained by “EA de Souza Neto, D Perić and DRJ Owen”. It is also of utter importance to observe the quadratic rate of convergence achieved by using the consistent tangent modulus.



## 5.2. Collapse of an End-Loaded Cantilever

In this application, we study the plastic collapse of an end-loaded cantilever beam with a rectangular cross-section. The load  $P$  is applied as a single nodal load on the node which is located at the middle of the cross-section height and at the right end of the cantilever. The boundary conditions consist of fixed supports at the bottom and top nodes of the left edge while only the horizontal displacement is constrained at all the other nodes of the edge. The geometry of the cantilever is illustrated in the following picture:



Geometry of the end-loaded cantilever.

For the material response, a plane stress projected von Mises constitutive model is assumed with material properties described below:

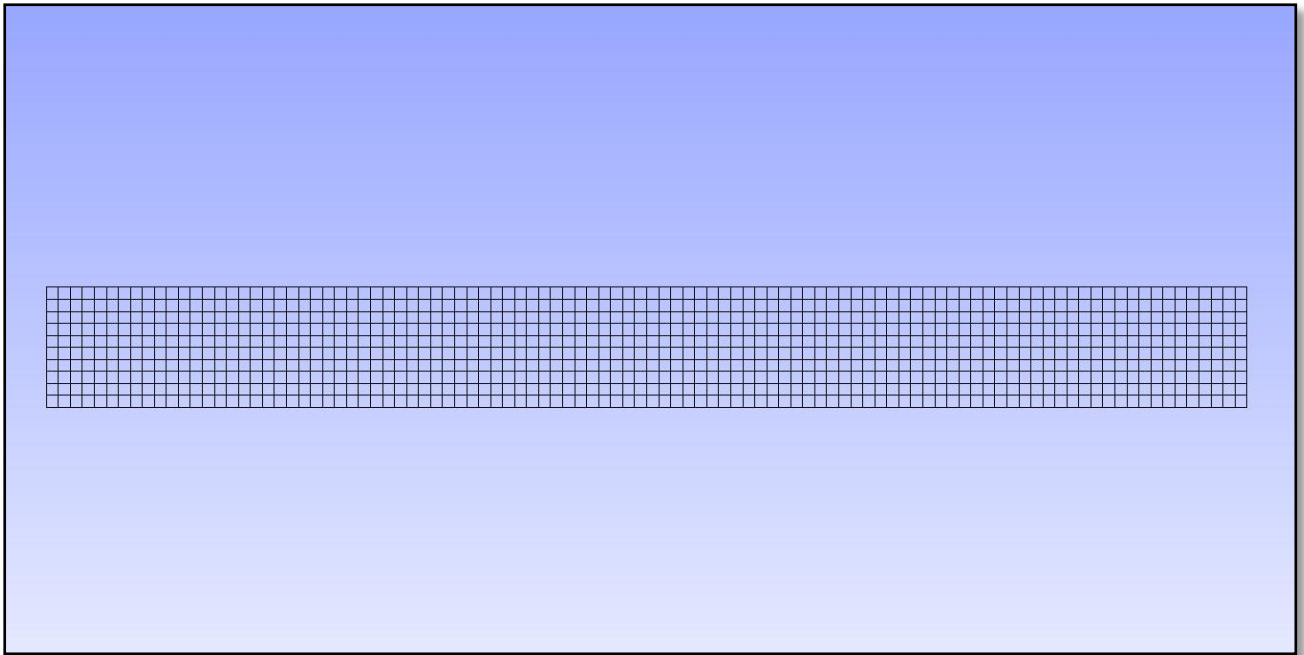
Material properties:

$$E = 210\text{Gpa}$$

$$\nu = 0.3$$

$$\sigma_y = 0.24\text{Gpa (perfectly plastic)}$$

The finite element mesh consists of 8-noded quadrilateral elements with (3x3 Gauss) integration and is illustrated in the following figure:



Finite element mesh consisting of 8-noded quadrilateral isoparametric elements.

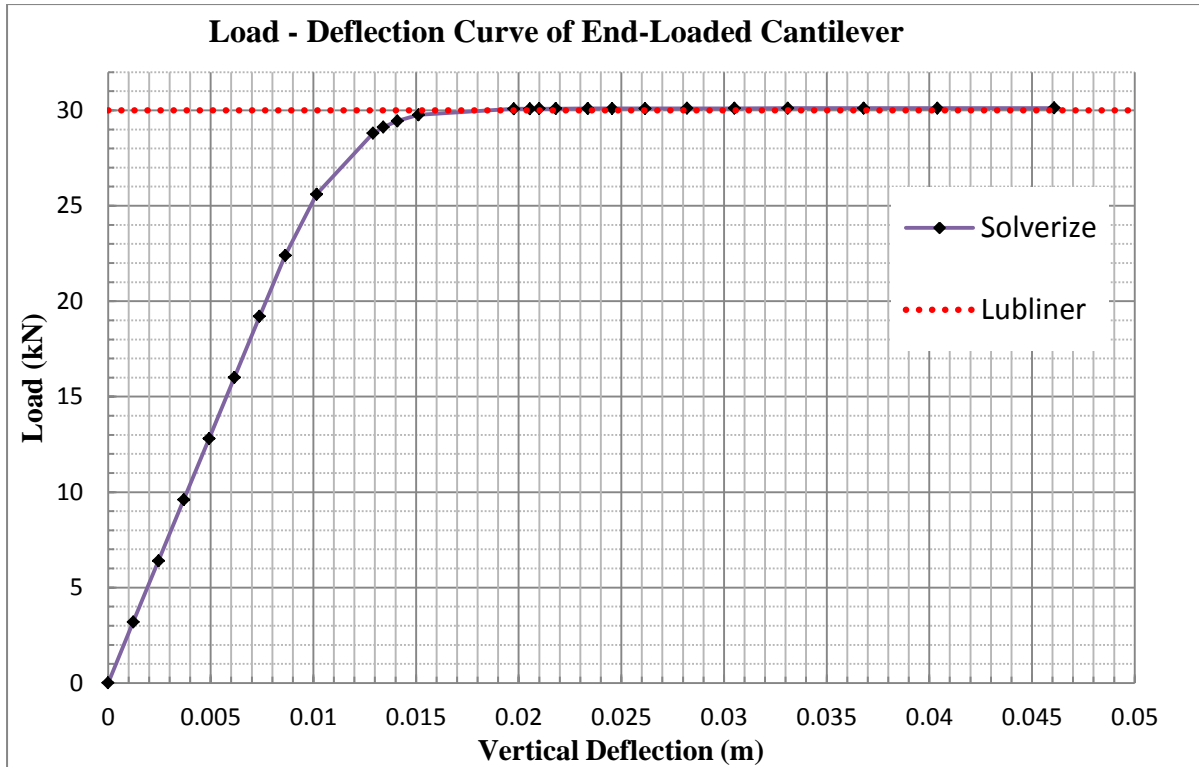
The analytical limit load for this problem is given by Lubliner (1990) and can be calculated by the following relation:

$$F_{lim} = \frac{\sigma_y b h^2}{4L}$$

which for this particular geometry and material properties gives:

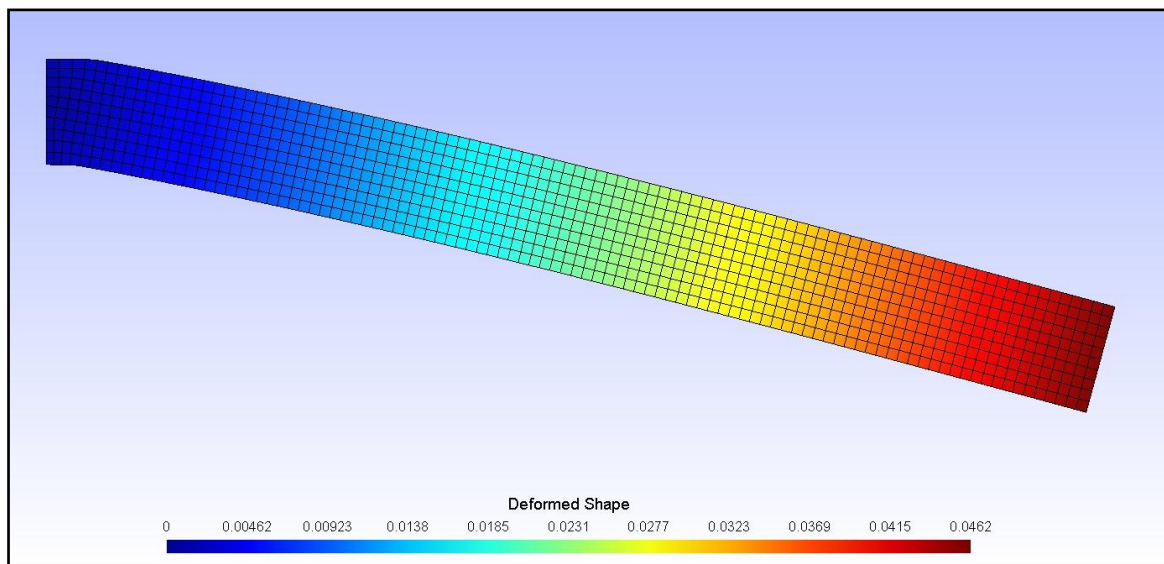
$$F_{lim} = 30kN$$

The following curve, gives the applied force versus the vertical deflection of the loaded node for the loading history until collapse is reached. The analytical limit load is plotted for comparison:



Load-deflection curve of the end-loaded cantilever

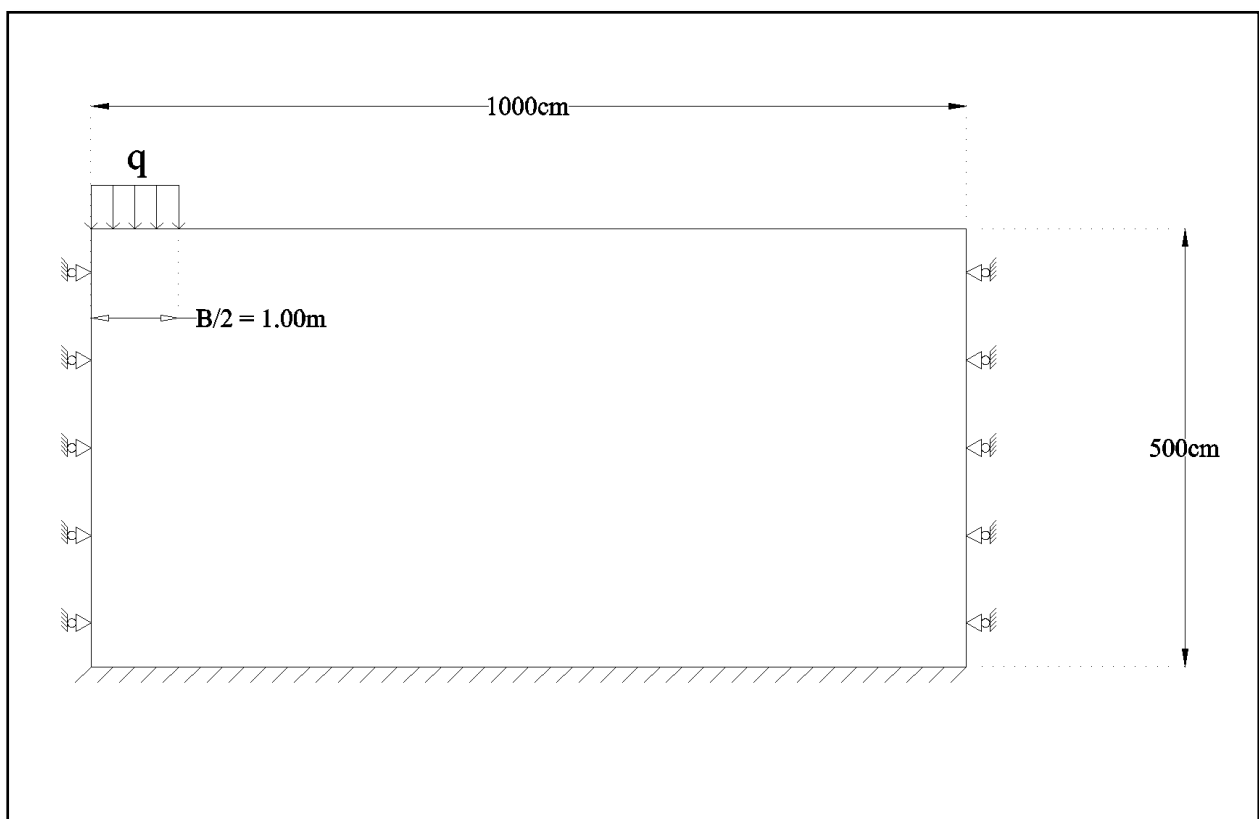
The numerically obtained collapse load  $P = 30.12\text{kN}$  is in excellent agreement with the theoretical limit load proposed by Lubliner. Finally, the following figure illustrates the deformed mesh during collapse:



Deformed mesh during plastic collapse.

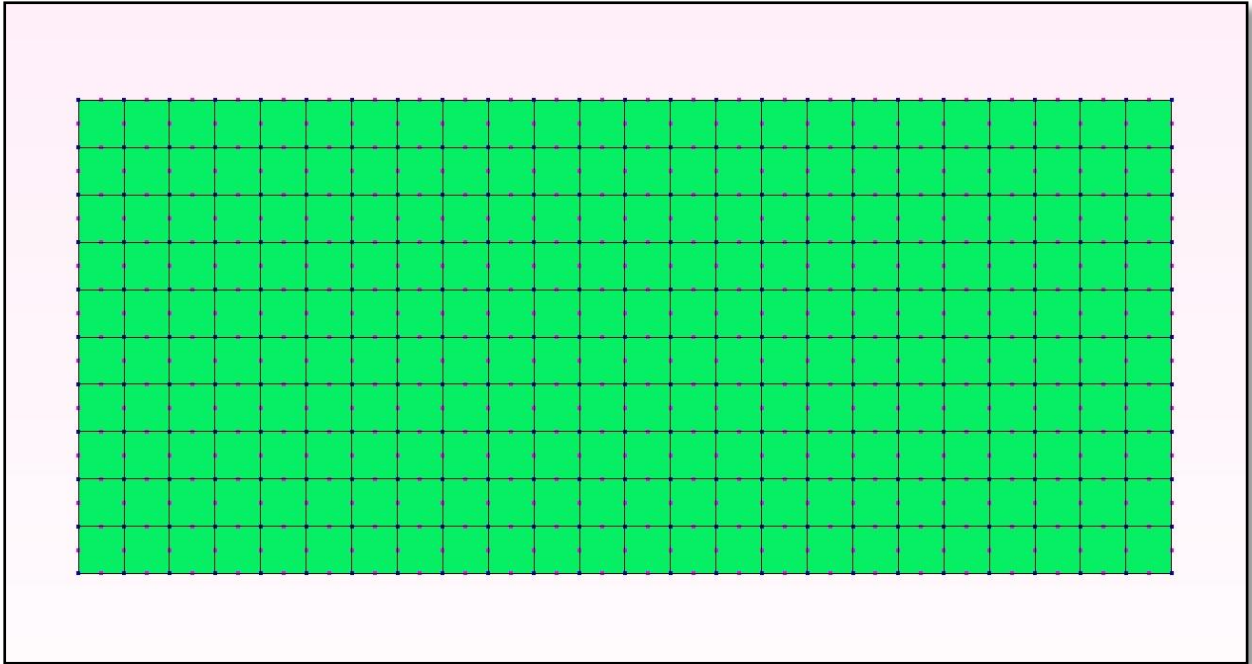
### 5.3. Strip-Footing Collapse

In this application, we want to determine the bearing capacity of a shallow strip footing. The problem consists of a long strip footing, of width  $B=2\text{m}$ , lying on soil which assumed as an infinite medium. The footing is subjected to a vertical pressure. The purpose of the present analysis is to find the collapse pressure  $P_{lim}$ . Two analyses are carried out. In both analyses, the soil is assumed to be weightless, while in the first case it is modeled as a von Mises perfectly plastic material and in the second case as a Drucker-Prager perfectly plastic material. The material constants for each case are given later. Due to the long length of the strip footing compared to its width, the problem is solved by assuming plane strain conditions. Also, by taking advantage of the symmetry of the problem, only half of the soil cross-section needs to be modeled. The geometry of the model is illustrated in the following figure.



Geometry of the cross-section of the soil domain.

The mesh of the model consists of 8-noded quadrilateral isoparametric elements with (3x3) Gauss integration. In order to properly simulate the infinite medium assumption of the soil, the soil domain extends far from the footing vicinity. The footing, is assumed flexible is subjected to a continuous line load  $q$ , which is applied as consistent nodal forces at the underlying nodes. The mesh which is used is illustrated in the following figure.



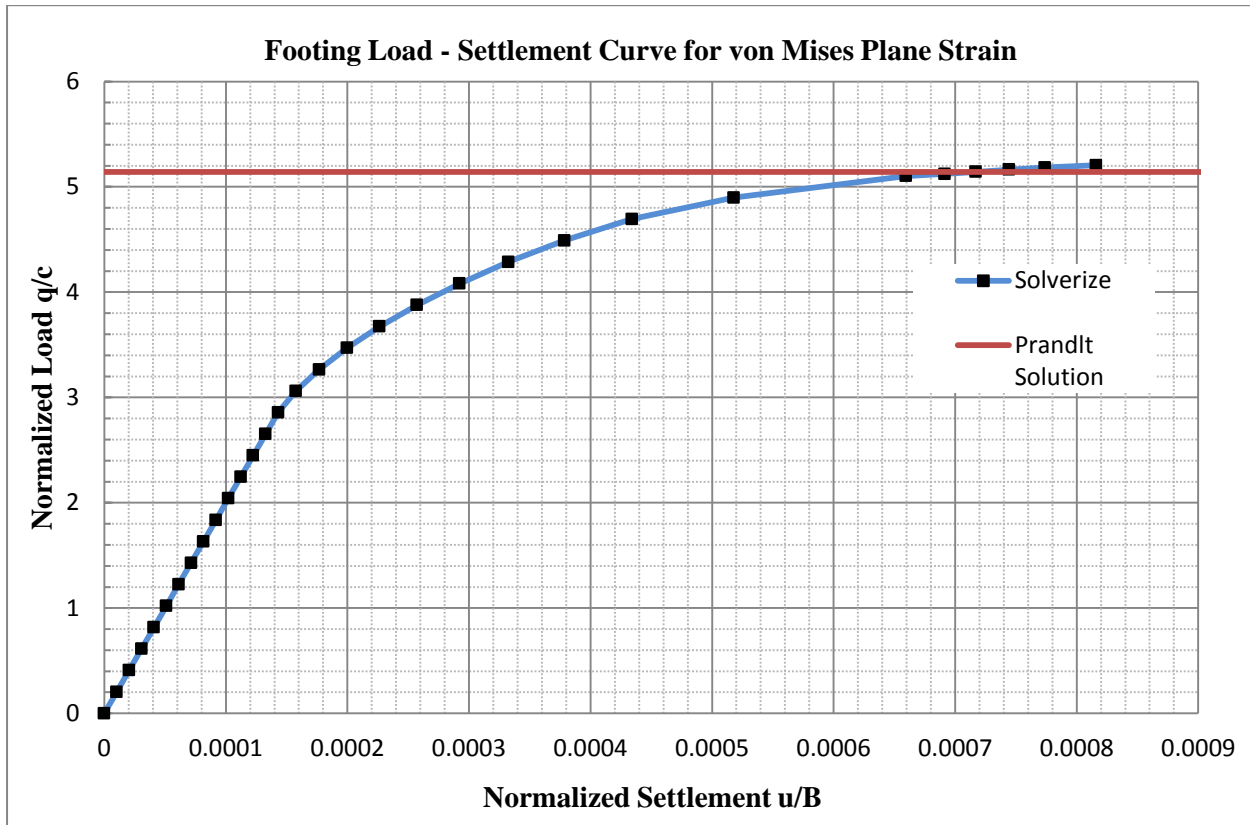
Finite element mesh of the soil domain.

As mentioned above, two analyses are carried out which differ in the material model used for the soil. The material properties for each analysis are given in the following:

1. The soil is modeled as a von Mises perfectly plastic material with the following material constants:
  - Young's Modulus  $E = 10^7 kPa$ .
  - Poisson Ratio  $\nu = 0.3$ .
  - Yield Stress  $\sigma_y = 848.8 kPa$  ( $\tau_y = 490 kPa$ )
2. The soil is modeled as a Drucker-Prager perfectly plastic material which follows the plane strain match approximation to the Mohr-Coulomb model. Associative flow-rule is assumed and the material parameters are the following:
  - Young's Modulus  $E = 10^7 kPa$ .
  - Poisson Ratio  $\nu = 0.3$ .
  - Cohesion =  $490 kPa$  .
  - Frictional angle (=dilatancy angle)  $\varphi = \psi = 20^\circ$ .

### 5.3.1. Results for the von Mises material model

In the following, the results obtained from the analysis using the von Mises material model are presented. First of all, we have the curve which gives the normalized pressure  $q/c$ , where  $c$  for this case equals the shear yield stress  $\tau_y$ , versus the normalized settlement  $u/B$  of the center of the footing, where  $B$  is the footing width.

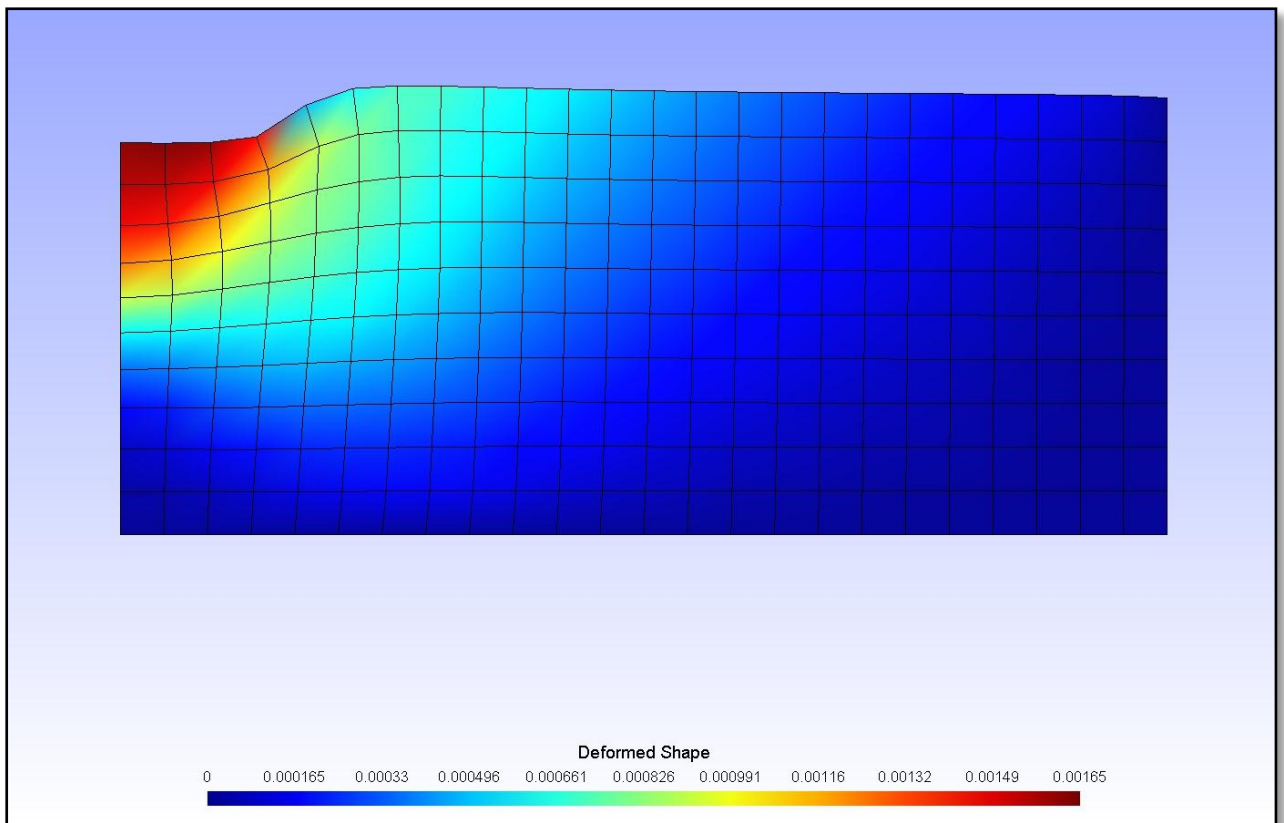


In the above curve, the limit load proposed by Prandtl is also illustrated for comparison. The analytical solution proposed by Prandtl is given from the following relation:

$$P_{lim} = (2 + \pi)c = 5.14c$$

The results obtained from the analysis with the program Solverize, are in excellent agreement with Prandtl's solution.

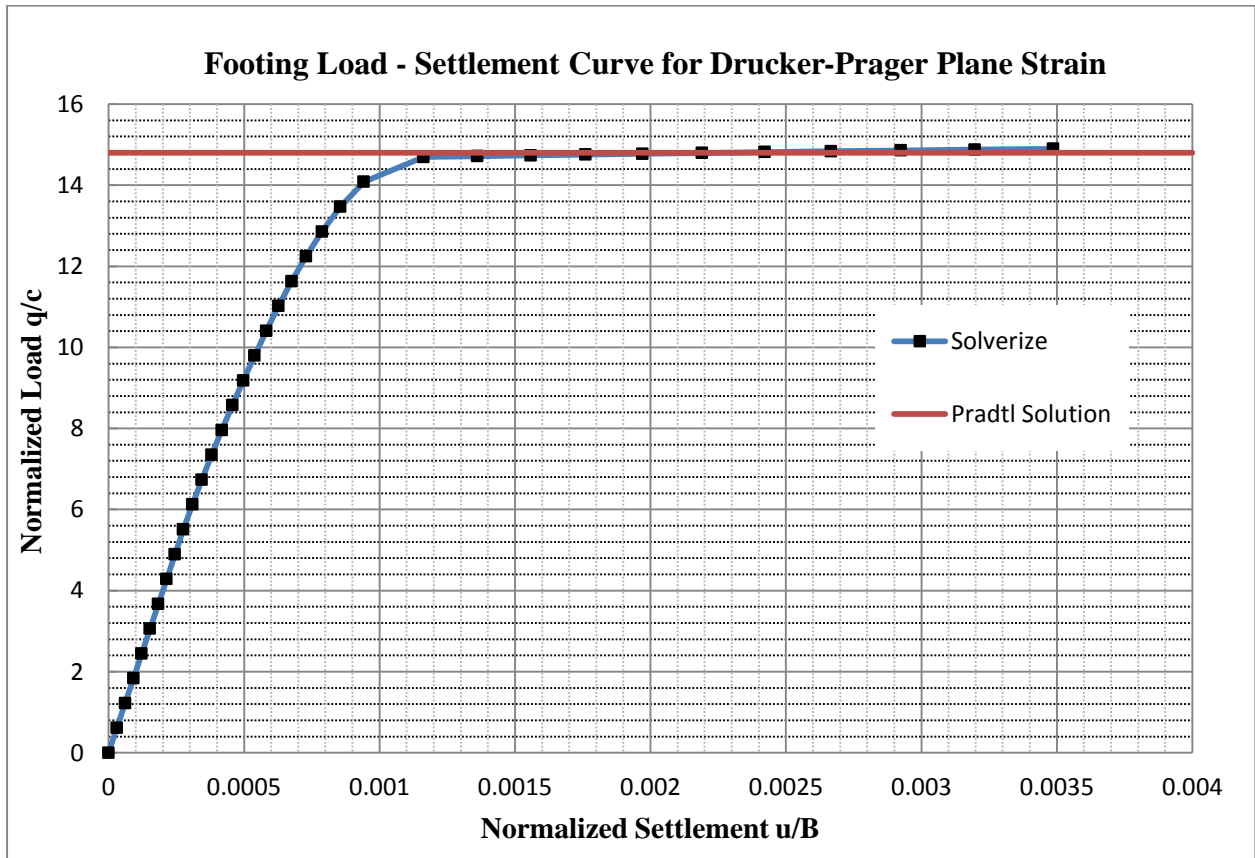
The following figure illustrates the deformed mesh during collapse:



Deformed shape for the von Mises material model during footing collapse.

### 5.3.2. Results for the Drucker-Prager material model

In the following, the results obtained from the analysis using the Drucker-Prager material model are presented. The normalized pressure versus normalized settlement curve is given, followed by the deformed shape figure during collapse.



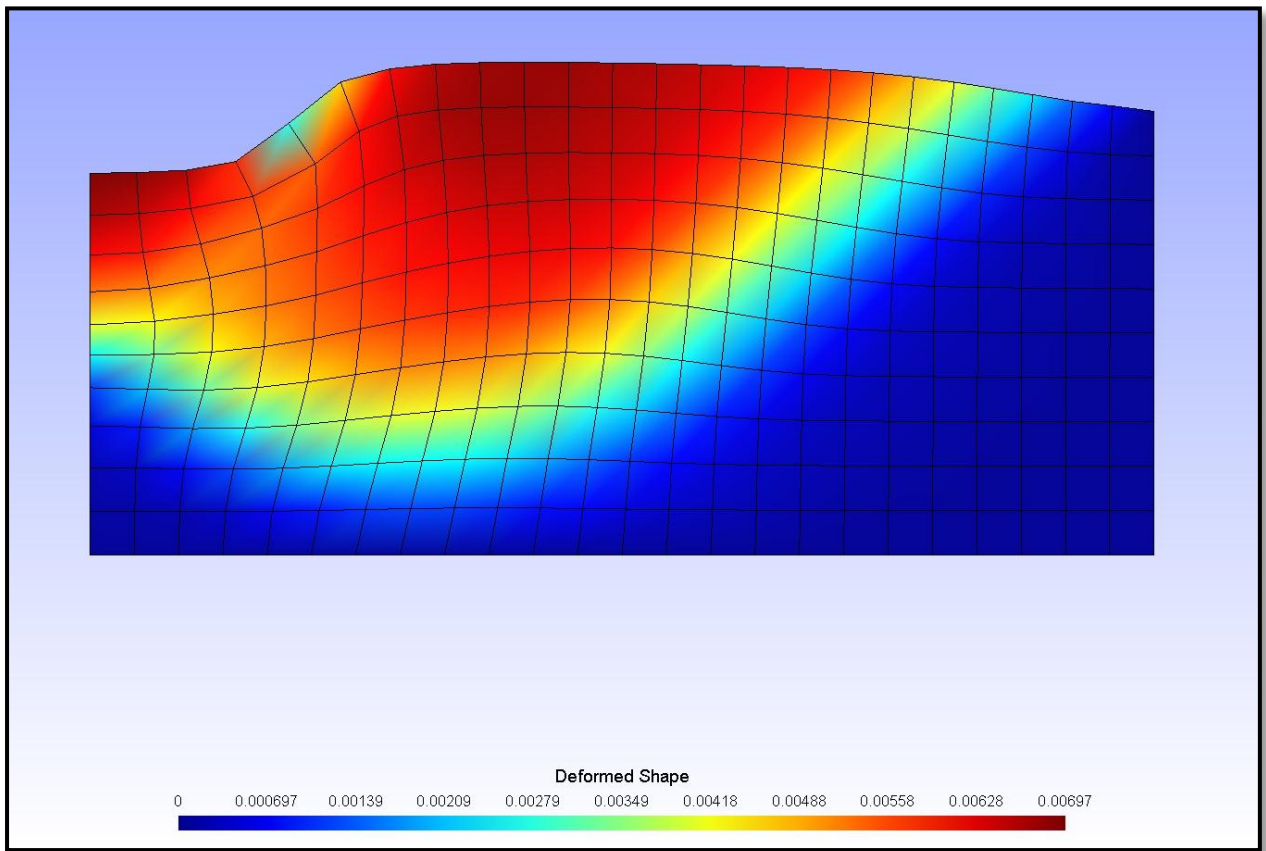
In the above curve, the limit load proposed by Prandtl for the Mohr-Coulomb model is also illustrated for comparison. The analytical solution proposed by Prandtl is:

$$P_{lim} = 14.8c$$

The limit load obtained from the analysis with the program *Solverize* by using the plane strain match approximation of the Drucker-Prager model to its Mohr-Coulomb counterpart is identical to the one given by Prandtl.



Finally the deformed mesh during the collapse of the footing is illustrated in the following figure.



Deformed shape for the Drucker-Prager material model during footing collapse.

## *References*

1. Μ. Παπαδρακάκης. 2001. *Ανάλυση Φορέων με τη Μέθοδο των Πεπερασμένων Στοιχείων*. Εκδόσεις Παπασωτηρίου.
2. EA de Souza Neto, D. Perić, DRJ Owen. 2008. *Computational Methods for Plasticity: Theory and Applications*. John Wiley & Sons Ltd.
3. Klaus-Jürgen Bathe. 2006. *Finite Element Procedures*. Klaus-Jürgen Bathe.
4. M. A. Crisfield. 1991. *Non-linear Finite Element Analysis of Solids and Structures, Volume 1: Essentials*. John Wiley & Sons Ltd.
5. W. Michael Lai, David Rubin, Erhard Krempl. 2010. *Introduction to Continuum Mechanics, Fourth Edition*. Elsevier Ltd.
6. Gerhard A. Hopzapfel. 2000. *Nonlinear Solid Mechanics: A Continuum Approach for Engineering*. John Wiley & Sons Ltd.
7. I. M. Smith, D. V. Griffiths. 2004. *Programming the Finite Element Method*. John Wiley & Sons Ltd.
8. Gene H. Golub, Charles F. Van Loan. 1996. *Matrix Computations*. The Johns Hopkins University Press.
9. Fridtjov Irgens. 2008. *Continuum Mechanics*. Springer-Verlag Berlin Heidelberg.
10. David M. Potts, Lidija Zdravkovic. 1999. *Finite Element Analysis in Geotechnical Engineering: Theory*. Thomas Telford Publishing.
11. A. J. M. Spencer. 1980. *Continuum Mechanics*. Dover Publications, Inc.
12. A.I. Borisenko, I.E. Tarapov, translated by Richard A. Silverman. 1968. *Vector and Tensor Analysis with Applications*. Dover Publications, Inc.
13. R. W. Ogden. 1984. *Non-Linear Elastic Deformations*. Dover Publications, Inc.
14. Helbert Schildt. 2011. *Java: The Complete Reference, Eighth Edition*. McGraw-Hill.
15. Joshua Bloch. 2008. *Effective Java, Second Edition*. Addison-Wesley.